

DEVELOPMENT OF MAGNESIUM POTASSIUM PHOSPHATE CEMENT  
PASTES AND MORTARS INCORPORATING FLY ASH

A THESIS SUBMITTED TO  
THE GRADUATE SCHOOL OF NATURAL AND APPLIED SCIENCES  
OF  
MIDDLE EAST TECHNICAL UNIVERSITY

BY

BAKİ AYKUT BİLGİNER

IN PARTIAL FULFILLMENT OF THE REQUIREMENTS  
FOR  
THE DEGREE OF MASTER OF SCIENCE  
IN  
CIVIL ENGINEERING

SEPTEMBER 2018



Approval of the thesis:

**DEVELOPMENT OF MAGNESIUM POTASSIUM PHOSPHATE  
CEMENT PASTES AND MORTARS INCORPORATING FLY ASH**

submitted by **BAKİ AYKUT BİLGİNER** in partial fulfillment of the requirements  
for the degree of **Master of Science in Civil Engineering Department, Middle  
East Technical University** by,

Prof. Dr. Halil Kalıpçılar  
Dean, Graduate School of **Natural and Applied Sciences** \_\_\_\_\_

Prof. Dr. İsmail Özgür Yaman  
Head of Department, **Civil Engineering** \_\_\_\_\_

Assoc. Prof. Dr. Sinan Turhan Erdoğan  
Supervisor, **Civil Engineering Dept., METU** \_\_\_\_\_

**Examining Committee Members:**

Prof. Dr. İsmail Özgür Yaman  
Civil Engineering Dept., METU \_\_\_\_\_

Assoc. Prof. Dr. Sinan Turhan Erdoğan  
Civil Engineering Dept., METU \_\_\_\_\_

Assoc. Prof. Dr. Berna Unutmaz  
Civil Engineering Dept., Hacettepe University \_\_\_\_\_

Asst. Prof. Dr. Çağla Meral Akgül  
Civil Engineering Dept., METU \_\_\_\_\_

Asst. Prof. Dr. Seda Yeşilmen  
Civil Engineering Dept., Çankaya University \_\_\_\_\_

**Date:** \_\_\_\_\_ 07.09.2018 \_\_\_\_\_

**I hereby declare that all information in this document has been obtained and presented in accordance with academic rules and ethical conduct. I also declare that, as required by these rules and conduct, I have fully cited and referenced all material and results that are not original to this work.**

Name, Last name: Baki Aykut Bilginer

Signature:

## ABSTRACT

### DEVELOPMENT OF MAGNESIUM POTASSIUM PHOSPHATE CEMENT PASTES AND MORTARS INCORPORATING FLY ASH

Bilginer, Baki Aykut  
MSc., Department of Civil Engineering  
Supervisor: Assoc. Prof. Dr. Sinan Turhan Erdoğan

September 2018, 94 pages

Magnesium potassium phosphate cements (MKPCs) have some promising properties to be considered as an alternative to ordinary Portland cement binders. The favorable properties of these cements are high early and ultimate strength. On the other hand, they have some problems like rapid setting, high heat of reaction, high cost and poor water stability. In this study, the effect of several factors like magnesium-to-phosphate molar ratio (M/P), water-to-binder ratio (W/B) and retarder (borax) content on properties such as setting time, compressive strength and on the microstructural evolution of MKPC pastes is investigated. Also, the effect of sand-to-binder ratio (S/B) and fly ash content on properties of MKPC mortar is investigated. The setting times of the paste samples were found to be between 4 and 10 min. The compressive strengths of the pastes were about 50 MPa. The 28 d compressive strength of the highest-strength mortar, prepared with S/B = 1.25, was almost 80 MPa. This value decreased with increasing fly ash content. Also, the strength loss in water did not seem to change with fly ash replacement. TGA and SEM investigations were also performed on paste samples used to study the effects of M/P and fly ash content.

Keywords: Magnesium, Phosphate, Strength, Water Stability.



## ÖZ

### UÇUCU KÜL İÇEREN MAGNEZYUM POTASYUM FOSFAT ÇİMENTOLARININ GELİŞİMİ

Bilginer, Baki Aykut  
Yüksek Lisans, İnşaat Mühendisliği  
Tez Yöneticisi: Doç. Dr. Sinan Turhan Erdoğan

Eylül 2018, 94 sayfa

Magnezyum potasyum fosfat çimentoları (MKPC), normal Portland çimentoları için alternatif bir bağlayıcı malzeme olarak düşünülebilecek bazı özelliklere sahiptir. Bu çimentoların elverişli özellikleri yüksek erken ve nihai dayanımdır. Diğer yandan, hızlı priz alma, yüksek reaksiyon ısısı, yüksek maliyet ve suya düşük dayanıklılık gibi bazı problemleri vardır. Bu çalışmada, MKPC hamurlarının magnezyum-fosfat molar oranına (M/P), su-bağlayıcı malzeme oranına (W/B) ve boraks içeriğine bağlı olarak, priz süresi, basınç dayanımı ve mikroyapısal gelişim gibi özellikleri araştırılmıştır. Ayrıca, kum-bağlayıcı malzeme (S/B) ve uçucu kül içeriğinin MKPC harcının özelliklerine etkisi araştırılmıştır. Hamur numunelerinin priz süresi 4 ile 10 dakika arasında değişim göstermiştir. Hamur numunelerinin 1 günlük basınç dayanımı yaklaşık 50 MPa olarak saptandı. S/B oranı 1.25 olan harc numunesinin 28 günlük basınç dayanımı yaklaşık 80 MPa idi. Uçucu kül miktarının artışıyla bu değerde azalma meydana geldi. Ayrıca, suda bekletilen harc numuneleri için, uçucu kül eklenmiş numunelerde dayanım kaybı neredeyse değişmedi. M/P ve uçucu kül miktarının etkilerini gözlemlemek için hazırlanan hamur numuneleri kullanılarak, TGA ve SEM incelemeleri de yapıldı.

Anahtar Kelimeler: Magnezyum, Fosfat, Dayanım, Suya Dayanıklılık.

To My Love, Nadire

To My Hero, Akif

To My Hope, Bekir

To My Truth, Berkay

To Fenerbahçe

## ACKNOWLEDGEMENTS

I wish to express my most profound gratitude to my supervisor Assoc. Prof. Dr. Sinan Turhan Erdoğan for his invaluable guidance, patience, motivation, and encouragement throughout this study. Also, I would like to thank all the thesis committee members.

I would like to thank my friends Oğulcan Canbek and Kadir Can Erkmn for everything.

I would like to thank my colleagues Kemal Ardoğa, Muhammet Ataseven, Meltem Tangüler Bayramtan for their great help.

I would like to thank Dr. Burhan Alessa Alam, Mr. Cuma Yıldırım and Mrs. Gülşah Bilici for their help with the problems in the laboratory.

I would like to thank my great friends from the Aikido Club, and Lifesaving and First-Aid Club of METU whose support cannot be underestimated.

I would also like to thank my friends Mustafa Aydoğan, Onur Tüysüz, Mithat Bayındır, Yiğit Genç, Onur Badem, Emre Karatepe, Mehmet Hilmi Somay, Eren Turgut, Hakan Gündüz, Naz Sürücü, Pınar Arıkoğlu, Berkay Akçören, Özgür Paşaoğlu, Mehran Ghasabeh, Büşra Elmas, and Sahra Shakouri for their great support and energy that made me feel better even at stressful times during my research.

I would like to express my respect towards Chet Baker, who was a very famous musician, without his great songs it would not have been possible to write my thesis.

I have to express my passion and love for Fenerbahçe, which made me stand even at stressful times during this study.

Finally, I would like to thank my lovely family; Nadire, Akif, Berkay, and Bekir for their great help throughout my years of study. This achievement would not have been possible without them.

## TABLE OF CONTENTS

ABSTRACT .....	v
ÖZ.....	vii
ACKNOWLEDGEMENTS .....	ix
TABLE OF CONTENTS .....	x
LIST OF TABLES .....	xiii
LIST OF FIGURES .....	xiv
CHAPTERS	
1. INTRODUCTION .....	1
1.1 Background.....	1
1.2 Objectives and Scope.....	2
2. LITERATURE REVIEW .....	3
2.1 Introduction .....	3
2.2 Magnesium Phosphate Cements .....	3
2.2.1 Reaction Mechanism of Formation.....	4
2.2.1.1 Using Acid Phosphates Instead of Phosphoric Acid.....	4
2.2.1.2 Calcination of MgO .....	6
2.2.1.3 Using Boric Acid or Borax .....	9
2.2.2 Types of Magnesium Phosphate Cement.....	10
2.2.3 Magnesium Potassium Phosphate Cements (MKPC).....	10
2.2.3.1 Influence of Water Content on the Properties of MKPC .....	11
2.2.3.2 Influence of M/P Ratio on the Properties of MKPC.....	14
2.2.3.3 Influence of Borax Content.....	18
2.2.3.4 Influence of S/B Ratio.....	19
2.3 Incorporating Fly Ash in MKPC .....	20
3. MATERIALS AND EXPERIMENTAL PROCEDURE .....	21
3.1 Introduction .....	21
3.2 Materials .....	21

3.2.1 Magnesia Powder .....	21
3.2.2 Dead-burned Magnesia Powder .....	22
3.2.3 Monopotassium Dihydrogen Phosphate.....	24
3.2.3 Sodium Tetraborate Decahydrate .....	24
3.2.4 Fly Ash .....	24
3.3 Experimental Procedure .....	25
3.3.1 Determination of the Calcination Process for the Magnesia Powder ....	25
3.3.1.1 Influence of calcination on physical properties .....	27
3.3.1.2 Influence of calcination on the oxide composition.....	27
3.3.1.3 Influence of calcination on setting time of MKPC pastes .....	27
3.3.2 Determination of the Mix Proportions for the MKPC.....	28
3.3.2.1 Setting time test for MKPC paste with different M/P and W/B ratios .....	29
3.3.2.2 Compressive strength of MKPC pastes with different M/P and W/B ratios .....	29
3.3.2.3 Determination of the suitable borax content for MKPC pastes.....	30
3.3.2.4 Determination of a suitable sand-to-binder (S/B) ratio for MKPC mortars .....	30
3.3.3 Incorporation of Fly Ash into MKPC Mortars .....	31
3.3.4 Thermogravimetric / Differential Analyses (TGA-DTA) Investigation on MKPC Pastes.....	31
3.3.5 Scanning Electron Microscopy (SEM) Investigation on MKPC Pastes	32
4. RESULTS AND DISCUSSION .....	33
4.1 Introduction .....	33
4.2 Analysis of the Effects of Calcination on the Magnesia Powder.....	33
4.2.1 Changes in Specific Gravity .....	33
4.2.2 Changes in Specific Surface Area .....	35
4.2.3 Changes in Microstructure .....	36
4.2.4 Changes in Reactivity.....	37
4.3 Analysis of the Effects of Mix Proportion on the Properties of MKPC Paste .....	40
4.3.1 Effects of the Mix Proportion on Setting Time .....	40
4.3.2 Effects of Mix Proportions on Compressive Strength.....	41
4.3.3 Effects of the Mix Proportion on the Microstructural Development ....	47

4.3.4 Effects of Borax Content on the Properties of MKPC Paste .....	50
4.4 Effects of Sand-to-Binder Ratio for the MKPC Mortar .....	54
4.5 Effects of Incorporating Fly Ash .....	55
4.5.1 Thermogravimetric / Differential Analyses .....	57
4.5.2 Scanning Electron Microscopy (SEM) Investigation .....	59
5. CONCLUSION .....	65
5.1 General.....	65
5.2 Recommendations for Future Studies.....	67
REFERENCES .....	69
APPENDICES .....	73
APPENDIX A .....	73
APPENDIX B.....	75
APPENDIX C.....	77
APPENDIX D .....	79

## LIST OF TABLES

Table 2.1 The dilution chart for phosphoric acid (Christensen and Reed, 1955) ...	5
Table 3.1 Oxide analysis of the magnesia powder used, determined with XRF. .	22
Table 3.2 Oxide analysis of the dead-burned magnesia powder used, determined with XRF.....	23
Table 3.3 Oxide analysis of the fly ash used, determined with XRF.....	25
Table 4.1 The percent mass loss of magnesia powder after calcination .....	35
Table 4.2 The early strength development of paste samples with different M/P and W/B .....	42
Table B.1 Compound composition of the magnesia samples calcined at different temperatures.....	75

## LIST OF FIGURES

Figure 2.1 Flow chart for phosphoric acid and acid phosphate production (NSP = normal super phosphate, TSP = triple super phosphate) (Wagh, 2004) .....	6
Figure 2.2 X-ray diffraction patterns of uncalcined and calcined MgO (Wagh and Jeong, 2003) .....	7
Figure 2.3 Change in the pH of an H <sub>3</sub> PO <sub>4</sub> solution with uncalcined and calcined MgO powders (Wagh and Jeong, 2003).....	7
Figure 2.4 Influence of calcination temperature on particle size distribution, M <sub>1-1</sub> : original sample, M <sub>1-2</sub> : calcined at 1000 °C, M <sub>1-3</sub> : calcined at 1200 °C (Li et al., 2014).....	8
Figure 2.5 Surface state of magnesia particles: A) original state, B) calcined at 1200 °C, C) calcined at 1600 °C (Li et al., 2014) .....	8
Figure 2.6 The influence of calcination temperature on the setting time of the paste samples with different liquid-to-solid ratios (L:S indicates liquid-to-solid ratio) (Wang et al., 2013) .....	9
Figure 2.7 Influence of W/B on setting time for MKPC pastes (Li and Chen, 2013) .....	12
Figure 2.8 Influence of W/B ratio on compressive strength of MKPC pastes. (Li and Chen, 2013).....	13
Figure 2.9 The effect of H <sub>2</sub> O : MgO on the X-ray diffraction patterns of pastes (Wang et al., 2013) .....	14
Figure 2.10 The effect of Mg/P ratio on setting time for MKPC pastes (Rouzic et al., 2017).....	15
Figure 2.11 The effect of phosphate to magnesium oxide molar ratio on compressive strength (Vertical axis shows compressive strengths in MPa) (Li et al., 2014).....	16
Figure 2.12 SEM images at 28 d of paste samples with M/P of 3 (left) and 5 (right) (Li et al., 2014) .....	16

Figure 2.13 The effect of Mg/P ratio on the compressive strength of MKPC pastes (Rouzic et al., 2017).....	17
Figure 2.14 SEM image of the $\text{KH}_2\text{PO}_4$ - reaction product interface for M/P=1 (Rouzic et al., 2017).....	17
Figure 2.15 Effect of borax content on the setting time and compressive strength of MKPC pastes (Qiao, 2010) .....	18
Figure 2.16 The effect of sand ratio on compressive strength of MKPC mortars (1.0-1.5 and 2.0 are S/B ratios) (Qiao, 2010) .....	20
Figure 3.1 The crucibles placed in the furnace (the top diameter of the crucible is almost 10 cm).....	23
Figure 3.2 Calcined samples: a) change in color (left to right – uncalcined, 600 °C, 1200 °C, 1300 °C, 1500 °C); b) The hard mass obtained (crucible - left, sample - right).....	26
Figure 3.3 A MKPC paste made with a low-temperature calcined MgO, dry and crumbly (image width is approximately 10 cm) .....	28
Figure 4.1 The influence of calcination on the specific gravity of the magnesia powder.....	34
Figure 4.2 The influence of calcination on the specific surface area of the magnesia powder.....	36
Figure 4.3 The influence of calcination on the microstructure .....	37
Figure 4.4 The effect of a) calcination temperature, b) calcination time on the setting time (at 1500 °C) of MKPC pastes .....	39
Figure 4.5 The setting times of MKPC pastes with different M/P and W/B .....	41
Figure 4.6 The effect of W/B ratio on the early strength gain of the samples with M/P = 3.....	43
Figure 4.7 The effect of W/B ratio on the early strength gain of the samples with M/P ratio of 4 .....	44

Figure 4.8 The effect of W/B ratio on the early strength gain of the samples with M/P ratio of 5.....	45
Figure 4.9 The effect of W/B on the early strength gain of samples with M/P = 6 .....	46
Figure 4.10 The evolution in microstructure for a) M/P=3, b) M/P=4, c) M/P=5, d) M/P=6 .....	49
Figure 4.11 The effect of borax content on the setting time.....	50
Figure 4.12 The effect of borax content on the compressive strength .....	52
Figure 4.13 The effect of borax content on the evolution in microstructure at a) 3 h, b) 7 d.....	53
Figure 4.14 The effect of sand-to-binder ratio on the compressive strength of the mortar samples.....	54
Figure 4.15 The effect of fly ash content on the compressive strength of the MKPC mortars .....	55
Figure 4.16 The effect of fly ash content on water stability of the mortar samples .....	56
Figure 4.17 The effect of fly ash content on the microstructural evolution .....	57
Figure 4.18 Heat flow and mass loss of the MKPC pastes .....	58
Figure 4.19 SEM Images for a large scale a) M/P=3, b) M/P=5, c) M/P=5 with 10 % FA, d) M/P=5 with 20 % FA.....	61
Figure 4.20 SEM images for a small scale a) M/P=3, b) M/P=5, c) M/P=5 with 10 % FA, d) M/P=5 with 20 % FA.....	63
Figure A.1 The change in X-ray diffraction patterns with calcination.....	73
Figure C.1 Cracks on the 5-cm cube sample with M/P = 6 and W/B = 0.20 at 24 h (before testing).....	77
Figure D.1 (a) W/B = 0.14, (b) W/B = 0.16, (c) W/B = 0.18, (d) W/B = 0.20 XRD results for M/P = 3 mixtures.....	80

Figure D.2 (a) 1 h (b) 3 h (c) 7 h (d) 24 h XRD results for M/P = 3 mixtures with W/B = 0.14, 0.16, 0.18, and 0.20.....	82
Figure D.3 (a) W/B = 0.14, (b) W/B = 0.16, (c) W/B = 0.18, (d) W/B = 0.20 XRD results for M/P = 4 mixtures.....	84
Figure D.4 (a) 1 h (b) 3 h (c) 7 h (d) 24 h XRD results for M/P = 4 mixtures with W/B = 0.14, 0.16, 0.18, and 0.20.....	86
Figure D.5 (a) W/B = 0.14, (b) W/B = 0.16, (c) W/B = 0.18, (d) W/B = 0.20 XRD results for M/P = 5 mixtures.....	88
Figure D.6 (a) 1 h (b) 3 h (c) 7 h (d) 24 h XRD results for M/P = 5 mixtures with W/B = 0.14, 0.16, 0.18, and 0.20.....	90
Figure D.7 (a) W/B = 0.14, (b) W/B = 0.16, (c) W/B = 0.18, (d) W/B = 0.20 XRD results for M/P = 6 mixtures.....	92
Figure D.8 (a) 1 h (b) 3 h (c) 7 h (d) 24 h XRD results for M/P = 6 mixtures with W/B = 0.14, 0.16, 0.18, and 0.20.....	94



# CHAPTER 1

## INTRODUCTION

### 1.1 Background

The most widely used hydraulic binding material is ordinary Portland cement. It is obtained by mixing a small amount of ground gypsum with Portland cement clinker that is produced by calcining calcareous and clayey raw materials in a rotary kiln, where the calcination temperature rises to  $\sim 1450$  °C (Erdogan, 2009). It is the most popular construction material which can be used for repair and maintenance work as Portland cement mortar and be used for structural components as Portland cement concrete reinforced with steel bars. Although it is very convenient to use ordinary Portland cement, there are some unfavorable outcomes of using it due mainly to the adverse environmental effect of the massive amount of CO<sub>2</sub> emission during its production. Producing 1000 kg of Portland cement generates 900 kg of CO<sub>2</sub> and consumes 5 million J of energy (Chau, Qiao and Li, 2011). Therefore, it is detrimental to use alternative binding materials to cope with these unfavorable properties of using ordinary Portland cement as much as possible. Magnesium potassium phosphate cements (MKPC), a type of magnesium phosphate cements (MPC), have been one of the most commonly used alternative binding materials, especially for the last decade. The raw materials of MKPCs are dead-burnt magnesia powder and potassium dihydrogen phosphate salts (Wagh, 2004). Acid-base reactions between the raw materials form the products of MKPCs. Since these reactions are very rapid, a retarder, often borax, is also included in the prepared

MKPCs. There are some advantages of using MKPC instead of ordinary Portland cement which are as follows: rapid setting, high early strength, high bonding strength, good abrasion resistance, durability in a wide pH range, and the ability to set and harden at low temperatures (Zheng et al., 2016; Liu and Chen, 2016; Li, Sun and Chen, 2014; Li et al., 2015; Li et al., 2015). Unfortunately, there are also some disadvantages such as poor water resistance, very high heat of hydration, high cost, which make it difficult for MKPC to be a candidate for structural applications (Li and Chen, 2013; Lu and Chen, 2016). Researchers have been working to minimize the problems concerning the use of MKPC for several decades. The most commonly studied application is to use of industrial by-products, generally fly ash, to take advantage of their possible favorable effects on workability, economy and sustainable development.

## **1.2 Objectives and Scope**

The main objectives of this research are:

- 1) Determination of suitable mix proportions for MKPC paste and mortar.
- 2) Investigate the effects of incorporating fly ash on the development of MPC mortar.

This dissertation is composed of five chapters. Chapter 1 gives the objective and scope of this study. In Chapter 2, a review of the literature on MPC is presented. Chapter 3 includes the physical and chemical properties of the raw materials used and the experimental procedures followed. In Chapter 4, the results of the experiments conducted and discussions of these results are presented. In Chapter 5, everything done for this research is finally summarized with concluding remarks and some recommendations for further studies.

## **CHAPTER 2**

### **LITERATURE REVIEW**

#### **2.1 Introduction**

A review of the literature is presented on magnesium phosphate cements which includes their formation and properties, types (especially magnesium potassium phosphate cements) and also a background for some industrial wastes like fly ash which have been used with these types of cements for several decades for some economical and durability advantages.

#### **2.2 Magnesium Phosphate Cements**

Magnesium phosphate cements are basically formed by the reaction between magnesium oxide and a phosphoric acid solution or an acid phosphate, which can be considered as the base and acid components, respectively. Normally, these acid-base reactions are very rapid and highly exothermic, giving rise to a noncoherent precipitate (Wilson and Nicholson, 1993). However, once the solubility of the reactant is controlled, especially for the metal oxide, the reaction can result in a coherent and crystalline hard mass that has found some potential applications as a quick-setting material for repair work and waste management. In the following, the detailed discussion of these cements is presented, starting from the most interesting and crucial concept; the reaction mechanism, which determines the end product.

### **2.2.1 Reaction Mechanism of Formation**

The reaction mechanism is related to the chemical and physical properties of the reactants mixed. The overall reaction can be termed a dissolution-precipitation process and the necessary steps could be summarized as follows: Magnesium oxide dissolves in a solution of phosphoric acid or acid phosphate solution, the dissolved magnesium cations and phosphate anions react to form the gel, then this gel saturates the solution, and finally the saturated gel solution precipitates and crystallizes (Wagh and Jeong, 2003). As the acid component inherently dissolves in water, one can only control the solubility or reactivity of magnesium oxide to get the desired end product. The definition of solubility is the maximum quantity of the substance, the solute, that can dissolve in a given quantity of solvent (Tro, 2008). There exist some ways to reduce the solubility of MgO, which include: Using acid phosphates instead of phosphoric acid, calcination of the MgO, and using boric acid or borax as a reaction retarder.

#### **2.2.1.1 Using Acid Phosphates Instead of Phosphoric Acid**

Phosphoric acid, generally referred to as orthophosphoric acid, is typically produced by the reaction of sulfuric acid ( $H_2SO_4$ ) with a phosphate ore. It is commercially available at different grades, at 70 and 85 wt. % concentration. Since it is a strong acid, the dilution of this acid is necessary for practical applications. Table 2.1 presents the change in pH value for diluted phosphoric acid solutions.

Table 2.1 The dilution chart for phosphoric acid (Christensen and Reed, 1955)

Phosphoric Acid (H <sub>3</sub> PO <sub>4</sub> )		
Concentration (%)	Molarity	pH
10	1.07	1.08
15	1.66	0.98
20	2.27	0.91
25	2.92	0.86
30	3.61	0.81
35	4.34	0.77
40	5.11	0.73
45	5.93	0.70
50	6.80	0.67
55	7.73	0.64
60	8.71	0.61
65	9.75	0.59
70	10.86	0.56
75	12.04	0.54
80	13.29	0.52
85	14.61	0.50

It is clear that the pH values of dilute phosphoric acid solutions are still very low which make it difficult to have a controlled reaction with magnesia powder. One possible way to solve this problem is to increase the water amount further. However, this will cause some stability problems related to the poorer structure formed. Therefore, using acid phosphates, produced by partial neutralization of the phosphoric acid, is a better way of solving this problem. This is achieved by reacting alkaline compounds such as chlorides, nitrates, oxides or carbonates of alkaline metals with phosphoric acid (Wagh, 2004). Figure 2.1 shows the schematic representation of the production process for phosphoric acid and acid phosphates.

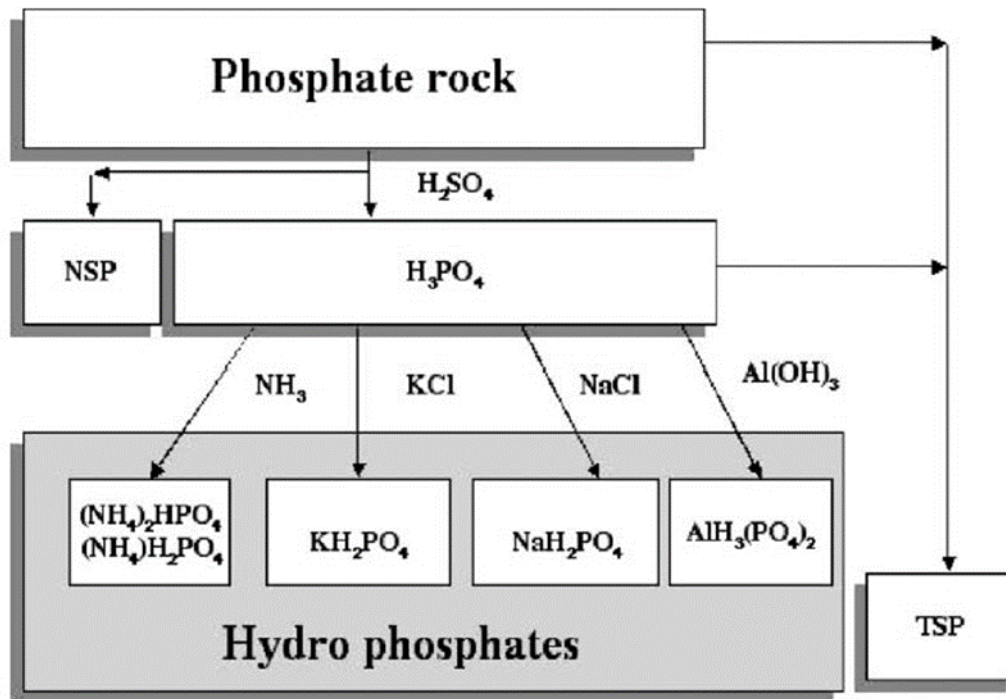


Figure 2.1 Flow chart for phosphoric acid and acid phosphate production (NSP = normal super phosphate, TSP = triple super phosphate) (Wagh, 2004)

### 2.2.1.2 Calcination of MgO

Eubank (1951) stated that calcination conditions of MgO determine its degree of reactivity, and solubility, by affecting particle size, porosity, lattice structure, and recrystallization. Eubank (1951) also pointed out that while the particle size increases, porosity and reactivity decrease by sintering and recrystallization processes for calcination temperatures higher than 900 °C. Therefore, it was important to study the influence of the calcination temperature and duration on the reactivity of the MgO used in the study presented here. Wagh and Jeong (2003) also performed some tests to study the effects of calcination on morphology and acid solubility of MgO powder by comparing uncalcined MgO powder with that calcined at 1300 °C. In Figure 2.2, one can see that the intensity of the magnesia X-

ray diffraction peak is higher and the peak is sharper for the calcined MgO, which indicates recrystallization.

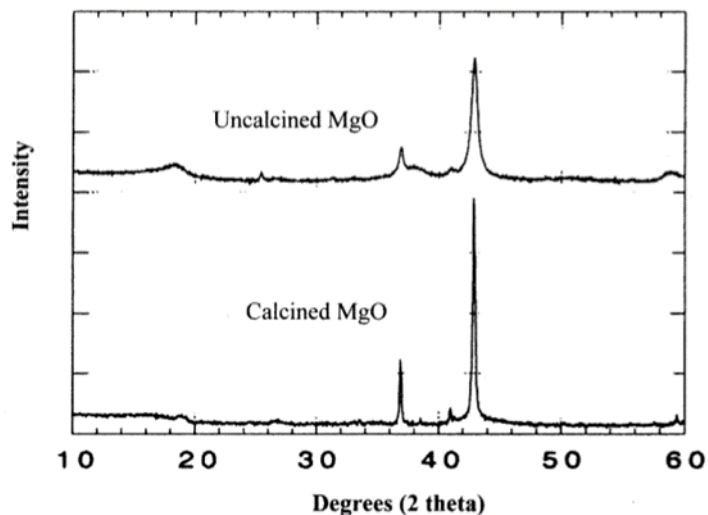


Figure 2.2 X-ray diffraction patterns of uncalcined and calcined MgO (Wagh and Jeong, 2003)

Figure 2.3 provides a comparison of the solubility of MgO powder in 50 % phosphoric acid solution before and after calcination. The slower increase in pH clearly shows that calcination slows down the neutralization rate of acid due to the lower reactivity of the MgO powder.

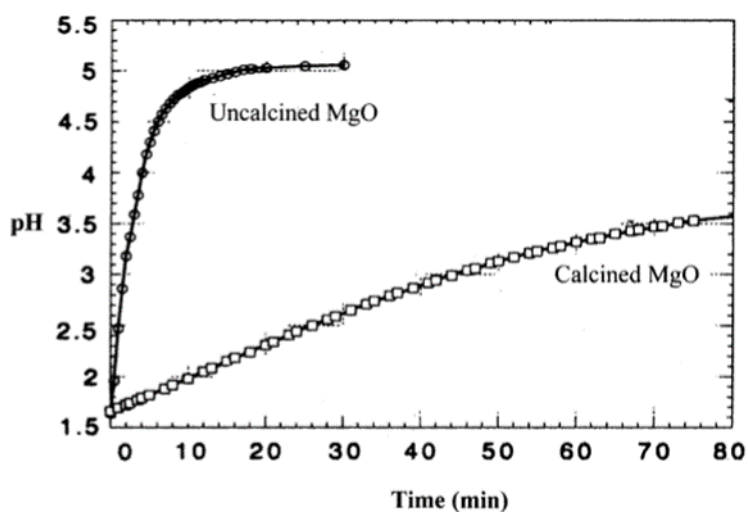


Figure 2.3 Change in the pH of an  $H_3PO_4$  solution with uncalcined and calcined MgO powders (Wagh and Jeong, 2003)

Li et al. (2014) studied the effect of calcination temperature on the particle size distribution and surface texture of magnesia powder which directly influence reactivity. Figure 2.4 shows the particle size distribution of magnesia powders calcined at different temperatures measured using laser diffraction. As the calcination temperature increases, the amount of finer particles decreases which result in a less reactive powder due to the decrease in surface area.

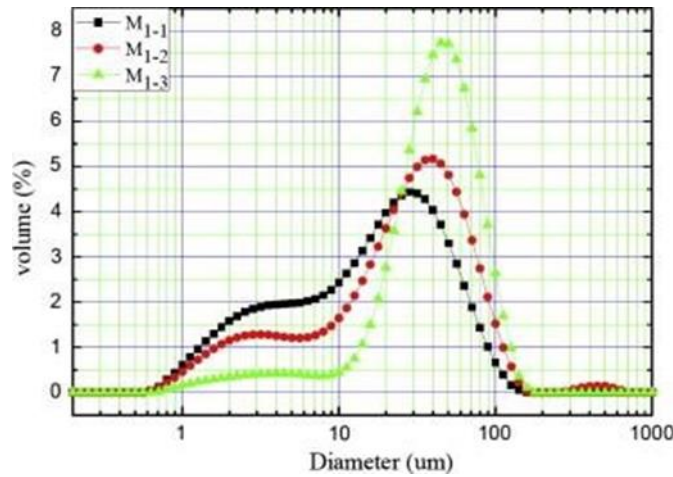


Figure 2.4 Influence of calcination temperature on particle size distribution, M<sub>1-1</sub>: original sample, M<sub>1-2</sub>: calcined at 1000 °C, M<sub>1-3</sub>: calcined at 1200 °C (Li et al., 2014)

Figure 2.5 shows the effect of different calcination temperatures on the surfaces of magnesia particles. Since the reaction starts on the particle surface, the reactivity of the sample is directly related to the change in surface texture.

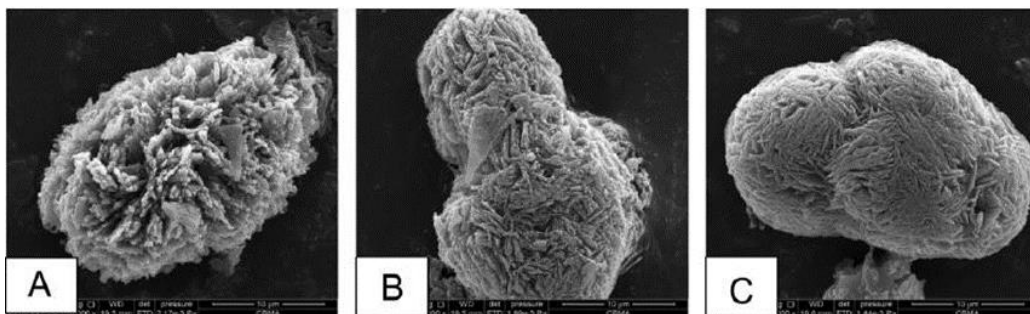


Figure 2.5 Surface state of magnesia particles: A) original state, B) calcined at 1200 °C, C) calcined at 1600 °C (Li et al., 2014)

Wang et al. (2013) investigated the effects of different calcination temperature on the setting times of the prepared magnesium phosphate cement pastes. Since setting time is directly related to the rate of reaction, it represents the effect of calcination on reactivity. Figure 2.6 shows the change in setting time for different paste samples prepared with the magnesia powder calcined at different temperatures. As the calcination temperature increases, the setting times also increase, which indicates that the reactivity of the powder reduces with the increase in calcination temperature.

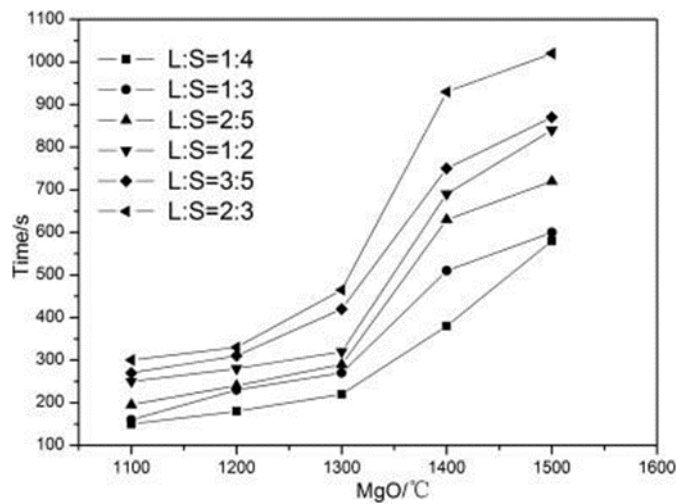


Figure 2.6 The influence of calcination temperature on the setting time of the paste samples with different liquid-to-solid ratios (L:S indicates liquid-to-solid ratio) (Wang et al., 2013)

### 2.2.1.3 Using Boric Acid or Borax

In addition to calcination of MgO powder, which causes some physical changes, using certain chemical additives as retarders is another way to control the overall reaction. In general, boron compounds, such as boric acid or borax, have been used to lower the rate of the fierce acid-base reaction by controlling the solubility of MgO to get enough time to work with the mixture more easily (Chau et al., 2011). Some studies in the literature discuss the reaction mechanism when these compounds are added to the system. It is basically described as the formation of an

amorphous coating around MgO particles preventing their continuous reaction with the phosphate ions (Mestres and Ginebra, 2011). As the pH of the system increases, the amorphous coating starts to dissolve which exposes the MgO particles to the dissolved phosphate ions after some delay (Wagh and Jeong, 2003). Although it is convenient to have a sufficiently long working time with the mixture, using this type of retarders gives rise to a decrease in the early mechanical strength and an increase in price (Tan et al., 2016). Thus, it is important to minimize the quantity of boron compounds used to make this type of cement useful for practical applications. Also, borax has been reported to be preferable for both academic studies and the commercial applications due to its easy storage and effectiveness (Liu and Chen, 2016).

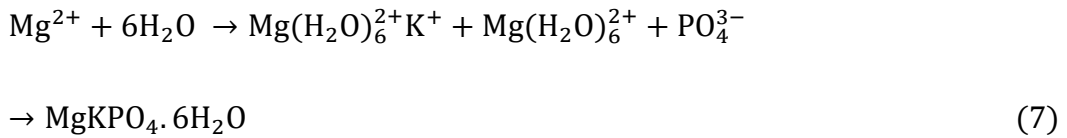
### **2.2.2 Types of Magnesium Phosphate Cement**

Based on the acid phosphate salt used, several types of magnesium phosphate cements exist. Commonly used acid phosphates are ammonium dihydrogen phosphate ( $\text{NH}_4\text{H}_2\text{PO}_4$ ), potassium dihydrogen phosphate ( $\text{KH}_2\text{PO}_4$ ) and sodium dihydrogen phosphate ( $\text{NaH}_2\text{PO}_4$ ). The corresponding types of cement are called magnesium ammonium phosphate cement (MAPC), magnesium potassium phosphate cement (MKPC) and magnesium sodium phosphate cement (MNPC). It is known that there are some problems with the use of MAPC and MNPC. For the former, one problem is the emission of ammonia leading to container corrosion and unpleasant environmental odor (Li and Chen, 2013; Li et al., 2016; Lai et al., 2016). For the latter, the problem is that the end product has an amorphous structure (Mestres and Ginebra, 2011; Hou et al., 2016). Because of these problems, MKPC is the most widely used type of MPC.

### **2.2.3 Magnesium Potassium Phosphate Cements (MKPC)**

The main raw materials for MKPC production are dead-burned magnesia powder (MgO), potassium dihydrogen phosphate ( $\text{KH}_2\text{PO}_4$ ) and a small amount of borax. The major reaction occurs between MgO and  $\text{KH}_2\text{PO}_4$ , which results in the main product called K-struvite ( $\text{MgKPO}_4 \cdot 6\text{H}_2\text{O}$ ) showing properties similar to the

mineral struvite (Zang et al., 2017). Ding et al. (2012) defined the reaction process by the following equations:



There are several factors that affect the properties of MKPC pastes and mortars such as setting time, compressive strength and microstructure. Some of these factors are water-to-binder ratio (W/B), magnesium-to-phosphate molar ratio (M/P), borax content and sand-to-binder ratio (S/B).

### **2.2.3.1 Influence of Water Content on the Properties of MKPC**

Similar to other traditional cementitious materials, water content plays a crucial role in forming desired end products of MKPC pastes and mortars. It affects several properties like setting time, compressive strength and microstructure.

Li and Chen (2013) studied the effects of water content on the setting time of MKPC paste for the range of W/B from 0.14 to 0.30 and an increase from almost 5 to 35 minutes was reported (Figure 2.7). Also, Wang et al. (2013) studied setting time with very small samples of MKPC pastes for a wider W/B range, from almost 0.25 to 0.65 and reported that there is an increase in the setting time from almost 10 to 16 minutes with the increasing W/B ratio. On the other hand, Qiao (2010) studied

the effect of lower W/B ratios on the setting time for a small range, from 0.105 to 0.135, with M/P = 12 and borax content of 5 %, and reported that all the samples prepared in that range are not affected by water content having setting time around 9 minutes. Therefore, it can be concluded that a sufficient increase in W/B, for a wider range, results in an increase in setting time.

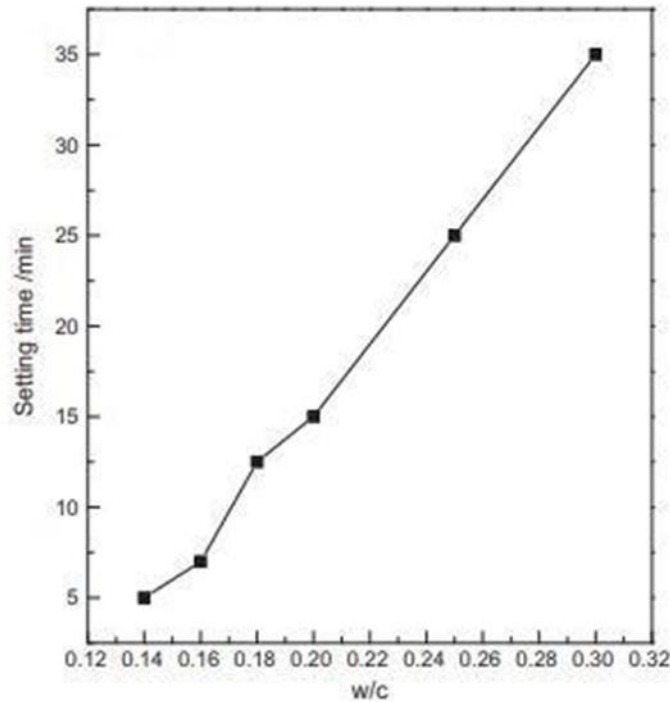


Figure 2.7 Influence of W/B on setting time for MKPC pastes (Li and Chen, 2013)

Although the increase in water content is preferable for field applications due to the increase in the setting time, there is an inverse relationship between the increasing water content and compressive strength, especially at late ages. The reason is that the excess water gives rise to an increase in porosity resulting in poor mechanical properties. There exist some studies which show the adverse effect of increasing water content on the compressive strength of MKPC pastes. Li and Chen (2013) studied the effect of increasing W/B from 0.14 to 0.20 and reported that the compressive strength of the samples, at 24 h, decreased from almost 52 to 40 MPa. They also reported that at an earlier age, 3 h, compressive strength increases from

almost 40 to 50 MPa with the increasing W/B from 0.14 to 0.16, which is explained by a problem in workability (Figure 2.8).

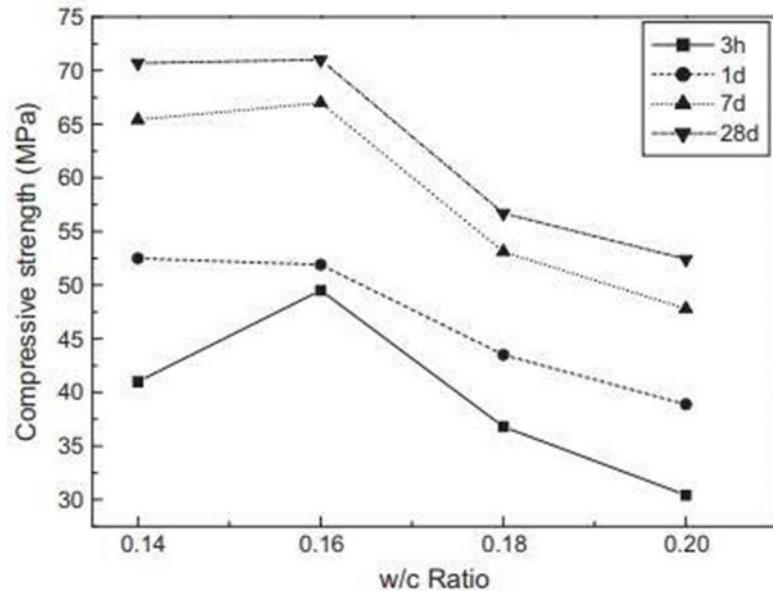


Figure 2.8 Influence of W/B ratio on compressive strength of MKPC pastes. (Li and Chen, 2013)

Wang et al. (2013) studied the effect of water content for a wider range of W/B from almost 0.15 to 0.35 and reported an adverse effect on compressive strength at 24 h. There is insufficient information in the literature about the effect of water content on the mineralogical evolution based on the XRD test results. Wang et al. (2013) studied this effect for a range of W/B from almost 0.15 to 0.35 and reported that the decrease in water content after a certain point results in amorphous K-struvite formation. This was explained by a lack of time for crystal formation due to the increase in supersaturation rate. Figure 2.9 represents the effect of water content on reaction product development.

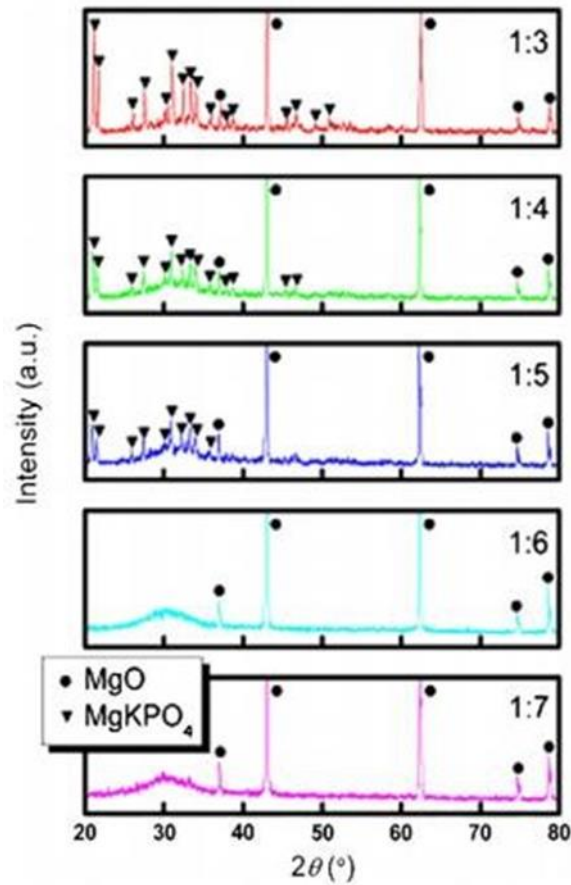


Figure 2.9 The effect of  $\text{H}_2\text{O} : \text{MgO}$  on the X-ray diffraction patterns of pastes (Wang et al., 2013)

It is clear that the decrease in water content, after some point, results in amorphous structure.

### 2.2.3.2 Influence of M/P Ratio on the Properties of MKPC

M/P is another important parameter that controls the reaction rate. Therefore, it affects some properties of the MKPC products like setting time, compressive strength and microstructure. There exist several studies in the literature investigating the effects of the M/P on these properties.

Qiao (2010) investigated the pH change of pastes and reported that as M/P increases, the pH of the system increases which results in the faster reaction. Therefore, it can be expected that an increase in M/P would result in a decrease in

setting time. Rouzic et al. (2017) investigated the effects of a wide range of M/P, from 1 to 10, on the setting time of MKPC pastes and found that the setting time decreases from almost 30 minutes to 5 minutes as the M/P increases for that range (Figure 2.10). Zhang et al. (2017) also reported that an increase in M/P shortens the setting time.

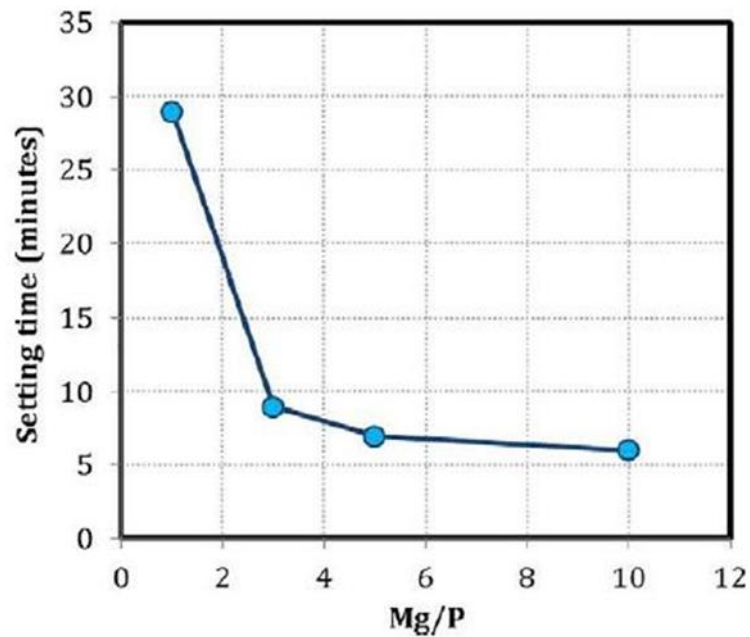


Figure 2.10 The effect of Mg/P ratio on setting time for MKPC pastes (Rouzic et al., 2017)

Li et al. (2014) studied the effects of M/P, from 3 to 6, on the compressive strength of the MKPC paste samples of 40-mm cubes. As M/P increased, the compressive strength increased from almost 20 to 35 MPa for 1 day of curing (Figure 2.11).

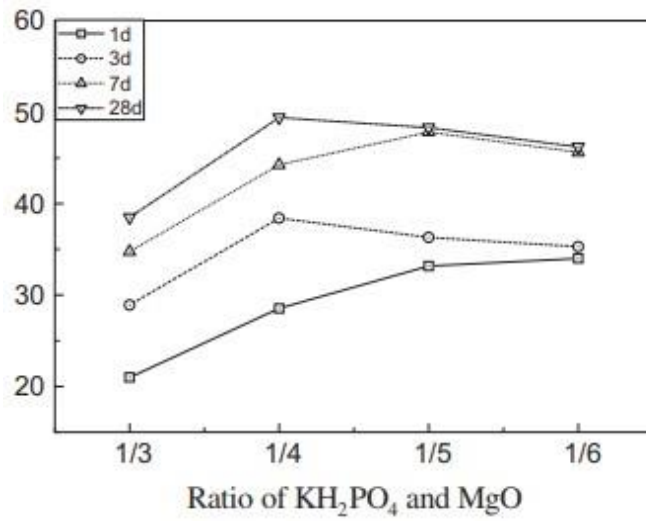


Figure 2.11 The effect of phosphate to magnesium oxide molar ratio on compressive strength (Vertical axis shows compressive strengths in MPa) (Li et al., 2014)

A cracked and less compact structure can explain the lower compressive strength obtained for the case of M/P of 3 compared to the one with M/P of 5 (Figure 2.12).

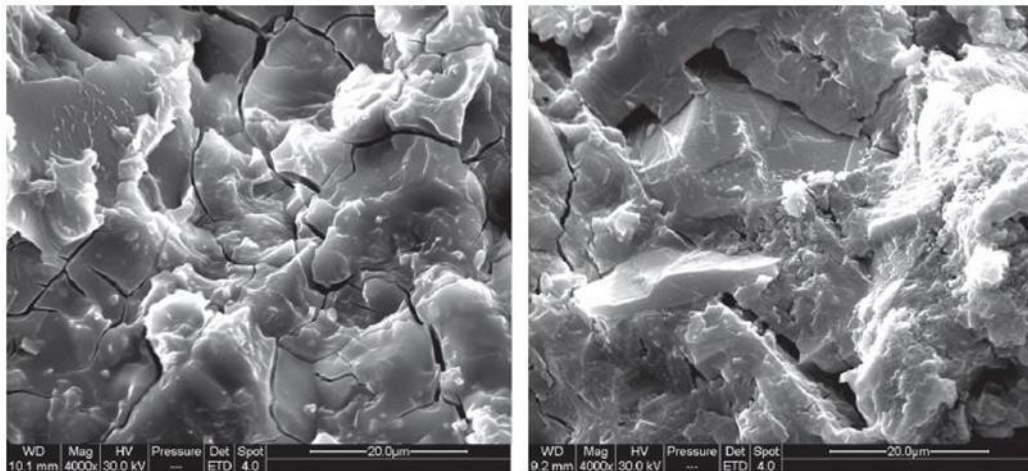


Figure 2.12 SEM images at 28 d of paste samples with M/P of 3 (left) and 5 (right) (Li et al., 2014)

Rouzic et al. (2017) also studied the effects of M/P on the compressive strength of 40x40x160 mm prisms, for a wider range of M/P (1, 3, 5 and 10) at a fixed W/B of 0.20. Figure 2.13 shows that maximum strength is achieved at M/P = 5.

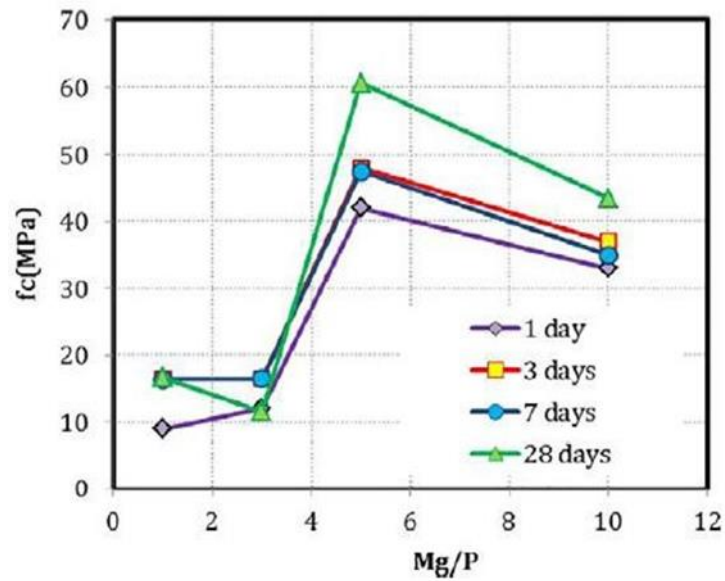


Figure 2.13 The effect of Mg/P ratio on the compressive strength of MKPC pastes (Rouzic et al., 2017)

The reasons for lower compressive strength at lower M/P ratios are explained as the increase in the amount of  $\text{KH}_2\text{PO}_4$  which has poorer mechanical properties than the reaction product of its reaction with MgO and the poor adhesion between the hydrated products and  $\text{KH}_2\text{PO}_4$  particles, which can be seen in Figure 2.14.

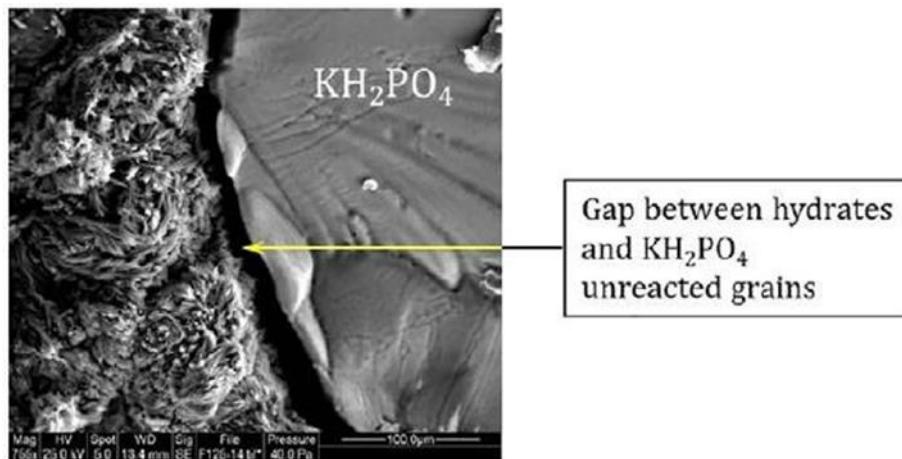


Figure 2.14 SEM image of the  $\text{KH}_2\text{PO}_4$  - reaction product interface for M/P=1 (Rouzic et al., 2017)

Wang et al. (2013) stated that while lower M/P results in low compressive strength due to the higher amount of the weak phase  $\text{KH}_2\text{PO}_4$ , higher M/P ratios give rise to lower compressive strengths due to a decrease in the amount of reaction products. Hence a balance between the two reactant powders is crucial.

### 2.2.3.3 Influence of Borax Content

Borax content plays a crucial role in decreasing the rate of reaction which is directly related to some properties of the MKPC samples like setting time, compressive strength and microstructural evolution. There exist some studies about the effects of borax content on these properties.

Qiao (2010) investigated the effects of borax content, for the range of 2.5 to 10 %, with a fixed M/P = 8, on setting time and compressive strength of MKPC pastes. Setting time increased from 6.5 to 26 minutes with the increase in borax content. It was stated that the earlier compressive strengths were adversely affected by increasing borax content at earlier ages while there was no significant change in the late strengths obtained at 28 day of curing (Figure 2.15).

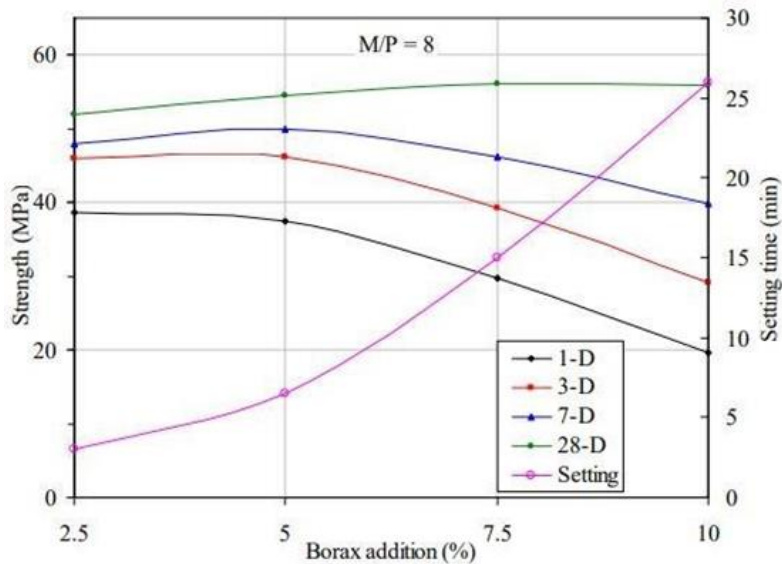


Figure 2.15 Effect of borax content on the setting time and compressive strength of MKPC pastes (Qiao, 2010)

Yang and Qian (2010) studied the effects of borax content on the microstructural evolution of MKPC pastes using XRD and SEM. They found that XRD showed a decrease in the diffraction peaks of the hydration product, with an increase in borax content from 5 to 12.5 %, giving rise to a poorer structure. SEM images showed that increasing borax contents from 5 to 12.5 % resulted in a hardened MKPC paste that has a looser microstructure with more cracks and defects.

#### **2.2.3.4 Influence of S/B Ratio**

Sand is used in MKPC mortars as an inert filler material to reduce costs and increase soundness. Since both the high heat of hydration and cost of MKPC are very important factors that make this type of cement hard to use as an alternative structural material, it is crucial to incorporate as much sand into the system as possible. Sand content influences some properties of MKPC mortars like setting time and compressive strength which are critical to obtain a desirable end product.

Qiao et al. (2010) stated that an increase in sand content results in less workable mortars with lower setting time. Qiao (2010) studied the effects of sand content on the compressive strength of the mortar samples with different M/P ratios, 8, 10 and 12 and reported that the increase in sand content results in lower compressive strength values. Figure 2.16 shows the effect of sand content on compressive strength.

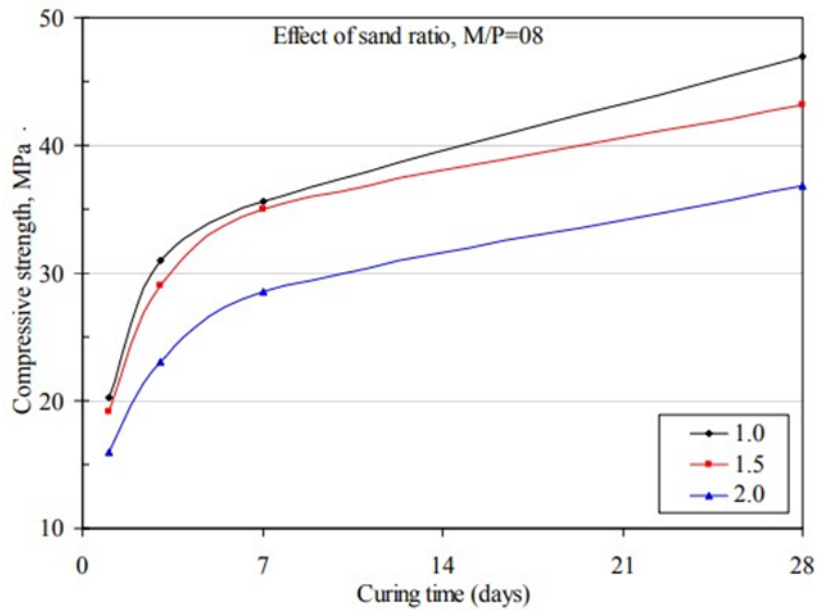


Figure 2.16 The effect of sand ratio on compressive strength of MKPC mortars (1.0-1.5 and 2.0 are S/B ratios) (Qiao, 2010)

It is observed that increasing S/B beyond 1.5 negatively impacts strength gain.

### 2.3 Incorporating Fly Ash in MKPC

One of the major drawbacks of MKPC products is their poor water resistance. Incorporating industrial wastes, especially fly ash, is a widely used way of improving the water stability problem. The basic idea is that the fine particles of fly ash fill in the pores of the hardened MKPC paste resulting in a less porous structure. Moreover, the use of fly ash is very important to get more economical MKPC products. The usage of fly ash can also influence some properties of MKPC mortars like setting time and compressive strength. There are some studies about the effects of using fly ash in MKPC system.

Li and Chen (2013) studied the influence of fly ash replacement up to 60 % and stated that this replacement increased setting time and compressive strength at later ages and improved water stability. Li et al. (2015) also stated that the fly ash replacement of 20 % for a MKPC mortar with M/P = 4 resulted in an increase in compressive strength.

## CHAPTER 3

### MATERIALS AND EXPERIMENTAL PROCEDURE

#### 3.1 Introduction

The materials used and the experimental procedure followed are presented in this chapter. Except for the X-ray fluorescence spectroscopy (XRF), scanning electron microscopy (SEM), and thermal gravimetric and differential thermal analysis (TGA-DTA) tests performed at METU Central Laboratory, all experiments conducted in the Materials of Construction Laboratory of the Department of Civil Engineering, METU.

#### 3.2 Materials

All materials used in this study, except the mixing water and sand, were either already in powder form or ground into a powder. For these materials, specific gravity and specific surface area were determined according to the related standards: ASTM C188 (2017) and ASTM C204 (2017), respectively.

##### 3.2.1 Magnesia Powder

Low-grade magnesia powder with an unknown calcination history was obtained from OSA Foreign Business in Ankara, Turkey. Its specific gravity and fineness (Blaine) were determined as  $\sim 3.10$  and  $\sim 11000 \text{ cm}^2/\text{g}$ , respectively. The compound composition of this powder, determined by XRF, is given in Table 3.1. This powder was later used to obtain the calcined powder samples.

Table 3.1 Oxide analysis of the magnesia powder used, determined with XRF.

Oxide	Mass (%)
MgO	81.30
SiO <sub>2</sub>	9.35
CO <sub>2</sub>	6.89
CaO	1.74
Fe <sub>2</sub> O <sub>3</sub>	0.60
NiO	0.12
Al <sub>2</sub> O <sub>3</sub>	0.06

It is clear that the purity of the MgO powder is around 80 %. A low cost, low purity MgO was intentionally chosen to obtain results for a viable MKPC. It also contains almost 10 % SiO<sub>2</sub>.

### 3.2.2 Dead-burned Magnesia Powder

Dead-burned magnesia powder was produced by calcining the magnesia powder at 1500 °C for one hour in a high-temperature tube furnace. For this process, it was not possible to place the magnesia powder directly into the furnace since the powder would stick to the surface of refractory material inside the furnace. Therefore, the magnesia powder was put into aluminum oxide crucibles, with a volume of 0.4 L each. The furnace and the crucibles before the calcination process can be seen in Figure 3.1.



Figure 3.1 The crucibles placed in the furnace (the top diameter of the crucible is almost 10 cm)

Upon heating and cooling the calcined magnesia powder was observed to have fused into a hard mass. It was ground for half an hour in a laboratory ball mill. The specific gravity and specific surface area for the powder were determined as  $\sim 3.42$  and  $\sim 3100 \text{ cm}^2/\text{g}$ , respectively. Hence the calcination process slightly increases the density of the material the oxide composition of the calcined MgO powder is given in Table 3.2.

Table 3.2 Oxide analysis of the dead-burned magnesia powder used, determined with XRF

Oxide	Mass (%)
MgO	82.80
SiO <sub>2</sub>	10.60
CO <sub>2</sub>	3.82
CaO	1.85
Fe <sub>2</sub> O <sub>3</sub>	0.72
NiO	0.13
Al <sub>2</sub> O <sub>3</sub>	0.08

It can be seen that calcination does not change the oxide composition of the powder significantly except for a decrease in the amount of CO<sub>2</sub> indicating decarbonation

of some minerals during calcination. This powder was used as the basic component in the magnesium potassium phosphate cement pastes and mortars.

### **3.2.3 Monopotassium Dihydrogen Phosphate**

Monopotassium dihydrogen phosphate ( $\text{KH}_2\text{PO}_4$ ) is generally produced by the reaction between diluted phosphoric acid solution and one of the following: potassium hydroxide, potassium carbonate or potassium chloride. This process is considered as the partial neutralization of the phosphoric acid solution since two of the three original H atoms in the acid remain after reaction. This acid phosphate salt was obtained in crystalline powder form from Kimetsan Production and Research & Development Center, in Ankara, Turkey. It was ground for 10 minutes in the laboratory ball mill. Its specific gravity and specific surface area were determined as  $\sim 2.40$  and  $\sim 2300 \text{ cm}^2/\text{g}$ , respectively. This powder was used as the acid component for the magnesium potassium phosphate cement pastes and mortars.

### **3.2.3 Sodium Tetraborate Decahydrate**

Sodium tetraborate decahydrate, generally known as borax, was already available in the laboratory. It was sieved through an ASTM No.100 sieve to get a more uniform powder. Its specific gravity and specific surface area were determined as  $\sim 1.80$  and  $\sim 2000 \text{ cm}^2/\text{g}$ , respectively. This powder was used as the set retarder, for the magnesium potassium phosphate cement mixtures.

### **3.2.4 Fly Ash**

Fly ash from Çatalağzı Thermal Power Plant was already available in the laboratory. Its specific gravity and specific surface area were determined as  $\sim 2.00$  and  $\sim 3500 \text{ cm}^2/\text{g}$ , respectively. The oxide composition for this material is given in Table 3.3. It was used to partially replace the calcined MgO in the magnesium potassium phosphate cement mixtures to cope with both water stability issues and to lower cost as much as possible.

Table 3.3 Oxide analysis of the fly ash used, determined with XRF

Oxide	Mass (%)
SiO <sub>2</sub>	42.70
Fe <sub>2</sub> O <sub>3</sub>	20.70
Al <sub>2</sub> O <sub>3</sub>	16.40
K <sub>2</sub> O	8.91
CaO	5.43
TiO <sub>2</sub>	3.21
P <sub>2</sub> O <sub>5</sub>	1.42
MgO	0.51
SO <sub>3</sub>	0.43
MnO	0.23

Since the total amount of SiO<sub>2</sub>, Fe<sub>2</sub>O<sub>3</sub> and Al<sub>2</sub>O<sub>3</sub> is higher than 70 %, this fly ash can be considered as Class F in accordance with ASTM C618 (2017).

### 3.3 Experimental Procedure

The experimental procedure followed in this study can be divided into three major categories as follows:

- 1) Development of a suitable calcination process for the magnesia powder,
- 2) Determination of suitable mixture proportions for the MKPC pastes and mortars,
- 3) Incorporation of the fly ash into the MKPC system.

#### 3.3.1 Determination of the Calcination Process for the Magnesia Powder

Magnesia powder was calcined for one hour at different temperatures ranging from 600 to 1500 °C. For these samples, the color gradually changed from light pink to dark yellow as the calcination temperature increased. Also, at 1100 and 1200 °C, the powder sample became lumpy, and at even higher temperatures, the powder samples were transformed into a hard mass. The physical changes mentioned are

shown in Figure 3.2. The physical and chemical properties of the calcined samples were compared to study the effect of calcination on the magnesia powder.

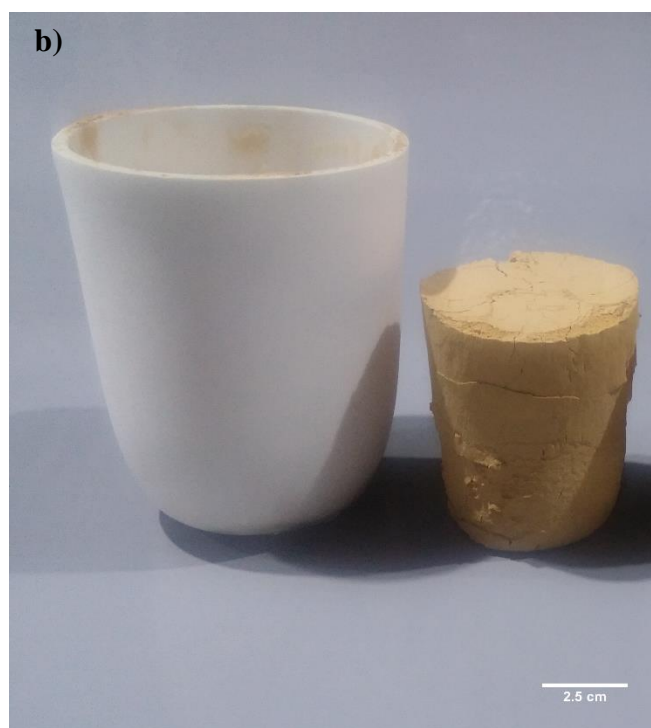


Figure 3.2 Calcined samples: a) change in color (left to right – uncalcined, 600 °C, 1200 °C, 1300 °C, 1500 °C); b) The hard mass obtained (crucible - left, sample - right)

### **3.3.1.1 Influence of calcination on physical properties**

Influence of calcination on physical properties was analyzed in terms of the changes in specific gravity and specific surface area of the calcined powder samples. The specific gravities of the samples were determined using a Le Chatelier flask in accordance with ASTM C188 (2017). The specific surface area values of the samples were determined using a Blaine air permeability apparatus in accordance with ASTM C204 (2017).

### **3.3.1.2 Influence of calcination on the oxide composition**

Influence of calcination on the oxide composition investigated with XRD and XRF to observe possible changes in microstructure and chemical composition.

### **3.3.1.3 Influence of calcination on setting time of MKPC pastes**

Magnesium potassium phosphate cement paste samples, very small in size, were prepared using the calcined magnesia to evaluate the effects of calcination on workability and setting time. Two different magnesium-to-phosphate molar ratios (M/P) of 1 and 2 were used, and water-to-binder ratio (W/B) was selected as 0.20 for both cases. While it was not possible to get workable mixtures for the samples prepared with the calcined samples from 600 to 1200 °C (as they were still too reactive), the samples prepared using the calcined magnesia samples at higher temperatures were sufficiently workable. A failed mixture representative of those prepared with the magnesia samples burnt at temperatures less than or equal to 1200 °C is given in Figure 3.3. These samples set while still mixing and could not be made into a monolithic specimen.



Figure 3.3 A MKPC paste made with a low-temperature calcined MgO, dry and crumbly (image width is approximately 10 cm)

Furthermore, setting time was determined for the MKPC paste samples prepared with the magnesia powders calcined at 1300, 1400 and 1500 °C. After deciding on a suitable calcination temperature as 1500 °C, the duration of calcination was determined again by setting time tests for paste samples. 1, 2 and 3 h were chosen as the calcination times. For the setting time test, magnesia and monopotassium dihydrogen phosphate powders were mixed intimately, and then water was added to the system which was mixed with a scraper for about 60 s. The setting time was measured using the Vicat needle (ASTM C191, 2018) as the time passed from the addition of water to the point where the needle did not leave an impression on the sample surface.

### **3.3.2 Determination of the Mix Proportions for the MKPC**

It is crucial to select proper mixture proportions to get a desirable end product in terms of workability, durability, and economy. The mix proportions for the MKPC system were determined through several steps as follows:

- 1) Determination of water-to-binder (W/B) ratio and magnesium-to-potassium molar ratio (M/P) by conducting setting time and compressive strength tests on the paste samples.
- 2) Determination of the borax content for the paste sample with the determined mix proportion in the previous step.
- 3) Determination of the sand-to-binder (S/B) ratio for the MKPC mortar to get a suitable end product.

#### **3.3.2.1 Setting time test for MKPC paste with different M/P and W/B ratios**

Setting time was measured for MKPC pastes with M/P of 3, 4, 5 or 6 and with W/B of 0.12, 0.14, 0.16, 0.18 and 0.20. The test procedure was as follows: Mixing the powders to ensure homogeneity as much as possible, adding water and then mixing the blend for about 60 s with a scraper, and determination of the setting time with the Vicat apparatus. It was very hard to work with the pastes with W/B of 0.12 and 0.14, but it became easier for the samples with higher W/B. Indeed, for W/B ratio of 0.20, the mixture was very fluid, with the consistency of soup.

#### **3.3.2.2 Compressive strength of MKPC pastes with different M/P and W/B ratios**

Compressive strength was determined for MKPC pastes with M/P of 3, 4, 5 or 6 and with W/B of 0.14, 0.16, 0.18 and 0.20. Since it was very hard to get a workable mixture, W/B ratio of 0.12 was not used for the compressive strength test mixtures. The mixing procedure was the same as that used for the setting time test. The pastes were cast into the 50-mm cubic molds at once, and hand tamped 50 times. Two cube samples were cast from each mixture. The samples were cured at ambient temperature for 1, 3, 7, and 24 h and were tested with a Universal Testing Machine, with a capacity of 250 kN, at a loading rate of 1.5 kN/s. Two samples were used to determine compressive strength at each age, and their average was taken. Also, XRD was performed on samples taken from a corner of the crushed cube samples for each curing time to observe changes in microstructure and mineralogy.

Since the specimen stuck to the inner surface of the mold, some problems occurred when removing the molds. In order to overcome this problem, several trials were made using different types of grease or placing a liner made by a thin acetate paper. Among these, placing a liner and using lithium grease gave better results. Since there was a problem with the use of liner for high W/B ratios, it was decided that the use of lithium grease on the molds was the best option.

### **3.3.2.3 Determination of the suitable borax content for MKPC pastes**

The next step was to determine the borax content needed to sufficiently retard the setting of the paste, with the selected M/P and W/B. The borax content was determined by investigating the effects on setting time and compressive strength for the pastes prepared with several borax contents taken as weight percentage of the magnesia powder. Setting time was measured for samples with 0, 1.0, 2.5, 5.0, 7.5 and 10.0 % borax following the procedure described in Section 3.3.1.3. For the compressive strength test, following the same procedure, samples with 0, 5 and 10 % borax were prepared. All samples were cured at ambient temperature and tested for compressive strength at 3 h and 7 d to study the effects on both the early and the late strength values. Since MKPC is an acid-base system, reactions and strength gain is rapid (compared to Portland cement systems, for example, and 7 d can be considered a later age). Also, XRD was performed on the samples for each curing time to observe the effects of borax content on the microstructure.

### **3.3.2.4 Determination of a suitable sand-to-binder (S/B) ratio for MKPC mortars**

A suitable sand-to-binder ratio was determined by investigating the workability and compressive strength of several mortar samples prepared with different S/B of 1.25, 1.50 and 1.75, by mass. For the compressive strength test, the mixing procedure was: Mixing of the dry powders to get the required homogeneity, addition of water and subsequently stirring the mixture for 30 s at moderate speed, and addition of sand to the system which was mixed for another 30 s, at moderate speed for the first half and at high speed for the second half. The mortar was cast into cubic molds,

and the samples were demolded after 1 h and then cured at ambient temperature as described in previous sections. The mortars were placed in two stages by hand tamping for 25 times after each stage due to their lower workability. The cured samples were tested for compressive strength at 1, 3 and 7 d. Also, about the workability, it can be said that the increase in S/B resulted in a less workable mortar. While it was easy to cast the sample with the S/B 1.25, it was very hard for the samples with S/B = 1.75.

### **3.3.3 Incorporation of Fly Ash into MKPC Mortars**

The effects of replacing calcined MgO and potassium dihydrogen phosphate in the MKPC mortars with fly ash at several dosages was investigated by measurement of workability, compressive strength and water stability of MKPC mortar mixtures. Three MKPC samples with 0, 10 and 20 % fly ash were used. The mix proportions for the mortar samples were taken as the ratios determined in Section 3.3.2.4. As the fly ash content increased the workability decreased. For the compressive strength test, by following the same procedure in the previous case exactly, the effects of different fly ash contents were analyzed in terms of both the early and the late strength by considering the strength values at 1, 7 and 28 d. For the water stability test, the samples air-cured for 28 d were immersed in water. After 1, 7 and 28 d in water, the retained strength of the samples was determined and compared with the reference mortar sample.

### **3.3.4 Thermogravimetric / Differential Analyses (TGA-DTA) Investigation on MKPC Pastes**

Several paste samples were prepared to investigate the influence of M/P and fly ash content on the properties of MKPC. The tests were performed on the samples cured at ambient temperature for 5 d.

### **3.3.5 Scanning Electron Microscopy (SEM) Investigation on MKPC Pastes**

Several paste samples prepared to investigate the influence of M/P and fly ash content on morphology of MKPC. The tests were performed on the samples cured at ambient temperature for 14 d.

## **CHAPTER 4**

### **RESULTS AND DISCUSSION**

#### **4.1 Introduction**

This chapter presents the analysis of the experimental work performed to investigate the effects of calcination on the magnesia powder, the effects of mixture proportioning on the properties of reaction products of MKPC, and the effects of incorporating fly ash into the system.

#### **4.2 Analysis of the Effects of Calcination on the Magnesia Powder**

The analysis of the effects of calcination is presented considering the changes in the properties of the magnesia powder such as specific gravity, specific surface area, microstructure, and reactivity.

##### **4.2.1 Changes in Specific Gravity**

The changes in specific gravity of the magnesia powder with calcination can be seen in Figure 4.1. As the calcination temperature increases, the specific gravity of the powder increases, from ~3.10 to ~3.50 at 1500 °C. There is a sharp change in specific gravity from the uncalcined powder to the powders calcined at 600 and 800 °C. After that, there is a slight or even no change in between 800 and 1200 °C. Beyond 1200 °C, there is again a continuous increase up to 1500 °C (the limit of the furnace). Eubank (1951) reported that the increase in calcination temperature

results in some decrease in the porous structure and also an increase in particle size for the magnesia samples calcined at the temperatures ranging from 500 to 900 °C, making the powder denser. Also, it was reported in the same study that for temperatures above 900 °C, the powder becomes even denser due to sintering process.

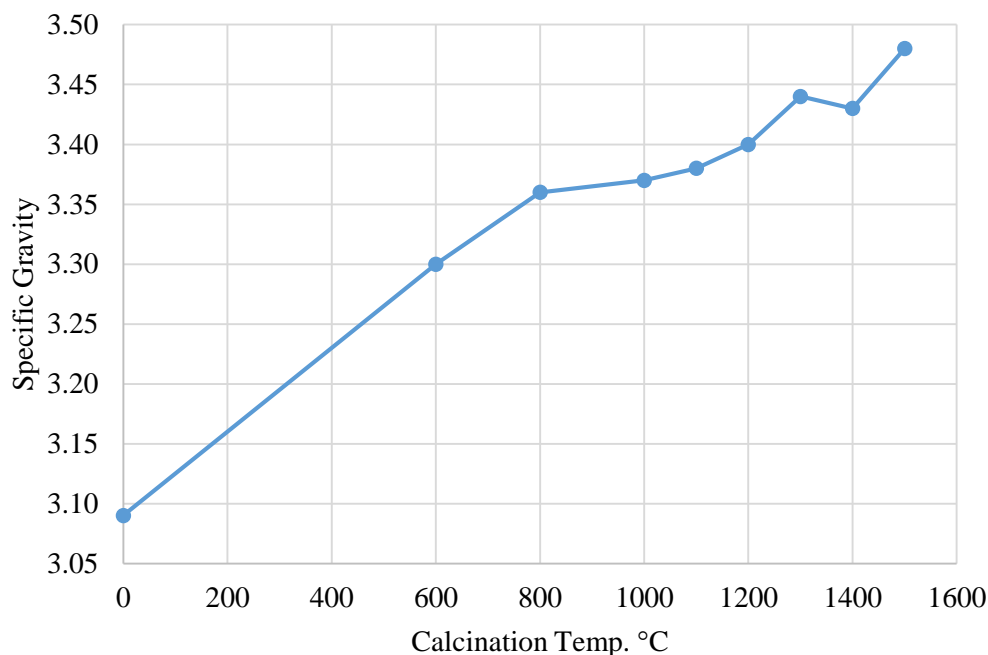


Figure 4.1 The influence of calcination on the specific gravity of the magnesia powder

Additionally, the mass loss after each calcination temperature measured after cooling to room temperature is provided in Table 4.1. The abrupt change in the specific gravity of the sample from 3.10 to 3.30 can be explained by the mass loss due to the evaporation of the lighter compounds upon calcining at 600 °C. Another point that can be supported by this mass loss issue is the sintering process. Although there is no significant change in the mass loss upon calcination beyond 1000 °C, the specific gravity of the powders increases.

Table 4.1 The percent mass loss of magnesia powder after calcination

Calcination Temperature (°C)	Mass Loss (%)
600	5.70
800	6.00
1000	6.60
1100	6.70
1200	6.70
1300	6.85
1400	6.90
1500	7.00

#### 4.2.2 Changes in Specific Surface Area

In Figure 4.2, the changes in specific surface area of the magnesia powder with calcination can be observed. As the calcination temperature increases the fineness remains almost the same up to 800 °C. After that point, the fineness starts to decrease with the increase in calcination temperature. The fineness value changes from ~12000 to ~6000 cm<sup>2</sup>/g starting from the uncalcined sample to the calcined sample at 1200 °C. Beyond that limit, the fineness values obtained for the samples calcined at 1300, 1400 and 1500 °C are ~2000 cm<sup>2</sup>/g, which is a very low value when compared with the other samples, but these samples were ground before testing for the fineness. Therefore, the decrease in the specific surface area can be explained by the increase in the particle size upon increasing calcination temperature (Li et al., 2014).

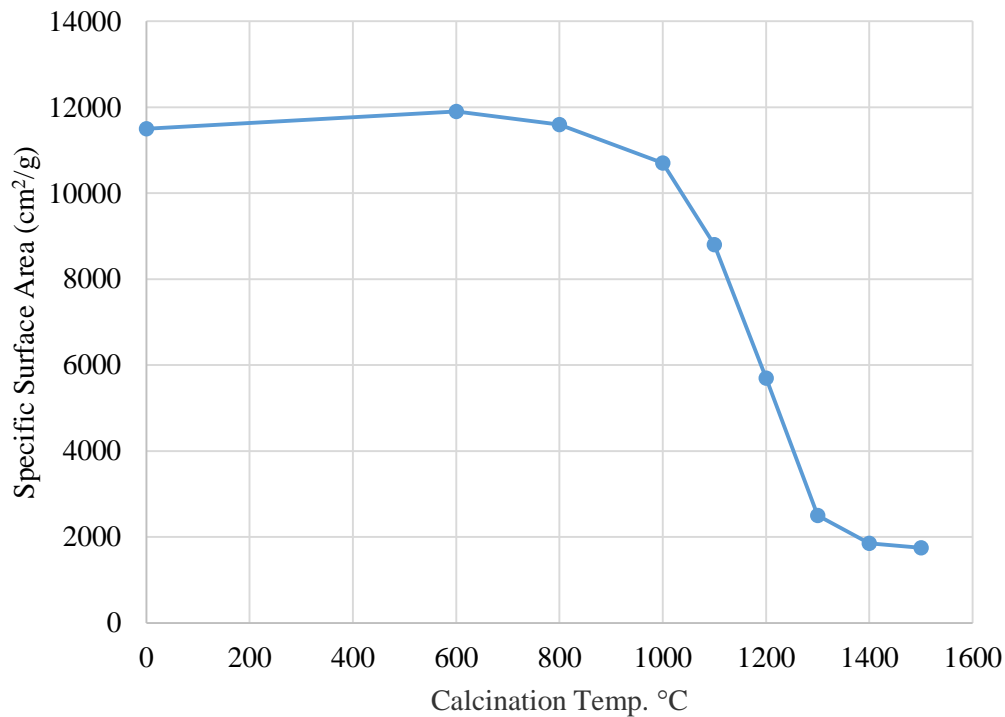


Figure 4.2 The influence of calcination on the specific surface area of the magnesia powder

#### 4.2.3 Changes in Microstructure

In Figure 4.3, the X-ray diffraction (XRD) test results, representing the changes in mineralogy with calcination, can be seen. For the uncalcined sample, the main peak at  $\sim 42.5$  ( $^{\circ}2\theta$ ) and the small peak at  $\sim 37$  ( $^{\circ}2\theta$ ) belong to periclase (MgO). Also, there is a very small peak at  $\sim 26.5$  ( $^{\circ}2\theta$ ) which is the main peak for quartz. For the calcined sample, on the other hand, this quartz peak is not present and a new phase, the forsterite ( $\text{MgSiO}_4$ ), can be easily identified. Forsterite is formed by the solid state reaction of MgO and  $\text{SiO}_2$  at high temperatures (Brindley and Hayami, 1965). This is the reason why the quartz peak vanishes with the calcination. Also, the formation of forsterite results in larger particles that may be considered as part of the cause of the decrease in fineness of the powder. Apart from these, there is a significant increase in the intensity of the periclase peak which can be related to the

increase in crystallinity of the powder. Wagh and Jeong (2003) explained this issue as the result of the recrystallization of the amorphous coating on individual grains. The more detailed representation of the gradual change in microstructure with increasing calcination temperature is provided in Appendix A. Also, the change in compound composition with increasing calcination temperature can be seen in Appendix B.

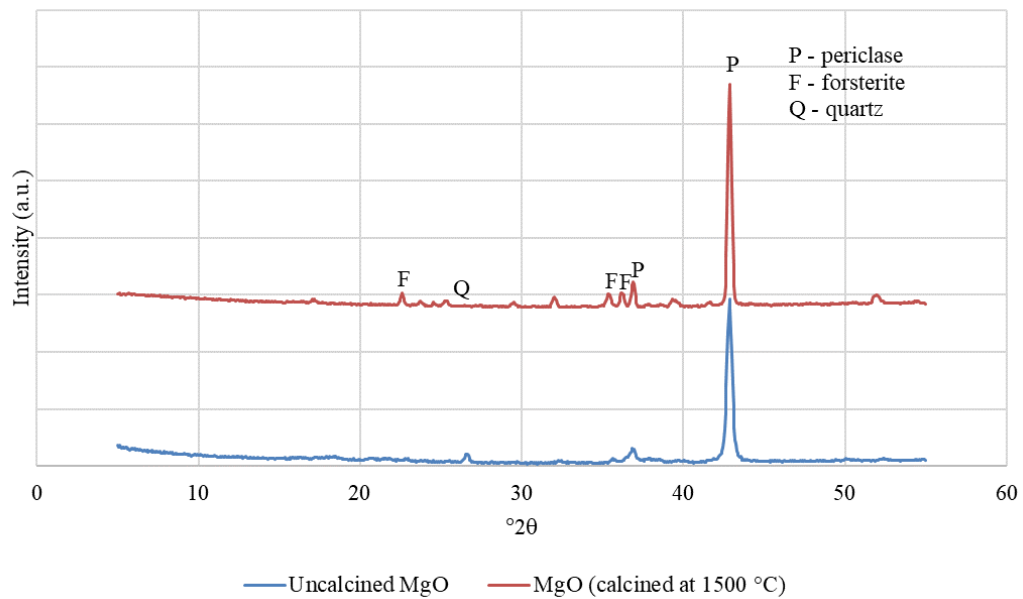


Figure 4.3 The influence of calcination on the microstructure

#### 4.2.4 Changes in Reactivity

An assessment of reactivity of the calcined magnesia samples was made by investigating the MKPC paste mixtures. Since there was no way to get a workable mixture for the samples prepared with the powders calcined at the temperatures less than or equal to 1200 °C due to rapid reaction, it can be concluded that there was not any observable change in reactivity for that range. On the other hand, for the remaining powder samples calcined at 1300, 1400 and 1500 °C, the reactivity assessment was made by considering the results of setting time test for the prepared paste mixtures. Although the properties of a powder such as the specific gravity,

specific surface area and the mineralogy affect the reactivity, since there is almost no change in the properties of the powder samples calcined at the temperatures higher than 1200 °C the setting time test could be a good way to investigate the change in reactivity. Figure 4.4a shows the results of the setting time test for the paste samples prepared with the magnesia powders calcined at different temperatures. As the setting time of the pastes is inversely proportional to the reactivity of the powder, it can be observed that the reactivity decreases with increasing calcination temperature. This is an expected result since there are several experimental works based on the neutralization of citric acid or acetic acid proving that the reactivity of the magnesia powder decreases with increasing calcination temperature (Aphane, 2007; Birchal et al., 2000). There is some decrease in setting time for the sample prepared with the calcined magnesia at 1500 °C when compared with the case for the calcined magnesia at 1400 °C. This change may be caused by an experimental error or some problem related to the mixing. The error in these test results is rather high due to the very low setting times, on the order of 10 minutes. In Figure 4.4b, the effect of calcination time can be seen for the calcination temperature of 1500 °C. There is some decrease in setting time, that is an increase in reactivity, but this may also be caused by problems related to the estimation or mixing. Therefore, it is considered that for that temperature range, there is no significant change in reactivity. The calcination study was limited to 1500 °C as this was the maximum temperature that could be sustained by the furnace.

While there were observable changes in reactivity with increasing calcination temperature, there was almost no significant change related to the calcination time. Therefore, to minimize the energy consumption as much as possible, the calcination time was selected as 1 h. Based on the calcination study, the calcination temperature and duration to be used for the remainder of the thesis study were selected as 1500 °C and 1 h, respectively.

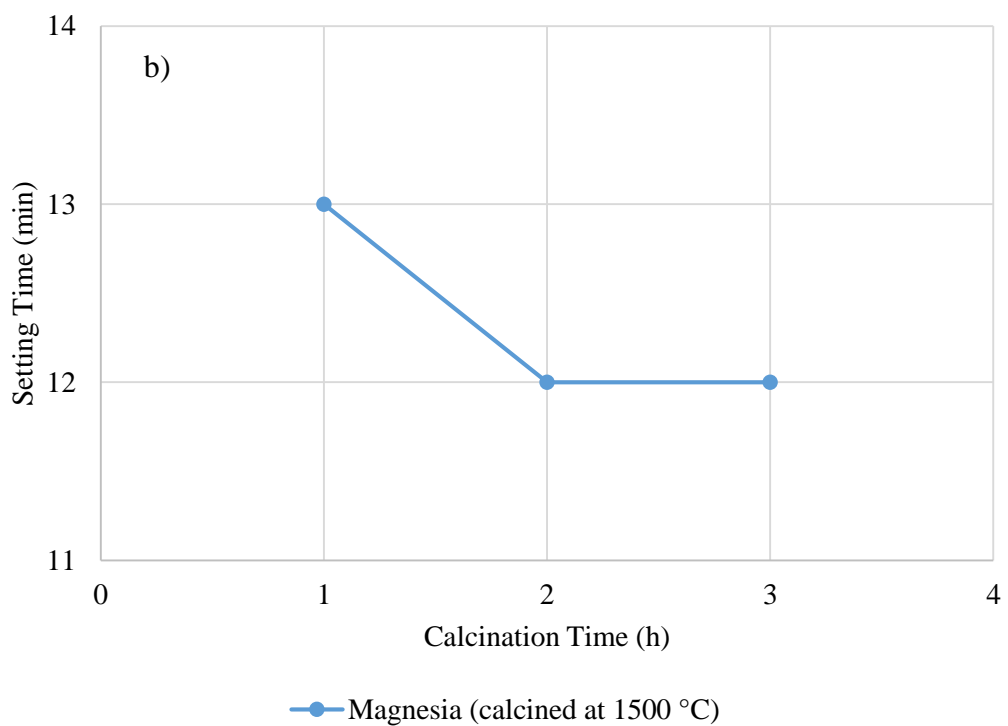
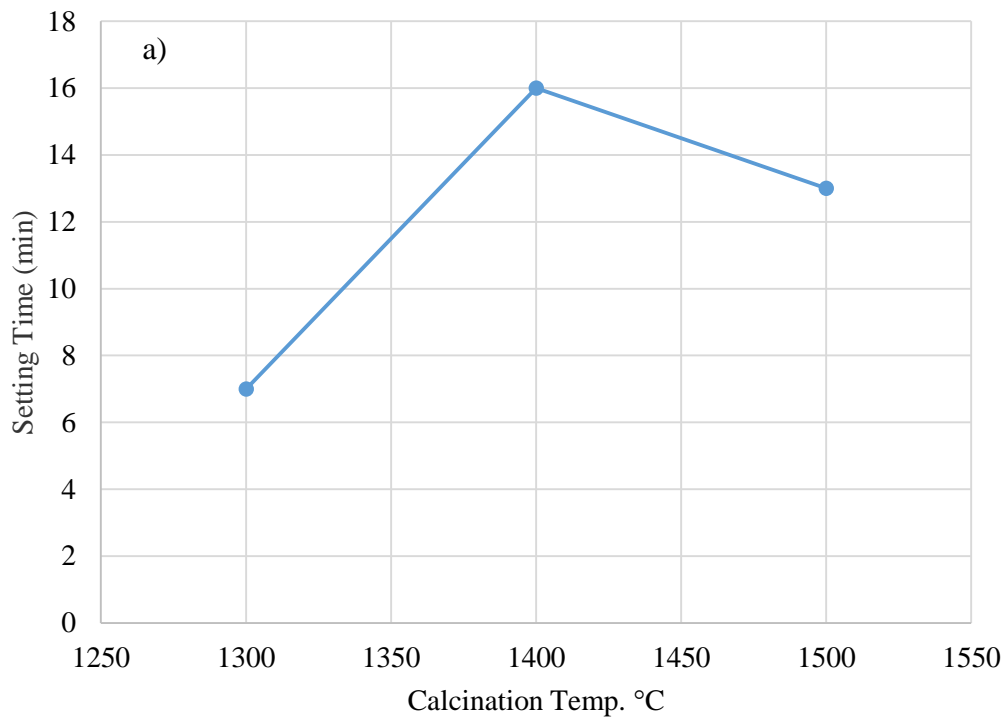


Figure 4.4 The effect of a) calcination temperature, b) calcination time on the setting time (at 1500 °C) of MKPC pastes

### **4.3 Analysis of the Effects of Mix Proportion on the Properties of MKPC Paste**

The analysis of the effects of mix proportion is presented considering the changes in the properties of the MKPC paste such as setting time, compressive strength, and microstructure. Also, the effects of borax content on the setting time and compressive strength of the MKPC paste with the selected mix proportion are presented.

#### **4.3.1 Effects of the Mix Proportion on Setting Time**

Setting time is a very crucial parameter to decide on the mix design for the end product since it represents the amount of time to be able to work with the mixture before the application. Figure 4.5 shows the effects of W/B and M/P on the setting time of the MKPC paste samples. It is clear that as the W/B increases, the setting time also increases. And, it is also clear that the decrease in M/P results in the increase of setting time. Moreover, as the M/P decreases, the effect of W/B increases. While, for the M/P = 3, the difference between the upper and the lower limit of setting time is greater than 4 minutes, for the M/P = 6, this difference is smaller than 2 minutes. Therefore, for the higher M/P of 5 and 6, the increase in W/B is not so effective to get a desirable mixture.

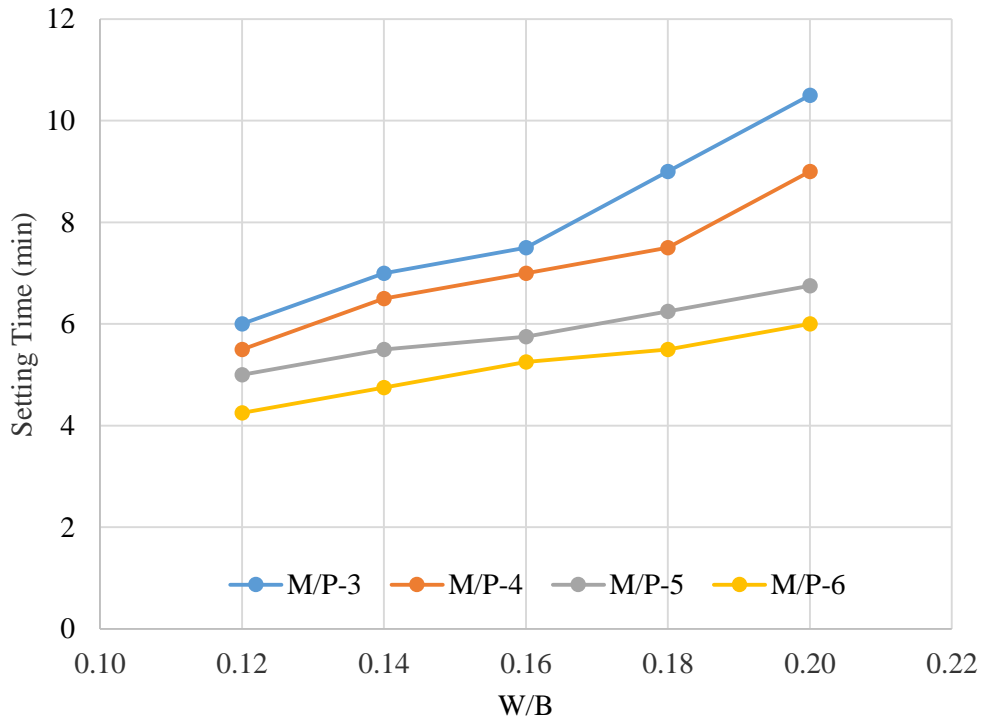


Figure 4.5 The setting times of MKPC pastes with different M/P and W/B

The unfavorable trend in setting time with decreasing water content is an expected result since lower water content implies a higher ionic concentration of phosphate anions which results in a faster reaction rate (Qiao, 2010). About the influence of M/P, the obtained results seem reasonable as it was reported that an increase in M/P results in faster reaction and higher pH environment, giving rise to a decrease in setting time (Yang and Wu, 1999; Xu, Ma and Li, 2015).

### 4.3.2 Effects of Mix Proportions on Compressive Strength

It is very important to analyze the strength gain of the paste mixtures prepared with a variety of M/P and W/B to decide on the most preferable mixture proportion. In Table 4.2, the compressive strength development of all studied mixtures is presented.

Table 4.2 The early strength development of paste samples with different M/P and W/B

		<b>Compressive Strength (MPa)</b>			
<b>M/P</b>	<b>W/B</b>	<b>1h</b>	<b>3h</b>	<b>7h</b>	<b>24h</b>
3	0.14	8.85	12.55	16.15	27.50
	0.16	8.70	13.00	18.05	35.35
	0.18	9.55	16.00	26.35	47.25
	0.20	9.80	20.15	39.55	44.65
4	0.14	12.80	18.10	25.00	41.60
	0.16	14.50	22.30	32.60	51.50
	0.18	15.60	32.75	43.80	53.20
	0.20	16.35	40.60	43.00	47.60
5	0.14	16.65	28.15	38.95	51.35
	0.16	17.90	31.60	44.00	53.10
	0.18	24.00	48.90	50.25	52.95
	0.20	33.90	43.95	47.55	48.50
6	0.14	28.20	48.60	48.20	51.40
	0.16	31.95	46.70	45.45	42.50
	0.18	36.75	42.80	42.45	42.90
	0.20	40.40	42.80	42.35	39.85

In Figure 4.6, the early strength gain can be observed for the case of M/P = 3. In general, as the W/B increases the strength measured at any given age also increases. Also, for the same curing time, the difference in the strength increases with increase in W/B. There is almost no difference between the 1 h compressive strengths of the samples (~10 MPa), so the effect of W/B can be observed starting from the curing time of 3 h. The highest 24 h compressive strength is almost 48 MPa which is obtained for the case of W/B = 0.18, and this value is slightly higher than the one obtained for the case of W/B = 0.20 sample. The lowest compressive strength is obtained for the case of W/B ratio of 0.14 which is almost 60 % of the case of W/B

ratio of 0.18. Also, another important thing to mention is that the strength at 7 h is almost equal to 90 % of the value at 24 h for the case of W/B of 0.20, which shows the crucial effect of W/B ratio on the early strength gain.

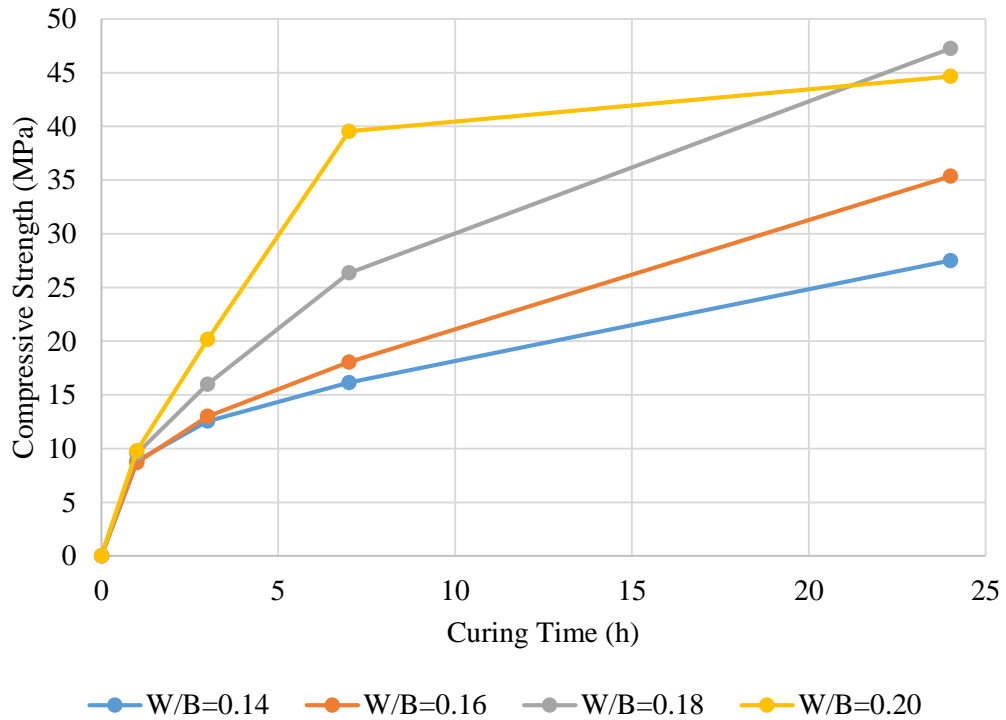


Figure 4.6 The effect of W/B ratio on the early strength gain of the samples with M/P = 3

The early strength gain of M/P = 4 paste samples is given in Figure 4.7. It is clear that an increase in curing time results in the increase in compressive strength. There are some small differences in the compressive strengths for the curing time at 1 h, but the effect of W/B on the difference in gain in strength can be clearly identified for the curing time of 3 h. The highest strength is almost equal to 53 MPa, obtained for the case of W/B = 0.18, slightly higher than the strength for the case of W/B = 0.16. For the case of W/B = 0.20, the strength attained at 3 h is almost equal to 85 % of the strength at 24 h, which is very high when compared to the relative strength gain of pastes with lower W/B.

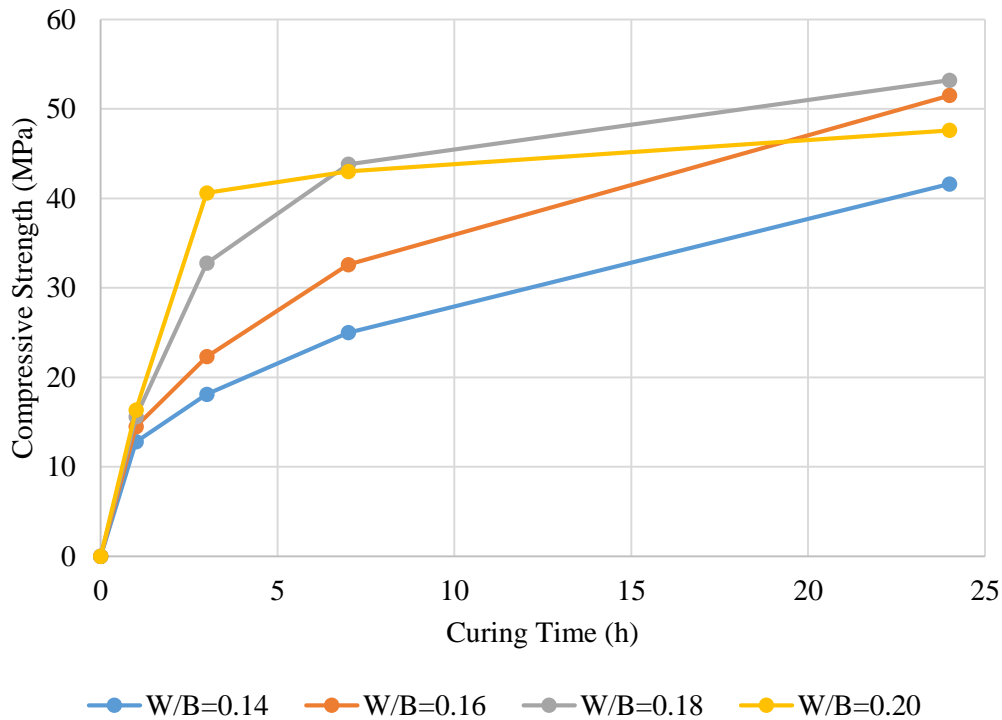


Figure 4.7 The effect of W/B ratio on the early strength gain of the samples with M/P ratio of 4

The early strength gain of M/P = 5 paste samples is given in Figure 4.8. Again, an increase in curing time results in a clear increase in compressive strength except for the W/B of 0.18 and 0.20 which show little or almost no difference after 7 h of curing. For these two cases, the samples reach almost 95 and 98 % of their 24 h of strengths at 7 h. The highest compressive strength is almost 53 MPa, obtained for of W/B of 0.18 and 0.16, slightly higher than the case of W/B = 0.14. Actually, while there are significant differences between the strength of the four pastes for the earlier curing times, there is no significant difference between the strengths at 24 h. Therefore, it can be said that, as M/P increases, the effect of W/B decreases.

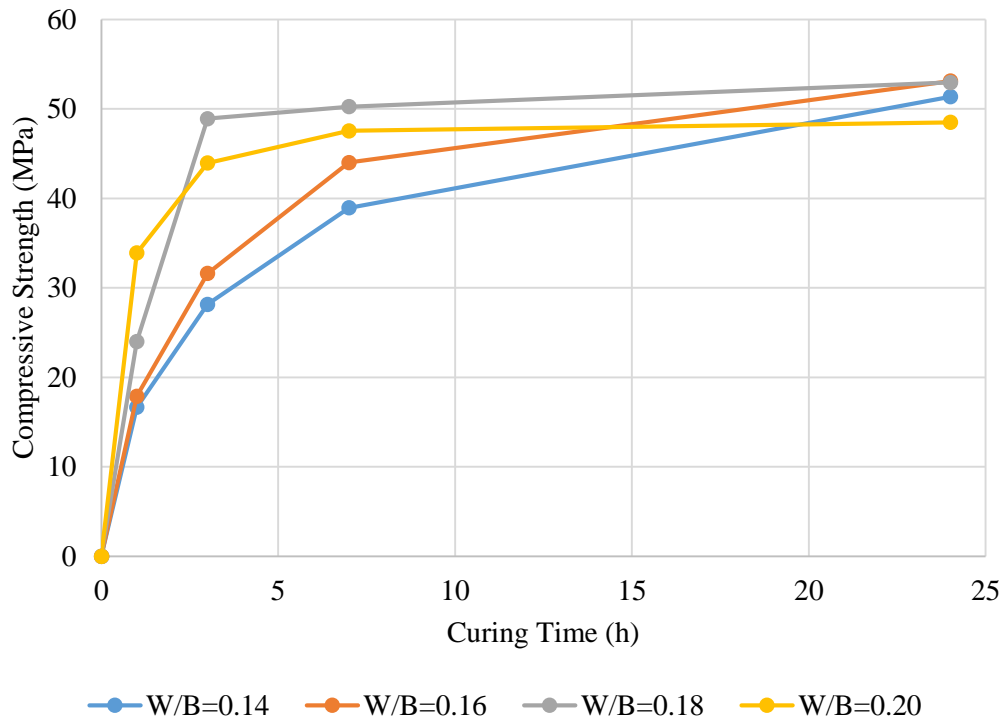


Figure 4.8 The effect of W/B ratio on the early strength gain of the samples with M/P ratio of 5

The early strength gain of M/P = 6 paste samples is given in Figure 4.9. For all the samples, there is some increase in compressive strength up to 3 h of curing. After, except for the W/B = 0.14 paste, the compressive strengths of the samples decrease showing the negative effect of curing time at higher W/B. The highest compressive strength obtained is almost 51 MPa, for W/B = 0.14, whereas the lowest one is 40 MPa for W/B = 0.20. Therefore, it is obvious that the compressive strength decreases with increasing W/B.

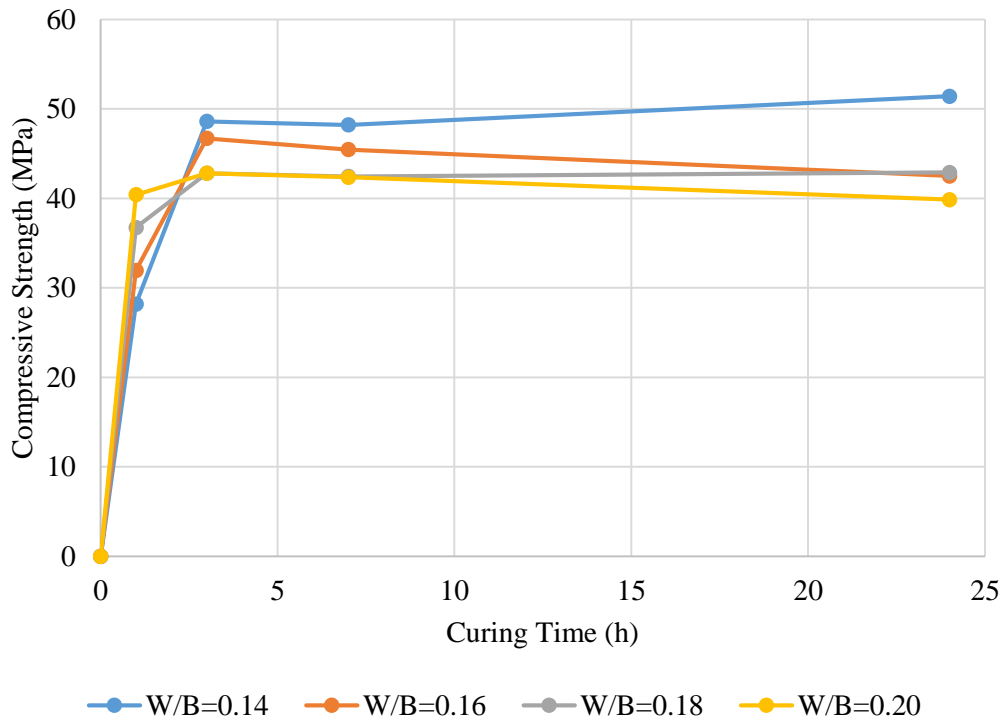


Figure 4.9 The effect of W/B on the early strength gain of samples with M/P = 6

Analyzing Figures 4.6 to 4.9, it can be clearly stated that as M/P increases, an increase in W/B results in higher compressive strengths after 1 h of curing, so the strength gain is faster at higher M/P. This is consistent with the setting time results since a higher M/P implies faster reaction (Xu et al., 2015). Also, the lower the M/P, the higher the residual amount of  $\text{KH}_2\text{PO}_4$  which poses poorer mechanical properties resulting in lower compressive strength for the earlier curing times. (Wang et al., 2013). On the other hand, while increasing W/B for the M/P from 3 to 5 causes no problems in terms of compressive strength, the adverse effect of increasing W/B on compressive strength can be clearly identified for the M/P = 6. There were some cracks on the surface of the sample, with M/P of 6 and W/B of 0.20, that can be seen the provided image in Appendix C. These cracks were most probably the main cause of the adverse effect of increasing W/B for the case of M/P = 6. Wang et al. (2013) stated that the total quantity of the hydrates decreases as the M/P increases, giving rise to a decrease in cohesion between the grains. This can be the main problem with higher M/P resulting in some decrease in compressive

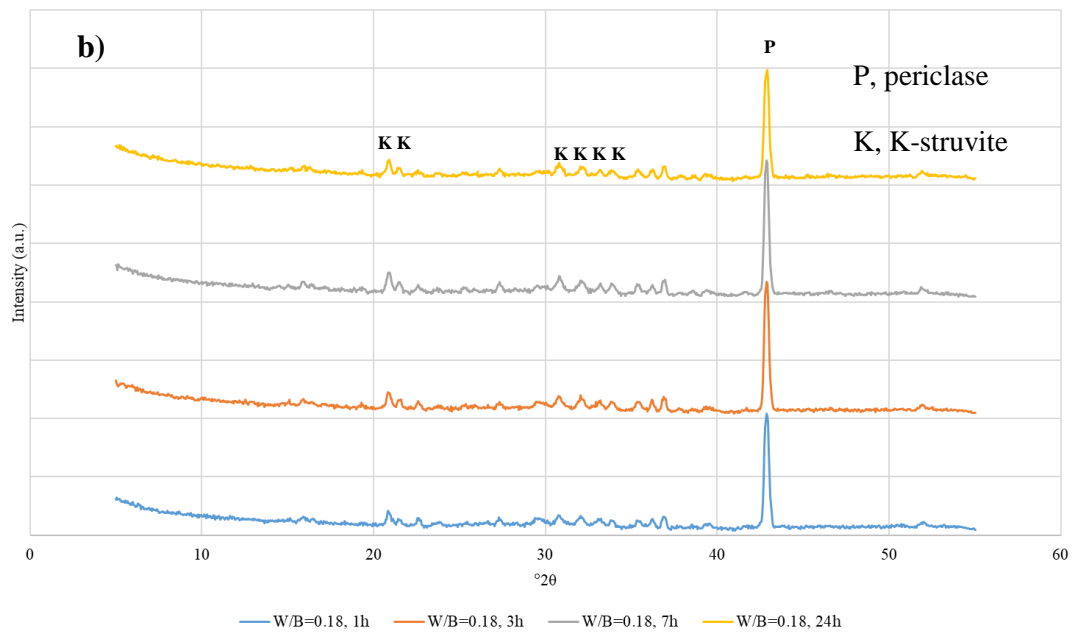
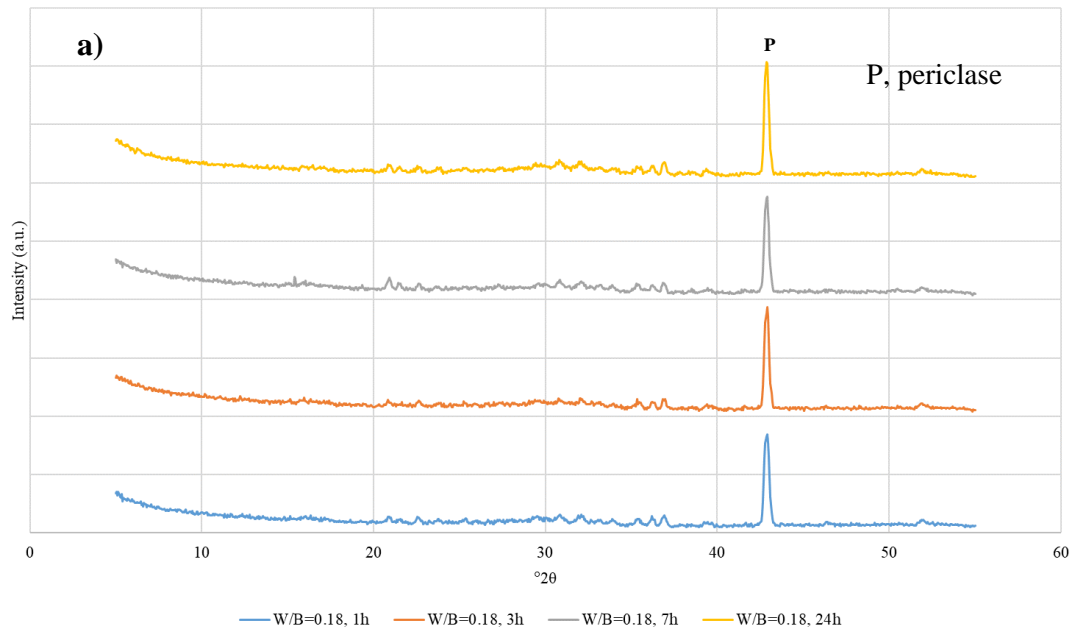
strength. Also, about the influence of increasing W/B, it is expected to have an adverse effect on the compressive strength due to the more porous structure formed. However, for the earlier curing times, it is obvious that the decrease in W/B gives lower compressive strengths, which can be related to the more porous structure being formed due to lower workability and faster setting (Li and Chen, 2013).

Based on the results obtained for the variety of mixtures in terms of setting time and compressive strength to ensure high early strength and high workability, M/P and W/B to be used for the remainder of tests were selected as 5 and 0.18, respectively.

#### **4.3.3 Effects of the Mix Proportion on the Microstructural Development**

The microstructural change for the first 24 h of hydration can be observed for the samples with a fixed W/B = 0.18 in Figure 4.10. As expected there are two main phases which are the unreacted MgO and magnesium potassium phosphate hexahydrate, generally known as the K-struvite. The unreacted MgO peak intensity increases with increasing M/P ratio, also an expected outcome. Also, there are some small humps around 30 ( $^{\circ}2\theta$ ) that can be clearly seen especially in Figure 4.10a, which could be the representation of the amorphous phase of K-struvite which making the crystal products cohere (Ding et al., 2012). The crystalline K-struvite peaks are getting easily observable as the M/P ratio increases which could be related to getting higher earlier strength as M/P ratio increases. Moreover, it is important to note that with the passing time there is almost no change in microstructure which can be explained by the fast reactions taking place.

The more detailed results for the change in microstructure for all the cases are presented in Appendix D. It is important to state that XRD tests were performed again using small paste samples to compare with the results obtained before. Since it is very difficult to observe some reasonable pattern in the XRD results provided in Appendix D, the results provided in Figure 4.10 could be more representative for the real case.



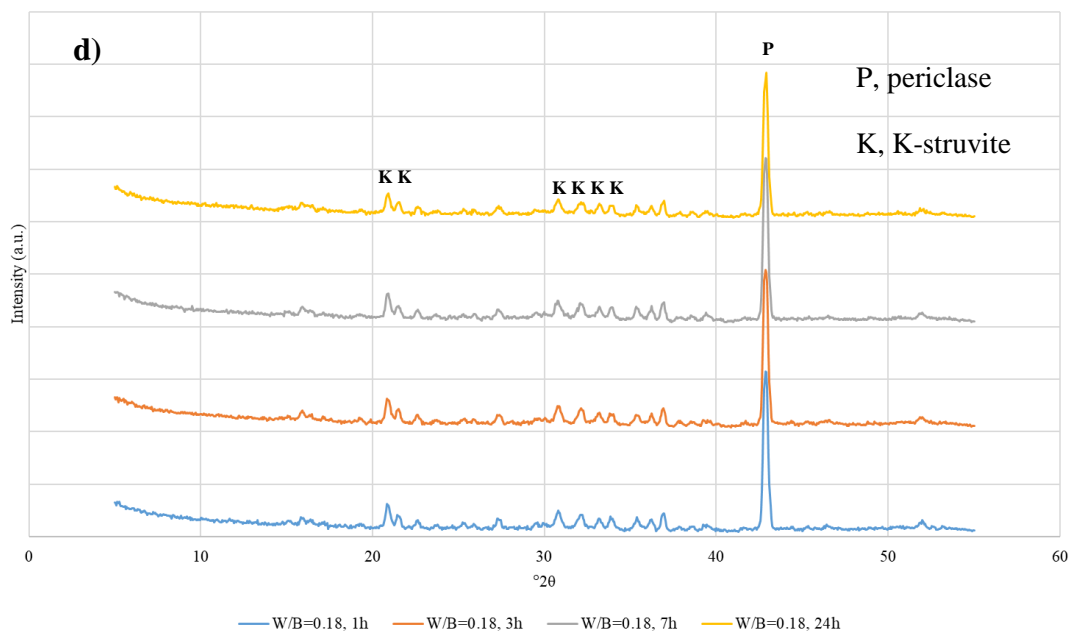
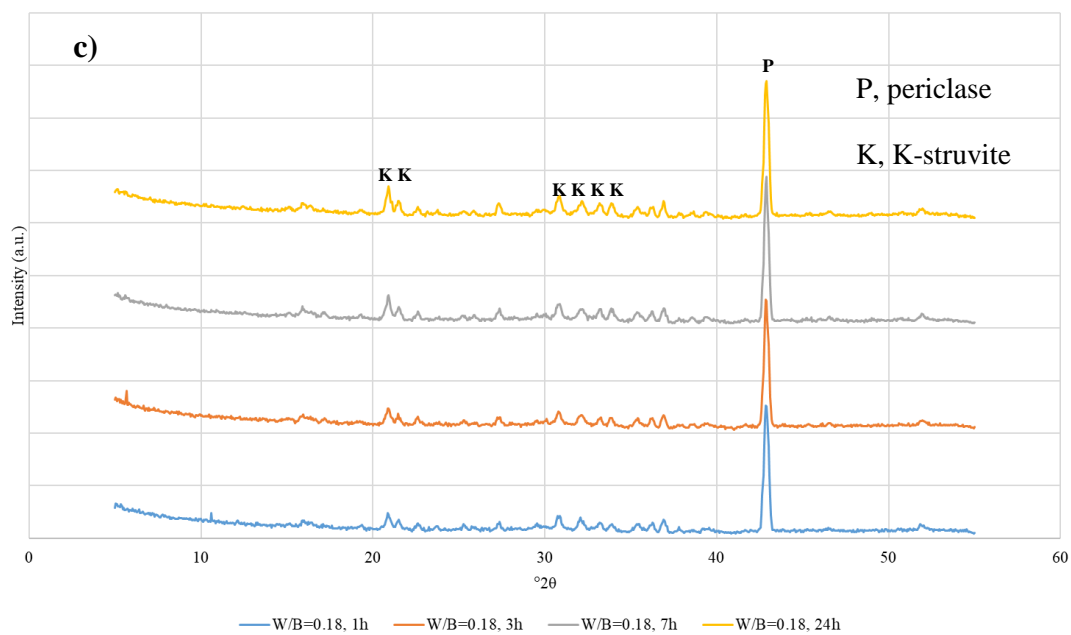


Figure 4.10 The evolution in microstructure for a) M/P=3, b) M/P=4, c) M/P=5, d) M/P=6

#### 4.3.4 Effects of Borax Content on the Properties of MKPC Paste

Figure 4.11 shows the effect of borax content on the setting time of the MKPC paste. As expected, addition of borax into the system retards setting of the MKPC paste. The increase in setting time can be explained by the decrease in reaction rate related to both the decrease in temperature and the increase in pH value of the system that is caused by the formation of a film on the magnesia surface (Yang and Qian, 2010). There is an almost linear relation between setting time and the borax content. While the setting time of the paste without borax is almost 6 minutes, the setting time for the paste with 10 % borax is almost 20 minutes. Although it is very good to have a mixture with the longest possible setting time, the effect of the use of borax on the compressive strength also needs to be considered to determine the suitable borax content for the MKPC products to be prepared in the remainder of the thesis.

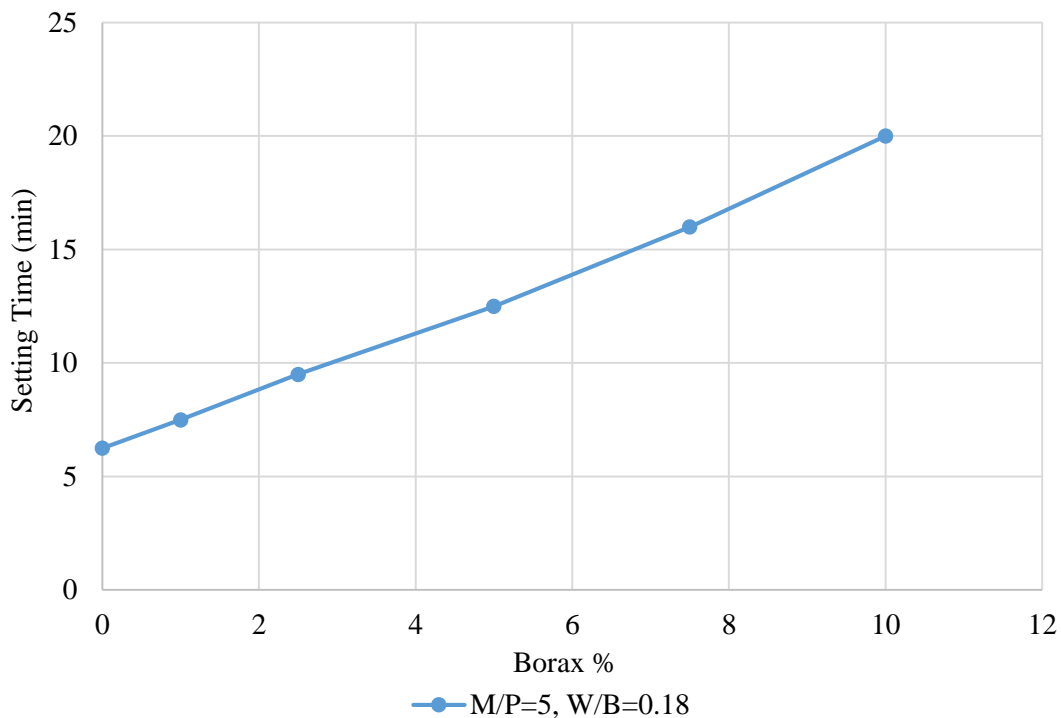


Figure 4.11 The effect of borax content on the setting time

Figure 4.12 shows the effect of different borax contents on the compressive strength of the MKPC pastes, evaluated at 3 h and 7 d. As expected, the increase in borax

content has a strong effect on early strength gain. While compressive strength at 3 h for the sample without borax is almost 50 MPa, it is almost 40 % of this value for the sample containing 10 % borax. The decrease in early strength is reasonable since the increase in borax content results in the decrease in reaction rate which is consistent with the setting time results. Although the increase in the borax content adversely affects the early strength gain, it does not cause a significant problem for the late strength of the samples with borax compared to the reference sample only a slight decrease is measured for the sample with 10 % borax. Indeed, the sample with 5 % borax content has higher late strength, reaching almost 65 Mpa, ~10 % higher than the reference sample. This favorable result of using the sample with 5 % borax content in terms of later age compressive strength can be caused by the fact that the decrease in reaction rate results in a more crystalline structure. On the other hand, considering the case for the sample with 10 % borax content, the unfavorable effect on the later compressive strength can be related to the use of higher amount of borax causing a decrease in the contents of the other reactants which form stronger structures than the borax, resulting in a poorer internal structure.

Based on the effects on setting time and compressive strength and also considering that it was important not to use higher borax content to decrease the cost as much as possible, the borax content to be used for the remainder of mixtures was determined as 5 %.

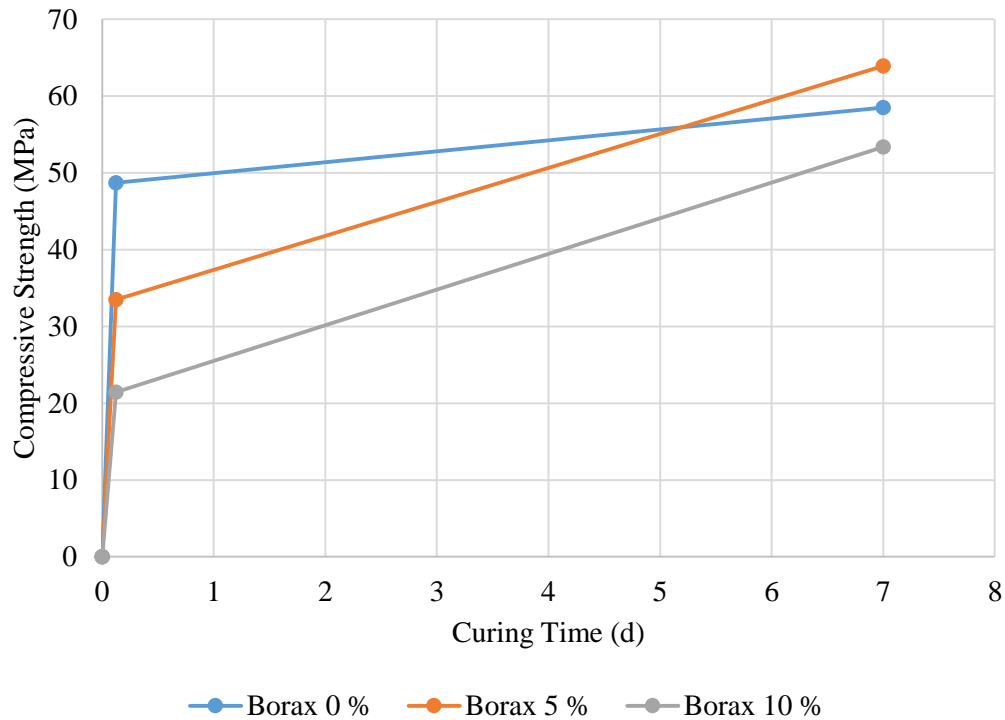


Figure 4.12 The effect of borax content on the compressive strength

Figure 4.13 shows the effect of different borax contents on the evolution of microstructure. The diffractograms presented in Figure 4.13a show the effect of the different borax contents on the evolution in microstructure for 3 h of curing. There is no significant change in the mineralogy except for the fact that the peak intensity of periclase decreases as borax content increases from 0 to 10 %. It could be better to investigate the earlier time in terms of mineralogical evolution to see the effect of borax content since 3 h can be considered as late age for this system. The diffractograms presented in Figure 4.13b show the effect of the different borax contents on the evolution in microstructure for 7 d of curing. The characteristic peaks are almost the same for the 7 d curing for different borax contents like the case for 3 h. Therefore, it is important to note that deeper investigation is needed for mineralogical evolution.

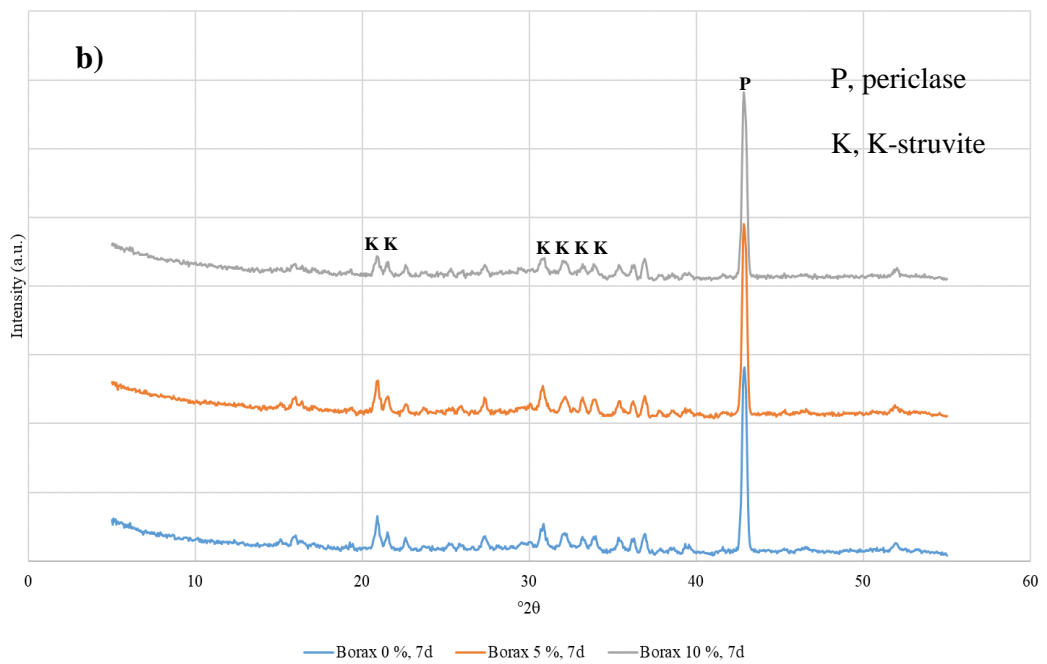
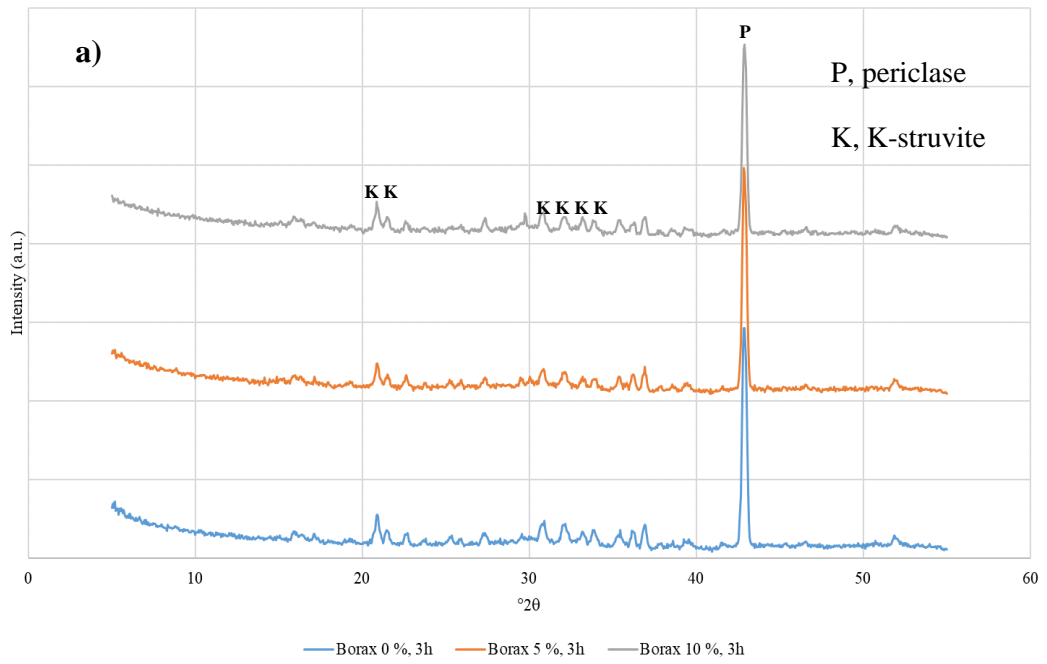


Figure 4.13 The effect of borax content on the evolution in microstructure at a) 3 h, b) 7 d

#### 4.4 Effects of Sand-to-Binder Ratio for the MKPC Mortar

Figure 4.14 represents the effect of S/B on the compressive strength of the MKPC mortar samples. Although for the case of S/B = 1.50, there is a small increase in the compressive strength at 1 d compared to the one with S/B = 1.25, it is obvious that for each curing age there is some decrease in the compressive strength as the S/B increases. Therefore, the increase in S/B adversely affects the compressive strength of the mortar samples. This can be caused by the decrease in the amount of binding material as the S/B increases. Also, another possible reason for that can be the decrease in workability as the S/B increases, which affects the compaction of the mortar. Since the highest strength was obtained for the S/B = 1.25, almost 74 MPa at 7 days, this was chosen as the sand-to-binder ratio for the mortar samples to be prepared for the remainder of the study.

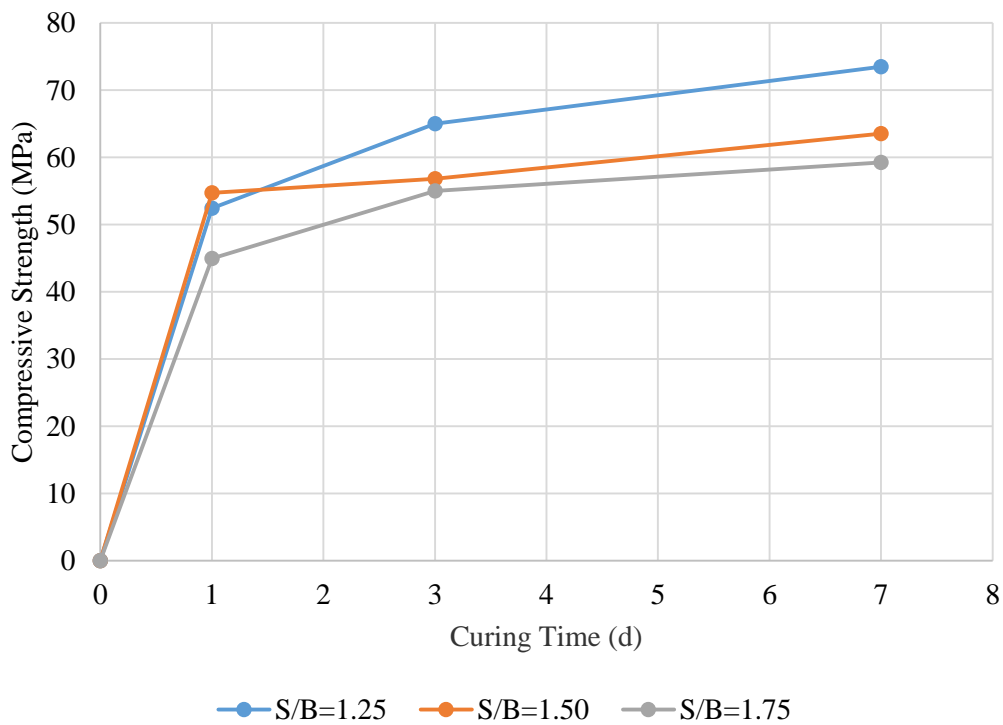


Figure 4.14 The effect of sand-to-binder ratio on the compressive strength of the mortar samples

#### 4.5 Effects of Incorporating Fly Ash

Figure 4.15 represents the effect of fly ash content on the compressive strength of the MKPC mortar samples. The increase in fly ash content results in lower strength values for the 28 d of strength decreasing from almost 80 to 70 MPa. Although in the literature, there are some studies stating that incorporating fly ash results in better compressive strength the decrease in compressive strength for this study can be explained due to the type of fly ash used and the unfavorable effect of including fly ash on workability.

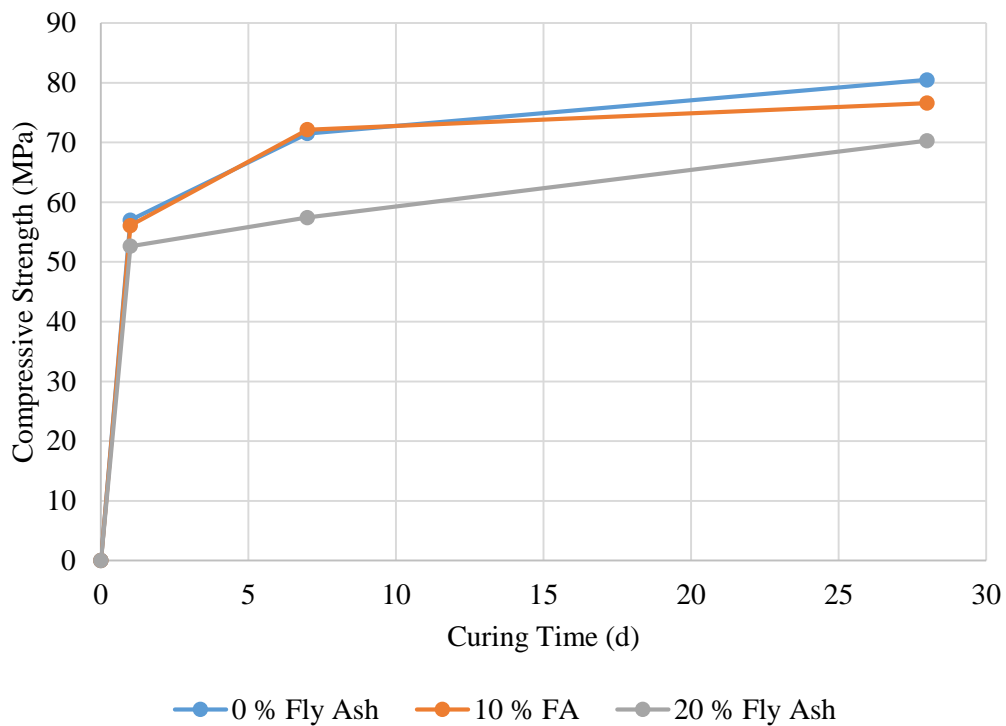


Figure 4.15 The effect of fly ash content on the compressive strength of the MKPC mortars

Figure 4.16 shows the effect of fly ash on the water stability on the MKPC mortar samples considering the retained strength after water curing at 1, 7, and 28 d. The mortar samples cured at ambient temperature for 28 d were immersed into water. All the samples, even the ones containing fly ash, lose some strength after immersed in water for a period of time. The strength loss is higher for 1 d for all the samples,

reaching almost 10 % for the reference sample and the sample with 10 % fly ash. Beyond that, all the samples continue losing some strength with a rate lower than the first day. Also, it is important to note that containing some fly ash does not seem beneficial for water stability. This may be caused by the type of fly ash used and its fineness. The main reason for the strength loss mainly attributed to dissolution of k-struvite in water (Zhang et al., 2017).

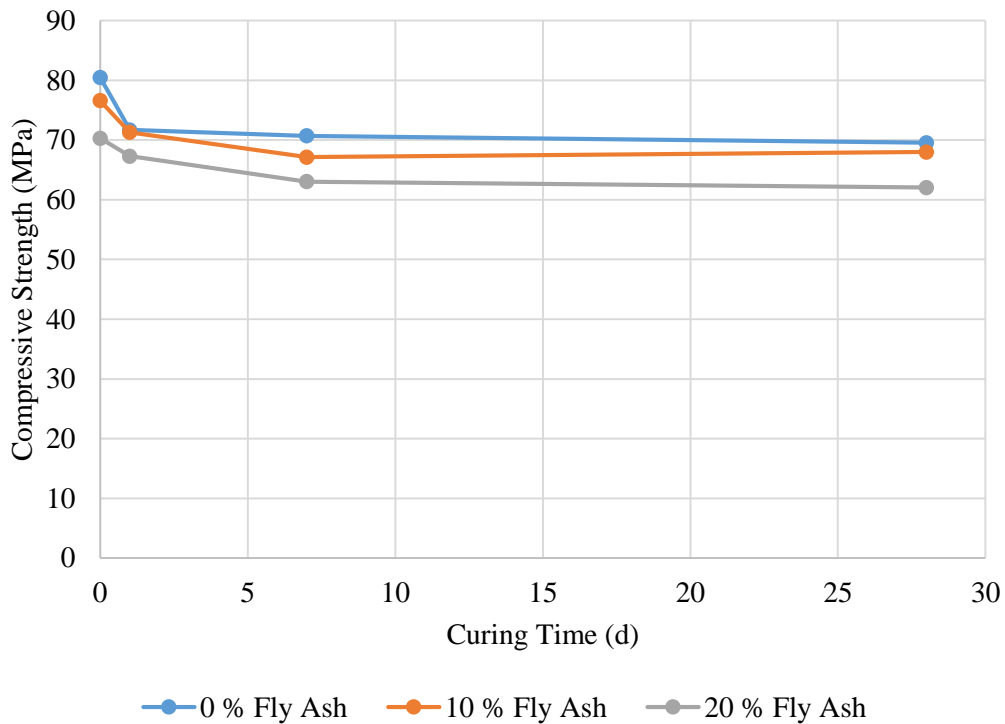


Figure 4.16 The effect of fly ash content on water stability of the mortar samples

Figure 4.17 shows the effect of different fly ash contents on the evolution of microstructure of MKPC paste samples air cured for 5 d. The X-ray diffractogram for the fly ash is also included in Figure 4.17. There is almost no change with increasing fly ash content in the mineralogy of the MKPC paste, except the fact that incorporation of fly ash results in some decrease in the intensity of the unreacted MgO peak.

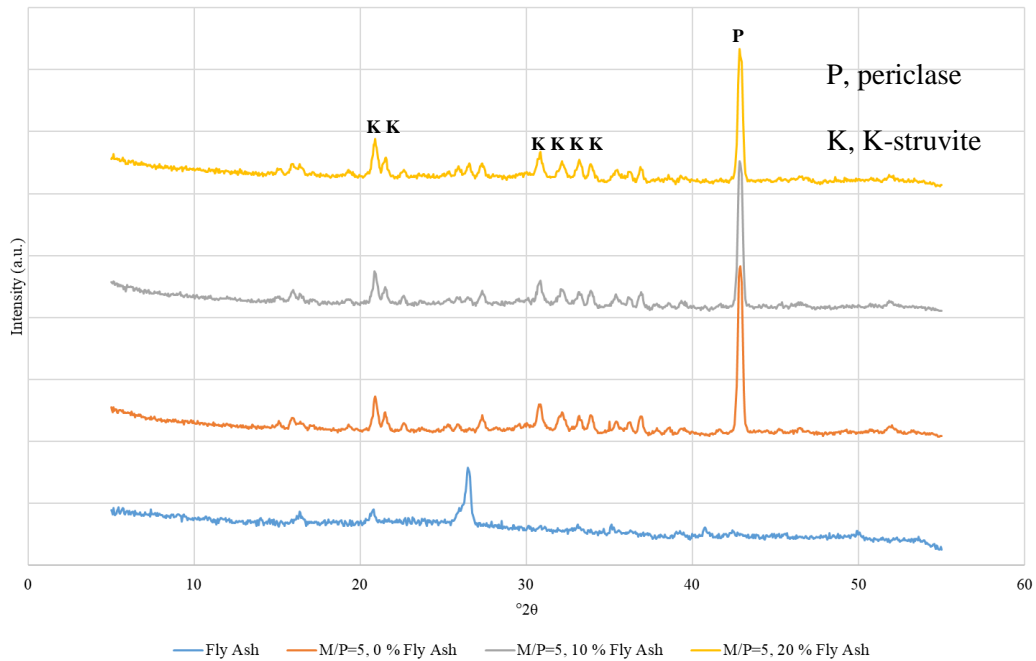


Figure 4.17 The effect of fly ash content on the microstructural evolution

#### 4.5.1 Thermogravimetric / Differential Analyses

The change in heat flow and percent mass loss upon heating to 1000 °C of different MKPC paste samples compared in Figure 4.18. There is a distinct endothermic peak around 125 °C associated with the mass loss caused by dehydration of the main reaction product K-struvite, which loses six water molecules during dehydration. The mass loss is very low up to 100 °C, beyond that the huge mass loss is associated with the loss of crystal water up to 200 °C (Li et al., 2015). After that point, there is a slight loss upon heating from 200 to 400 °C. The total mass loss does not change significantly beyond 400 °C, reaching almost 16 % loss for each sample. Liu and Chen (2016) reported a second characteristic endothermic peak related to the unreacted monopotassium dihydrogen phosphate (KDP) peak around 200 °C, which is not observed for this study. The reason for that issue can be simply explained by the fact that there is no remaining unreacted KDP in the samples.

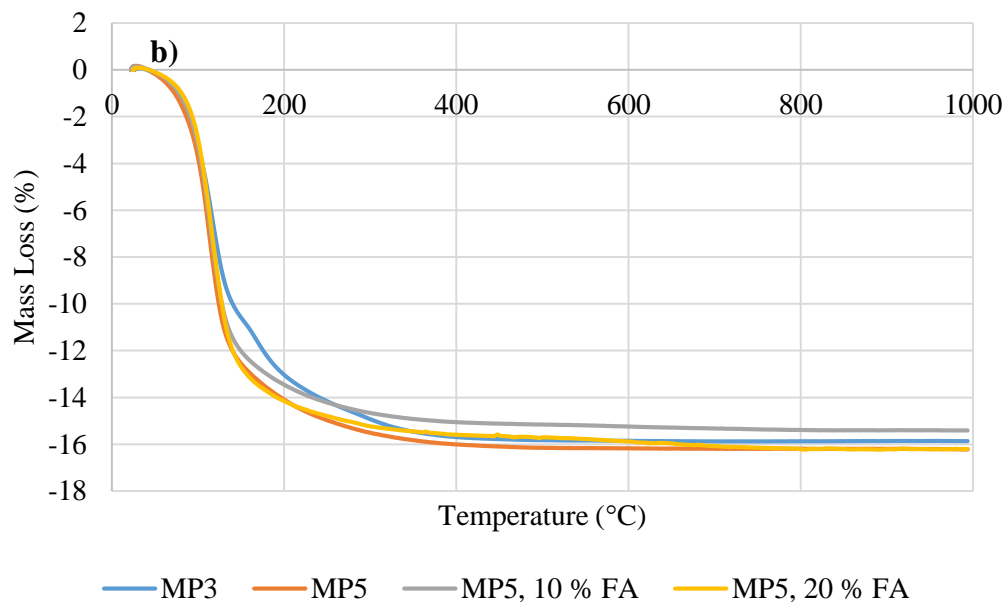
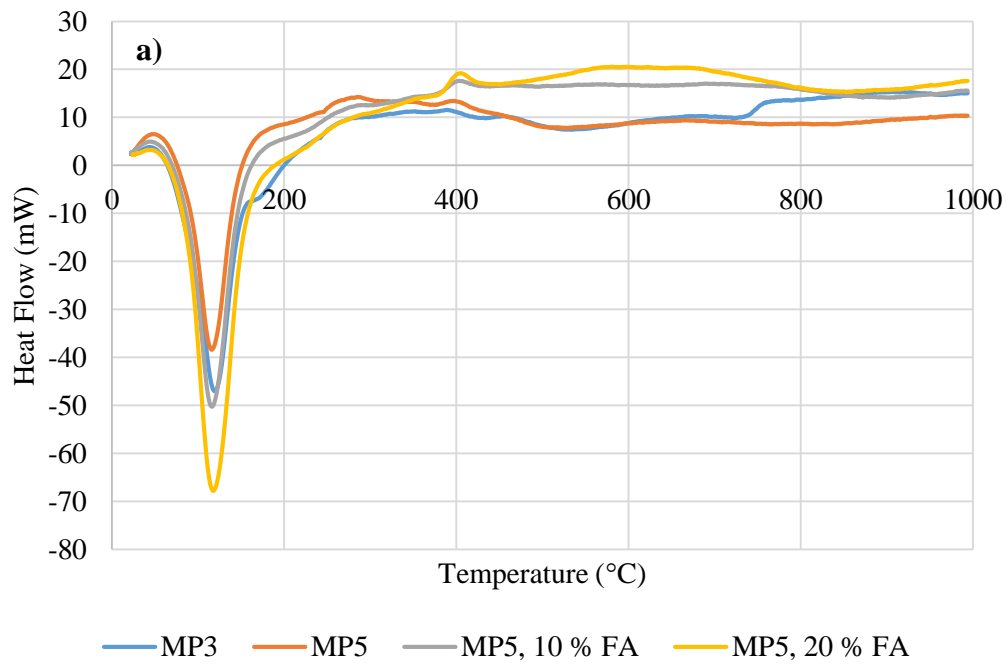
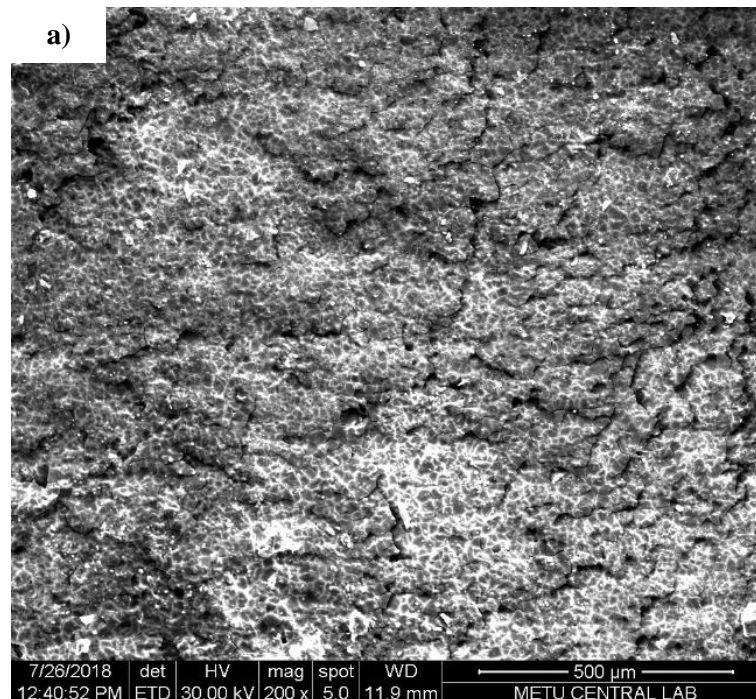


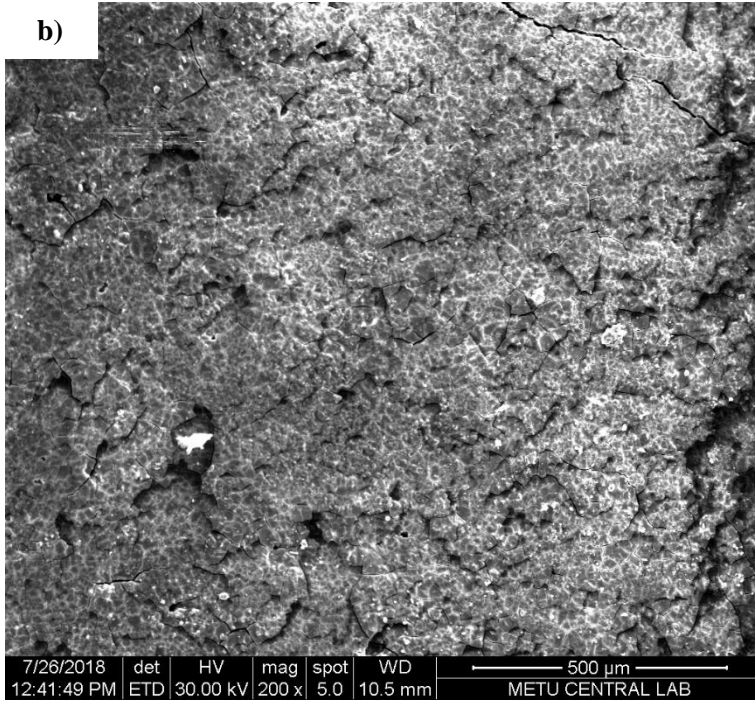
Figure 4.18 Heat flow and mass loss of the MKPC pastes

#### 4.5.2 Scanning Electron Microscopy (SEM) Investigation

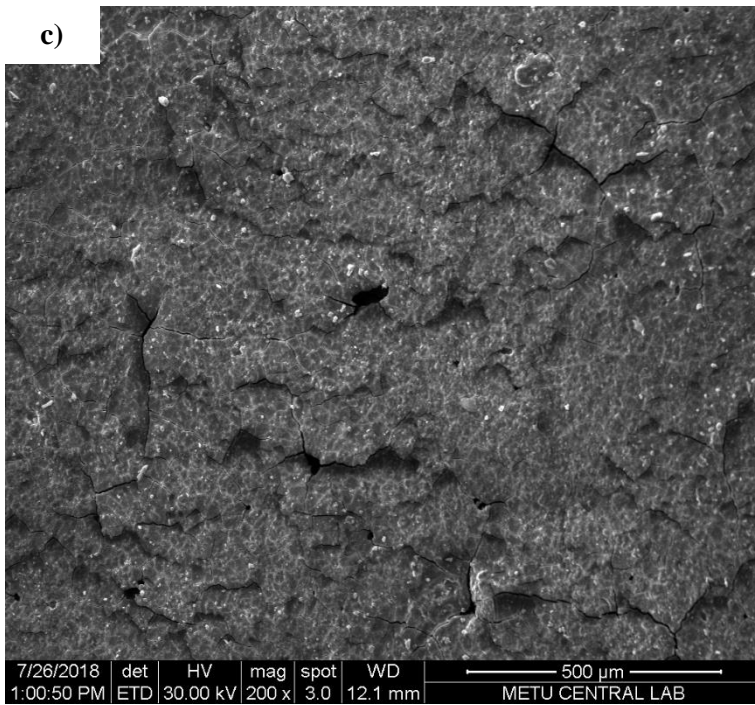
Scanning electron microscopy images for different MKPC paste samples air cured for 14 d are presented in Figure 4.19 and Figure 4.20. The increase in M/P ratio from 3 to 5 results in a less compact structure that could be seen in Figure 4.19a and 4.19b. Although the sample with M/P=3 has more cracks, the cracks are larger in size for the sample with M/P=5, which can be seen in Figures 4.20a and 4.20b. Also, for M/P=5, the increasing fly ash content seems to be ended with a more porous structure that could be seen in Figure 4.19c and 4.19d. Figure 4.20 shows the microstructure of much greater magnification. The increase in M/P ratio results in morphology with fewer microcracks, which can be seen in Figure 4.20a and 4.20b. Also, there are some rod-like crystals observed for the case of M/P=3, which could be K-struvite or unreacted KDP. Moreover, the increase in fly ash content seems to result in less a compact microstructure with more cracks.



b)



c)



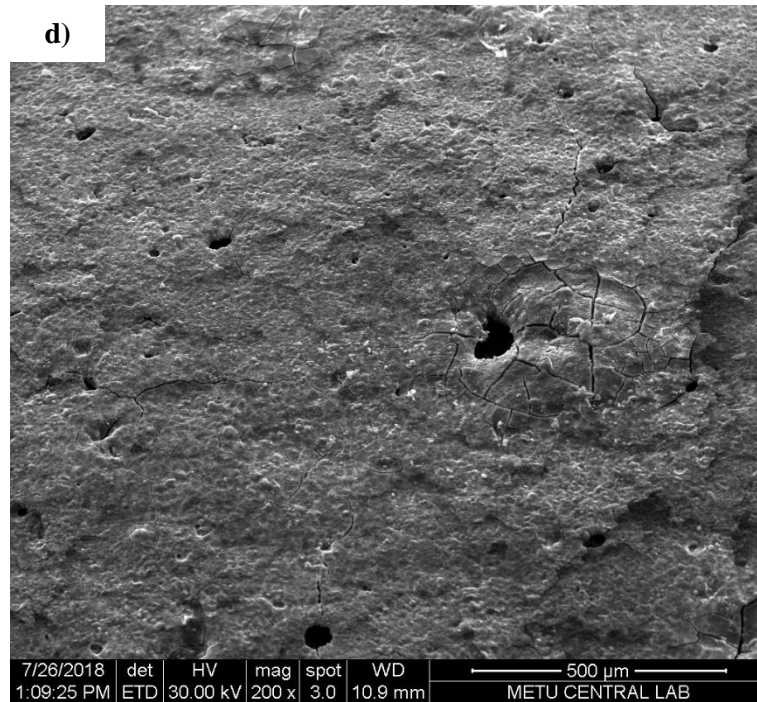
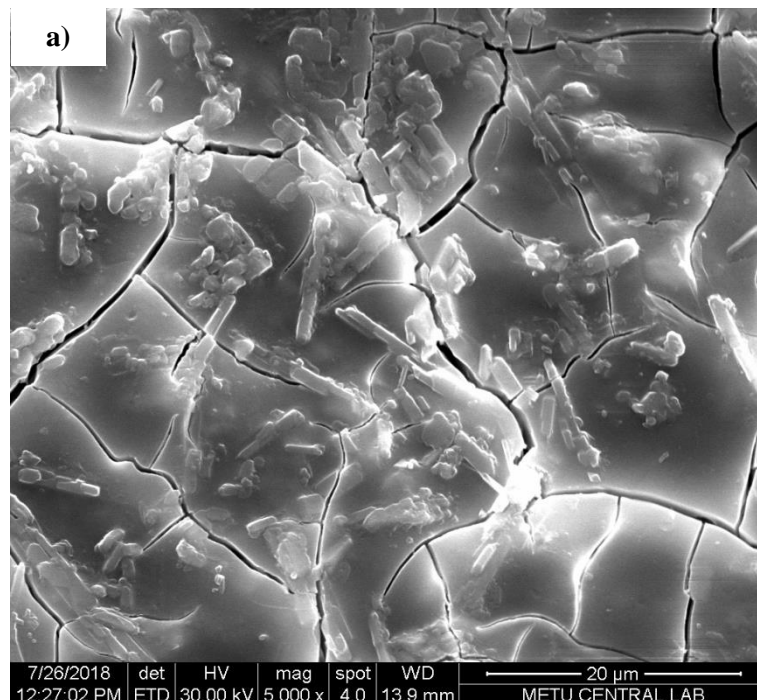
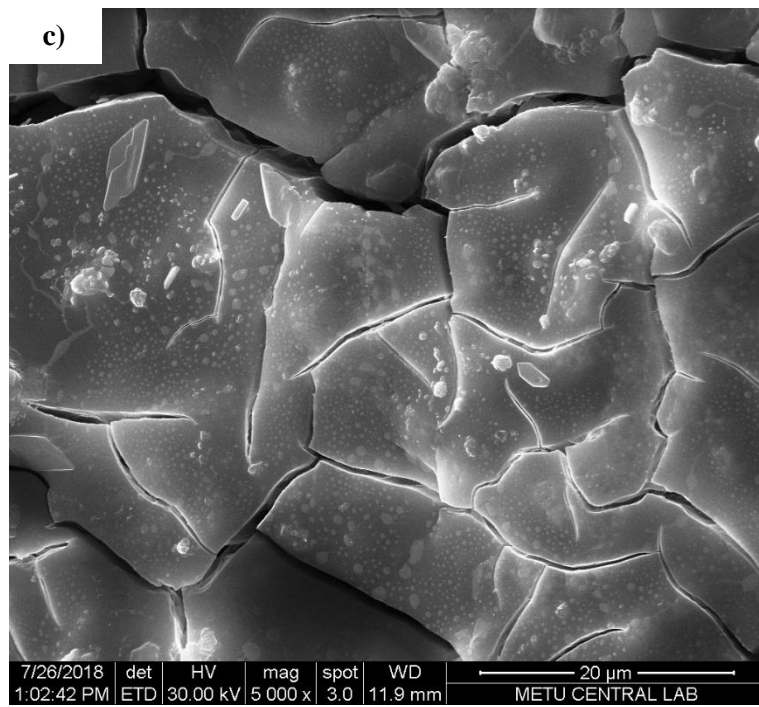
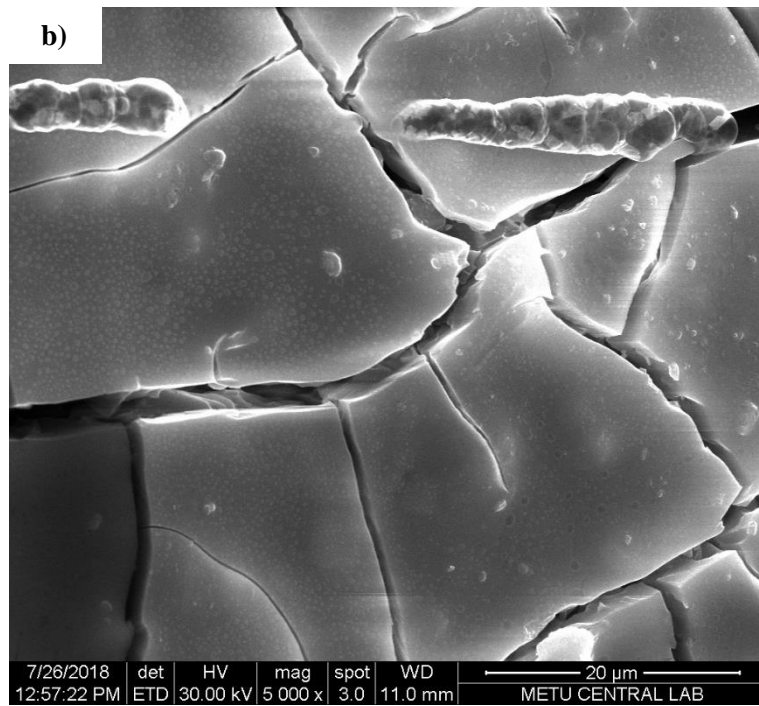


Figure 4.19 SEM Images for a large scale a) M/P=3, b) M/P=5, c) M/P=5 with 10 % FA, d) M/P=5 with 20 % FA





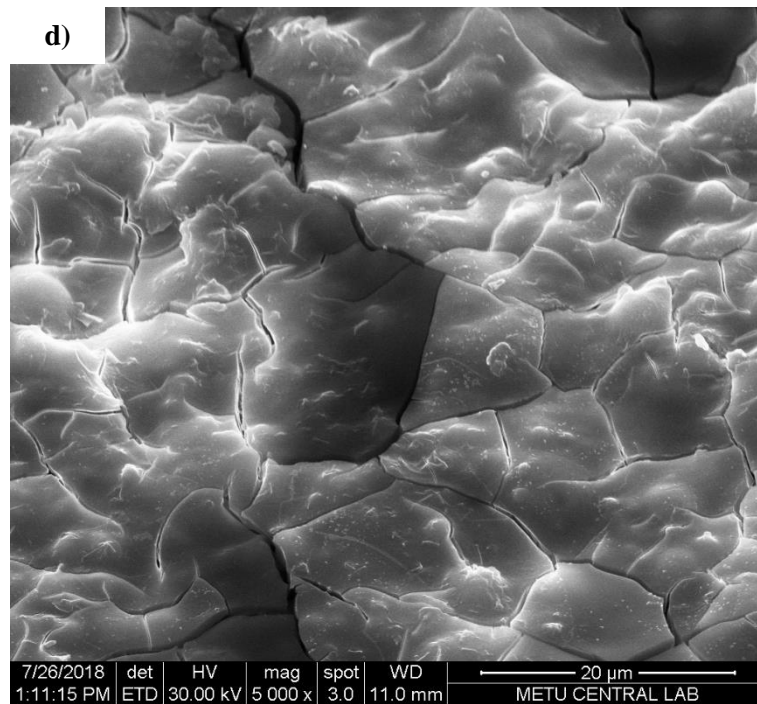


Figure 4.20 SEM images for a small scale a) M/P=3, b) M/P=5, c) M/P=5 with 10 % FA,  
d) M/P=5 with 20 % FA



## CHAPTER 5

### CONCLUSION

#### 5.1 General

In this study, the following investigations were performed:

- 1) The effects of calcination on the properties of magnesia powder in terms of changes in specific gravity and specific surface area.
- 2) The effects of M/P and W/B on the properties of MKPC pastes in terms of setting time and early compressive strength gain.
- 3) The effects of borax content on the properties of MKPC pastes with selected M/P and W/B in terms of setting time and compressive strength gain.
- 4) The effects of S/B on the compressive strength gain of the MKPC mortars.
- 5) The effects of incorporating fly ash on the compressive strength gain and water stability of MKPC mortars with selected S/B.
- 6) XRD tests to observe the effects of mix proportions on the mineralogy of the reaction products.
- 7) TGA/DTA investigations of different MKPC paste samples.

8) SEM investigations on different MKPC paste samples to observe the effects of M/P and fly ash content on the morphology.

The following can be concluded:

1) The specific gravity of the MgO powder sample increases from ~3.10 to 3.50 upon calcination at 1500 °C. The higher the calcination temperature, the lower the specific surface area of the magnesia sample which results in some decrease in reactivity.

2) An increase in W/B results in some increase in setting time as expected. However, as the M/P increases, the W/B loses its effectiveness on setting time. Also, the higher the M/P, the higher the early strength gain of the samples with increasing W/B. The paste samples with M/P=5 reach compressive strengths around 50 MPa at 24 h.

3) The setting time of the MKPC paste with M/P = 5 and W/B = 0.18 increases from ~6 to 20 minutes with 10 % borax addition. The strength gain decreases significantly for the earlier (3 h) strength with increasing borax content, but there are small differences for the late (7 d) strength.

4) The increase in fly ash content results in some decrease in 28 d compressive strength. While the compressive strength of the reference sample is around 80 MPa, the one containing 20 % fly ash reaching almost 70 MPa at 28 d. About the water stability, the increase in fly ash does not seem working well with the water stability problem.

5) The main diffraction peaks observed through the XRD investigations are K-struvite and unreacted MgO.

6) The characteristic endothermic peak related to dehydration of K-struvite around 125 °C has been observed through TGA-DTA investigations.

7) SEM investigation shows that the increase in M/P from 3 to 5 results in a less compact structure. Also, while some crystals are observed for the case of M/P = 3,

the structure for the case of  $M/P = 5$  is mainly amorphous. Apart from these, the increase in fly ash content seems to result in a more porous structure.

## **5.2 Recommendations for Future Studies**

The following recommendations can be useful for future studies:

- 1) It is important to find a way to use MgO powders calcined at lower temperatures in order to get more efficient end products in terms of energy consumption.
- 2) Wider ranges of M/P and W/B should be studied to get more reliable outcomes.
- 3) Incorporation of different types of fly ash and some other industrial wastes should be studied.



## REFERENCES

- Aphane, M. E. (2007). *The hydration of magnesium oxide with different reactivities by water and magnesium acetate*. (Master's thesis, University of South Africa, Pretoria, South Africa).
- ASTM C188-17. (2017). *Standard Test Method for Density of Hydraulic Cement*. ASTM International, West Conshohocken, PA.
- ASTM C191-18. (2018). *Standard Test Methods for Time of Setting of Hydraulic Cement by Vicat Needle*. ASTM International, West Conshohocken, PA
- ASTM C204-17. (2017). *Standard Test Methods for Fineness of Hydraulic Cement by Air-Permeability Apparatus*. ASTM International, West Conshohocken, PA.
- ASTM C618-17. (2017). *Standard Specification for Coal Fly Ash and Raw or Calcined Natural Pozzolan for Use in Concrete*. ASTM International, West Conshohocken, PA.
- Birchal, V. S. S., Rocha, S. D. F., Ciminelli, V. S. T. (2000). The effect of magnesite calcination conditions on magnesia hydration. *Minerals Engineering*, 13(14-15), 1629-1633.
- Brindley, G. W., & Hayami, R. (1965). Kinetics and mechanism of formation of forsterite ( $Mg_2SiO_4$ ) by solid-state reaction of MgO and  $SiO_2$ . *The Philosophical Magazine: A Journal of Theoretical Experimental and Applied Physics*, 12(117), 505-514.
- Chau, C. K., Qiao, F., & Li, Z. (2011). Microstructure of magnesium potassium phosphate cement. *Construction and Building Materials*, 25(6), 2911-2917.
- Christensen, J. H., & Reed, R. B. (1955). Density of Aqueous Solutions of Phosphoric Acid. *Industrial and Engineering Chemistry*, 47(6), 1277-1280.
- Ding, Z., Dong, B., Xing, F., Han, N., & Li, Z. (2012). Cementing mechanism of potassium phosphate based magnesium phosphate cement. *Ceramics International*, 38(8), 6281–6288.
- Erdoğan, T. Y. (2009). *Materials of Construction*. Ankara, Turkey: METU Press Publishing Company.
- Eubank, W. R. (1951). Calcination Studies of Magnesium Oxides. *Journal of the American Ceramic Society*, 34(8), 225–229.

- Hou, D., Yan, H., Zhang, J., Wang, P., & Li, Z. (2016). Experimental and computational investigation of magnesium phosphate cement mortar. *Construction and Building Materials*, 112, 331-342.
- Lai, Z., Lai, X., Shi, J., & Lu, Z. (2016). Effect of  $Zn^{+2}$  on the early hydration behavior of potassium phosphate based magnesium phosphate cement. *Construction and Building Materials*, 129, 70-78.
- Li, Y., & Chen, B. (2013). Factors that affect the properties of magnesium phosphate cement. *Construction and Building Materials*, 47, 977-983.
- Li, Y., Li, Y., Shi, T., & Li, J. (2015). Experimental study on mechanical properties and fracture toughness of magnesium phosphate cement. *Construction and Building Materials*, 96, 346-352.
- Li, Y., Shi, T., & Li, J. (2016). Effects of fly ash and quartz sand on water-resistance and salt-resistance of magnesium phosphate cement. *Construction and Building Materials*, 105, 384-390.
- Li, Y., Shi, T., Chen, B., & Li, Y. (2015). Performance of magnesium phosphate cement at elevated temperatures. *Construction and Building Materials*, 91, 126-132.
- Li, Y., Sun, J., & Chen, B. (2014). Experimental study of magnesia and M/P ratio influencing properties of magnesium phosphate cement. *Construction and Building Materials*, 65, 177-183.
- Liu, N., & Chen, B. (2016). Experimental research on magnesium phosphate cements containing alumina. *Construction and Building Materials*, 121, 354-360.
- Lu, X., & Chen, B. (2016). Experimental study of magnesium phosphate cements modified by metakaolin. *Construction and Building Materials*, 123, 719-726.
- Mestres, G., & Ginebra, M. P. (2011). Novel magnesium phosphate cements with high early strength and antibacterial properties. *Acta Biomaterialia*, 7(4), 1853-1861.
- Qiao, F. (2010). *Reaction Mechanisms of Magnesium Potassium Phosphate Cement and Its Application*. (Doctoral dissertation, Hong Kong University of Science and Technology, Hong Kong).
- Qiao, F., Chau, C. K., & Li, Z. (2010). Property evaluation of magnesium phosphate cement mortar as patch repair material. *Construction and Building Materials*, 24(5), 695-700.
- Rouzić, M. L., Chaussadent, T., Stefan, L., & Saillio M. (2017). On the influence of Mg/P ratio on the properties and durability of magnesium potassium phosphate cement pastes. *Cement and Concrete Research*, 96, 27-41.

- Tan, Y., Yu, H., Li, Y., Bi, W., & Yao, X. (2016). The effect of slag on the properties of magnesium potassium phosphate cement. *Construction and Building Materials*, 126, 313-320.
- Tro, N. J. (2008). *Chemistry: A molecular approach*. Pearson Custom Publishing, New York.
- Wagh, A. S. (2004). *Chemically bonded phosphate ceramics: Twenty-first-century materials with diverse applications*. Elsevier Sci Ltd.
- Wagh, A. S., & Jeong, S. Y. (2003). Chemically bonded phosphate ceramics: I, A dissolution model of formation. *Journal of the American Ceramic Society*, 86(11), 1838-1844.
- Wang, A., Yuan, Z., Zhang, J., Liu, L., Li, J., & Liu, Z. (2013). Effect of raw material ratios on the compressive strength of magnesium potassium phosphate chemically bonded ceramics. *Materials Science and Engineering: C*, 33(8), 5058-5063.
- Wang, A., Zhang, J., Li, J., Ma, A., & Liu, L. (2013). Effect of liquid-to-solid ratios on the properties of magnesium phosphate chemically bonded ceramics. *Materials Science and Engineering: C*, 33(5), 2508-2512.
- Wilson, A. D., and Nicholson, J. W. (1993). *Acid-base cements: Their biomedical and industrial applications*. Cambridge University Press, Cambridge.
- Xu, B., Ma, H., & Li, Z. (2015). Influence of magnesia-to-phosphate molar ratio on microstructures, mechanical properties and thermal conductivity of magnesium potassium phosphate cement paste with large water-to-solid ratio. *Cement and Concrete Research*, 68, 1-9.
- Yang, J., & Qian, C. (2010). Effect of borax on hydration and hardening properties of magnesium and potassium phosphate cement pastes. *Journal of Wuhan University of Technology – Material Science Edition*, 25(4), 613-618.
- Yang, Q., & Wu, X. (1999). Factors influencing properties of phosphate cement-based binder for rapid repair of concrete. *Cement and Concrete Research*, 29(3), 389–396.
- Zhang, G., Li, G., & He, T. (2017). Effects of sulphoaluminate cement on the strength and water stability of magnesium potassium phosphate cement. *Construction and Building Materials*, 132, 335-342.
- Zheng, D. D., Ji, T., Wang, C. Q., Sun, C. J., Lin, X. J., & Hossain, K. M. A. (2016). Effect of the combination of fly ash and silica fume on water resistance of Magnesium-Potassium Phosphate Cement. *Construction and Building Materials*, 106, 415-421.



## APPENDICES

### APPENDIX A

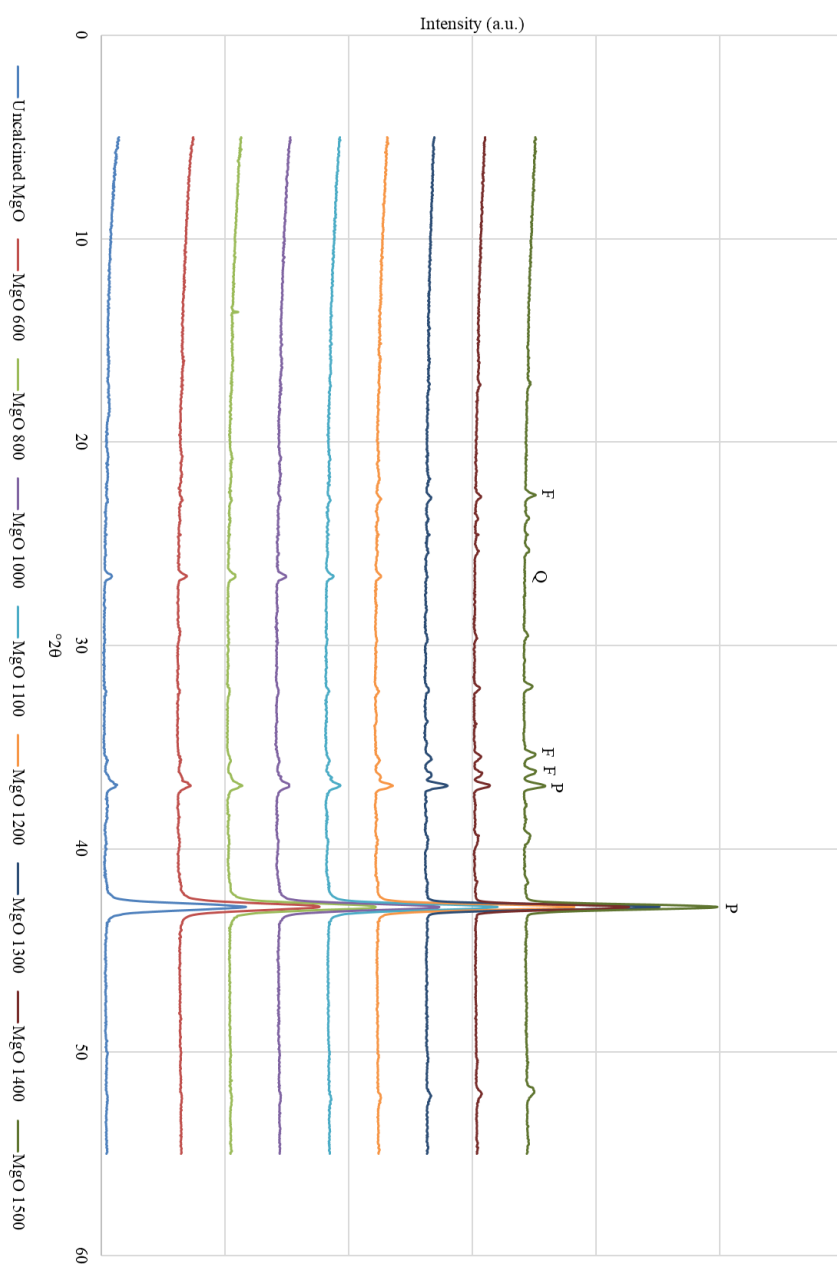


Figure A.1 The change in X-ray diffraction patterns with calcination.



## APPENDIX B

Table B.1 Compound composition of the magnesia samples calcined at different temperatures

Oxide	Compound Composition (%)		
	A	B	C
MgO	81.30	82.80	82.80
SiO <sub>2</sub>	9.35	7.19	10.60
CO <sub>2</sub>	6.89	7.78	3.82
CaO	1.74	1.57	1.85
Fe <sub>2</sub> O <sub>3</sub>	0.595	0.526	0.724
NiO	0.116	0.105	0.127
Al <sub>2</sub> O <sub>3</sub>	0.058	0.037	0.077

- A- The uncalcined magnesia powder  
B- The magnesia powder calcined at 600 °C  
C- The magnesia powder calcined at 1500 °C



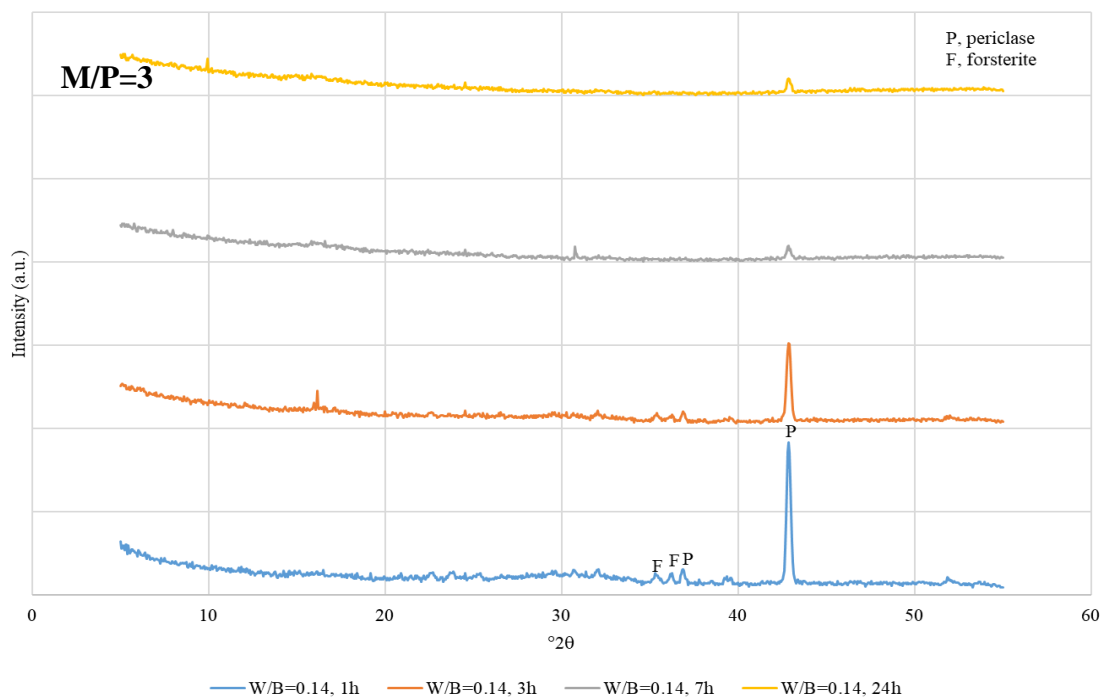
## APPENDIX C



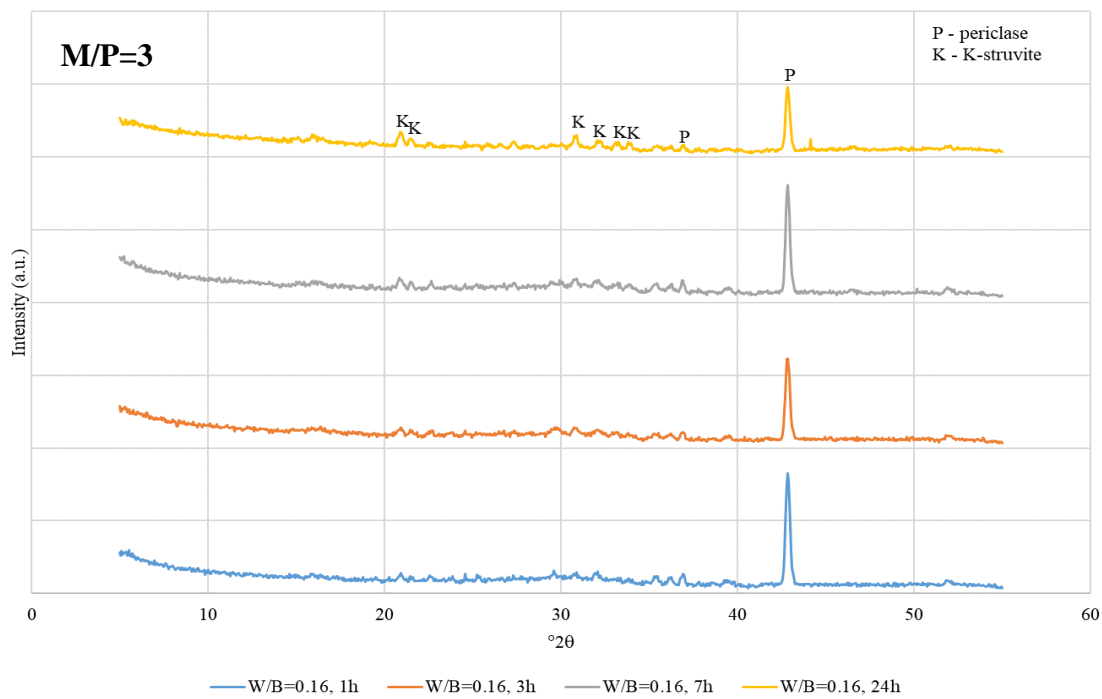
Figure C.1 Cracks on the 5-cm cube sample with  $M/P = 6$  and  $W/B = 0.20$  at 24 h (before testing)



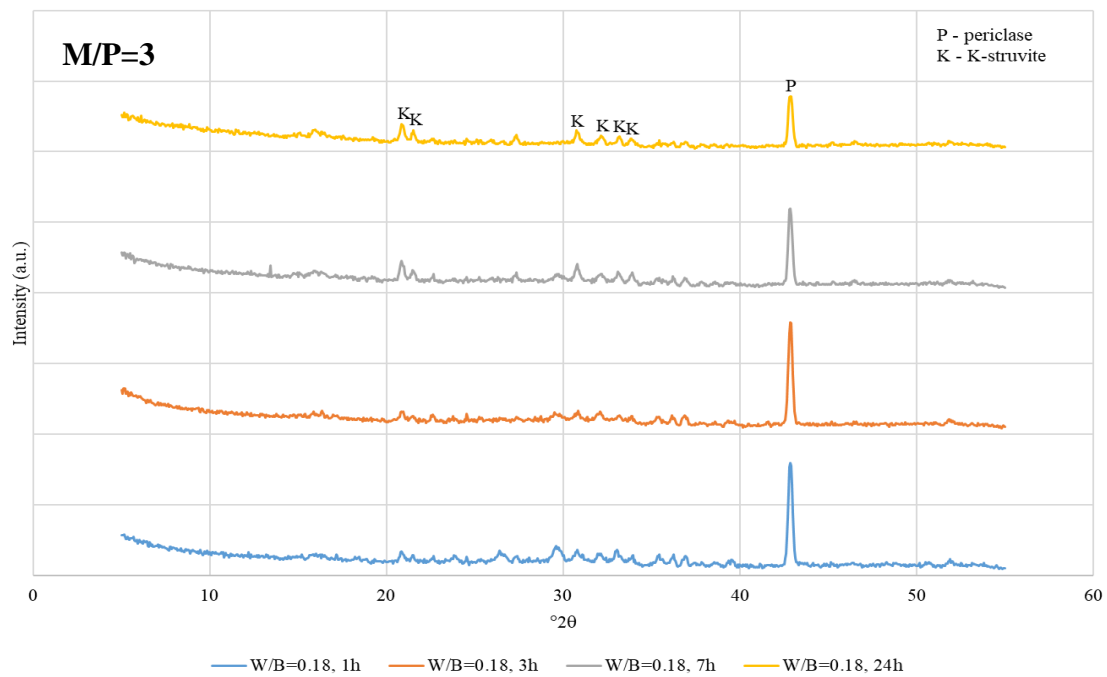
## APPENDIX D



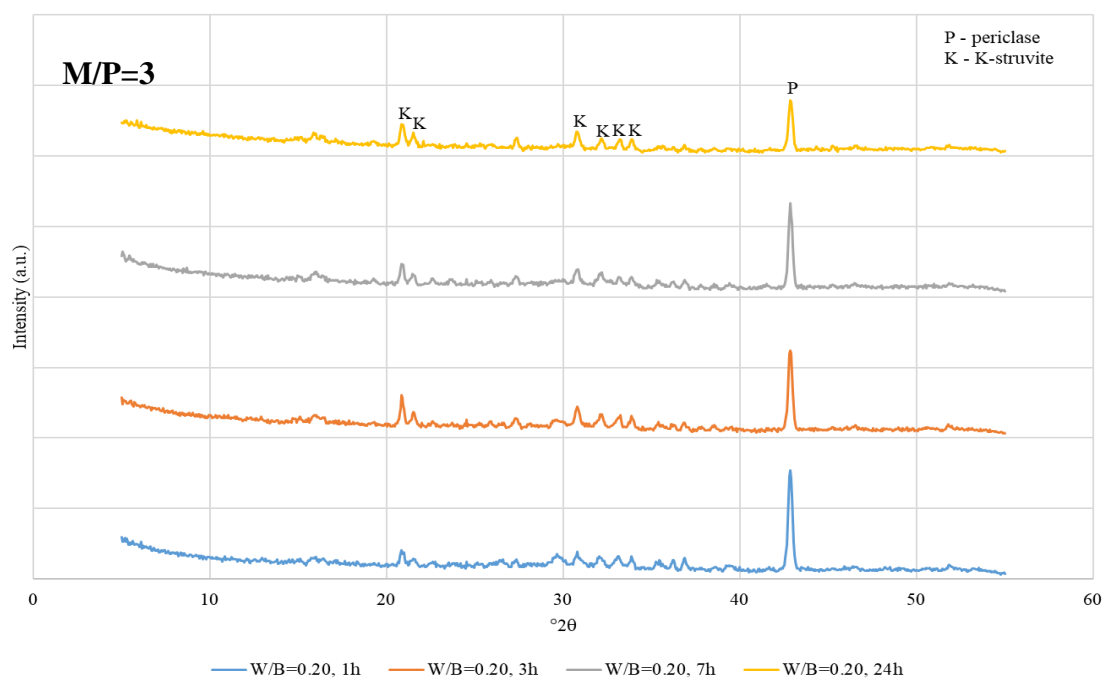
(a)



(b)

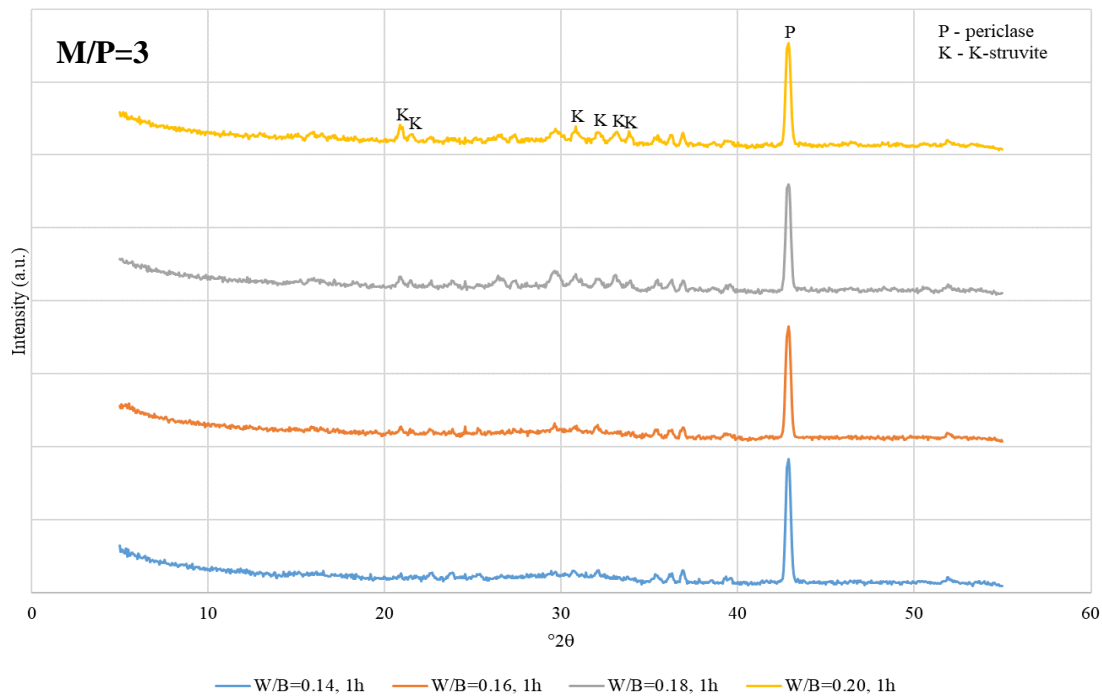


(c)

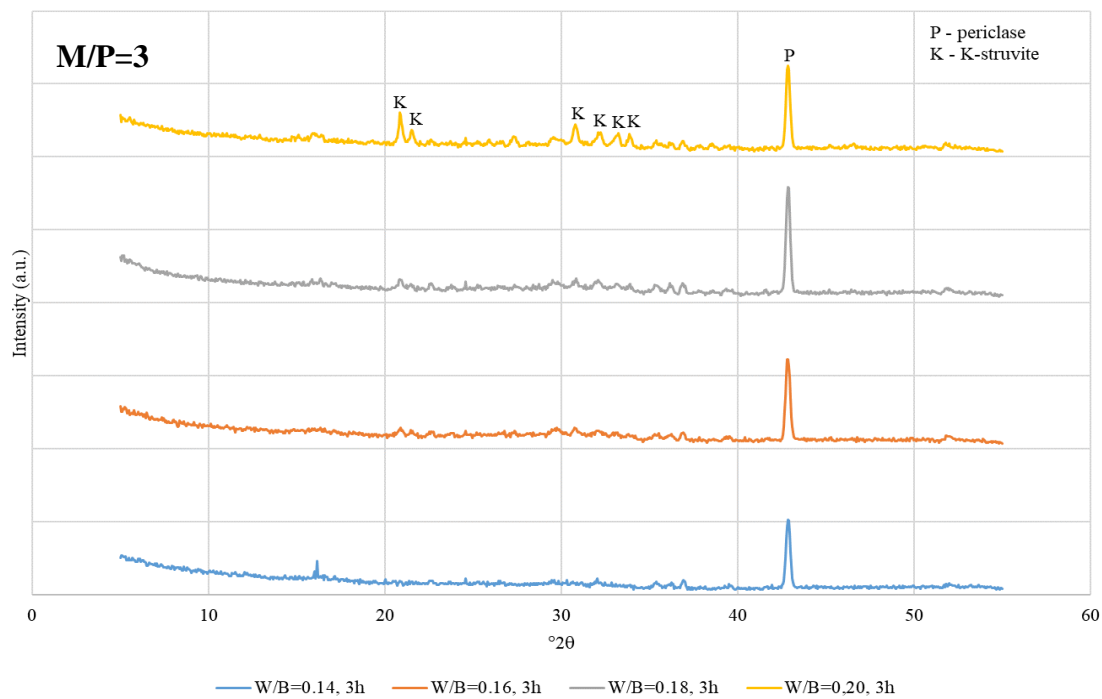


(d)

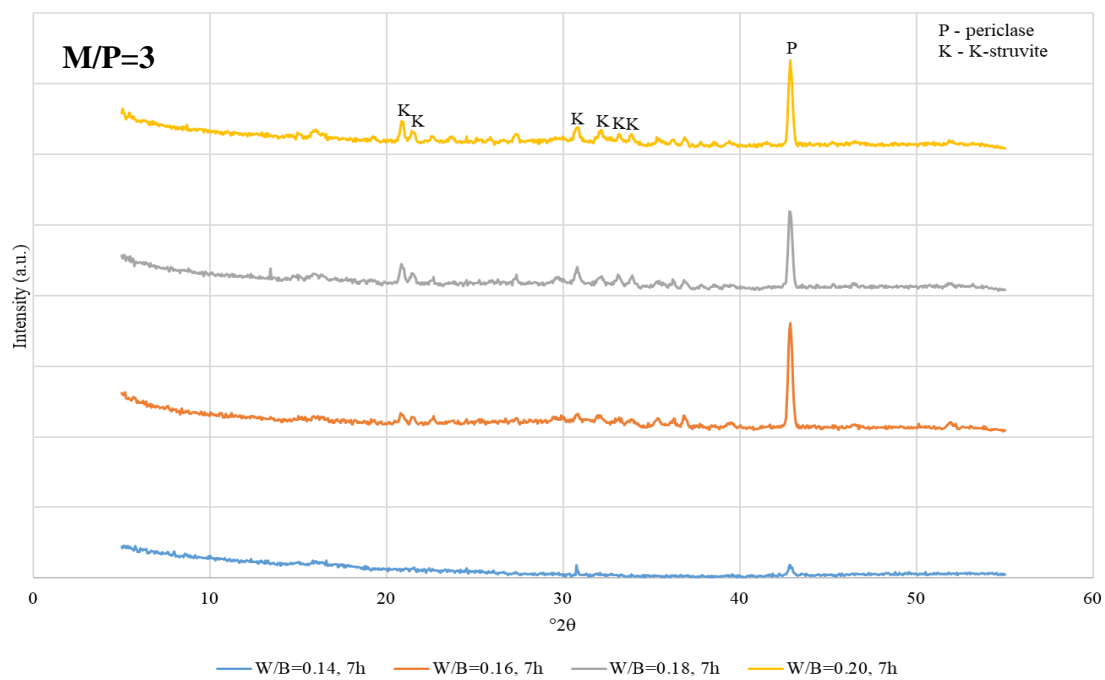
Figure D.1 (a) W/B = 0.14, (b) W/B = 0.16, (c) W/B = 0.18, (d) W/B = 0.20 XRD results for M/P = 3 mixtures



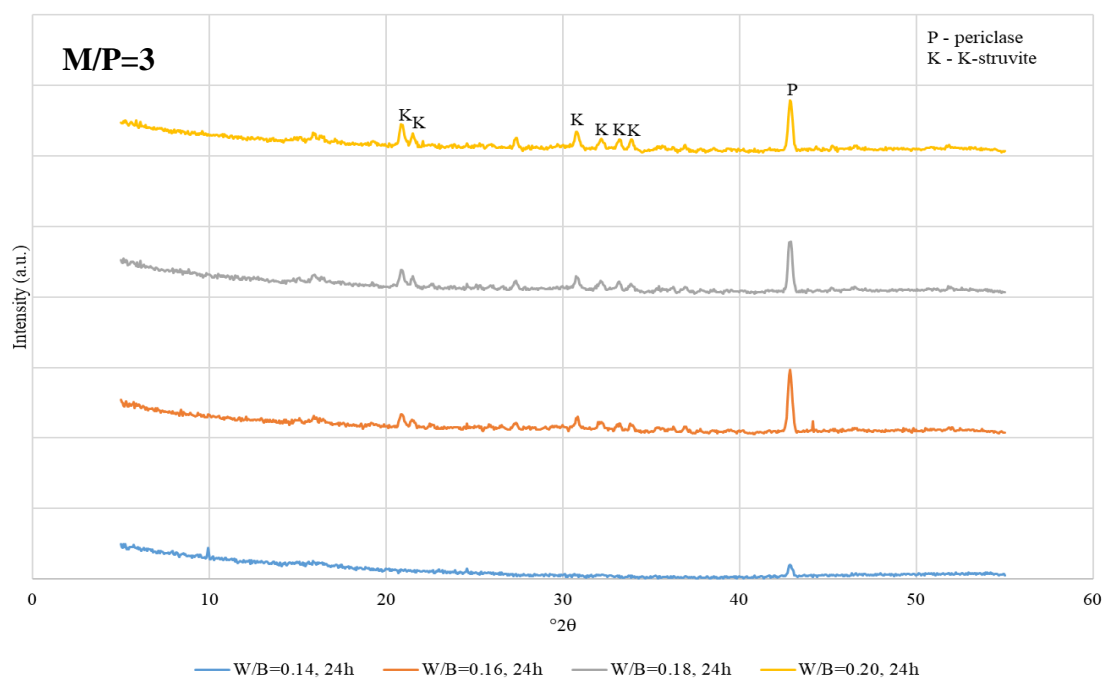
(a)



(b)

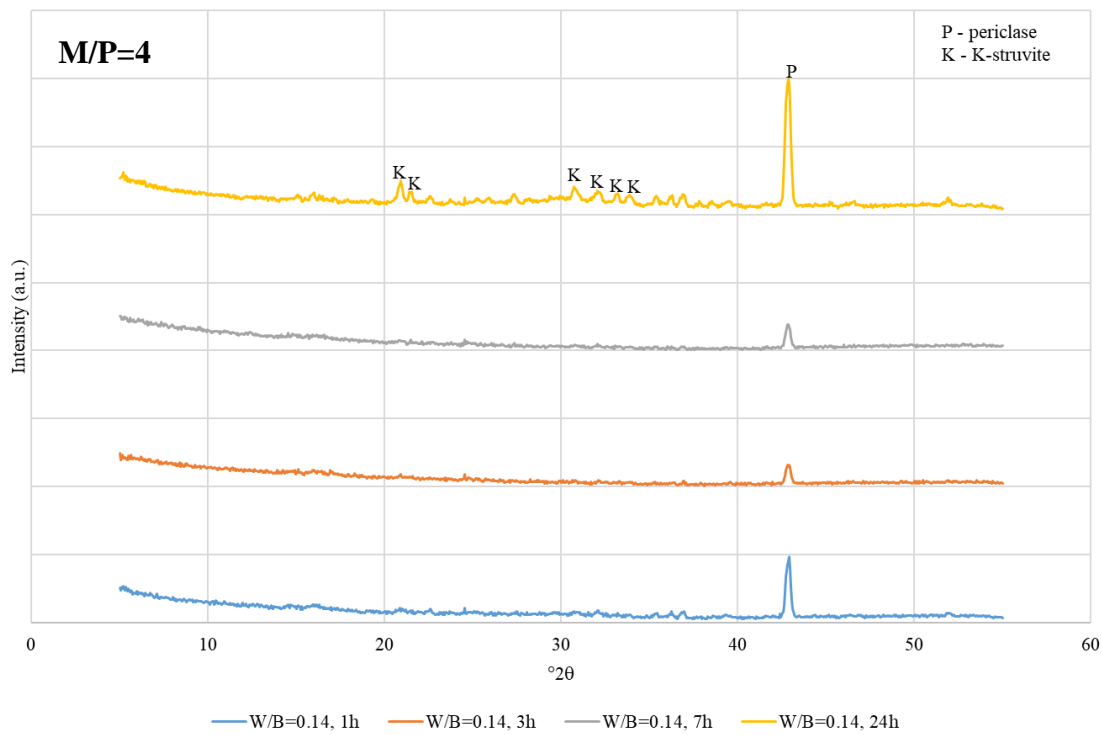


(c)

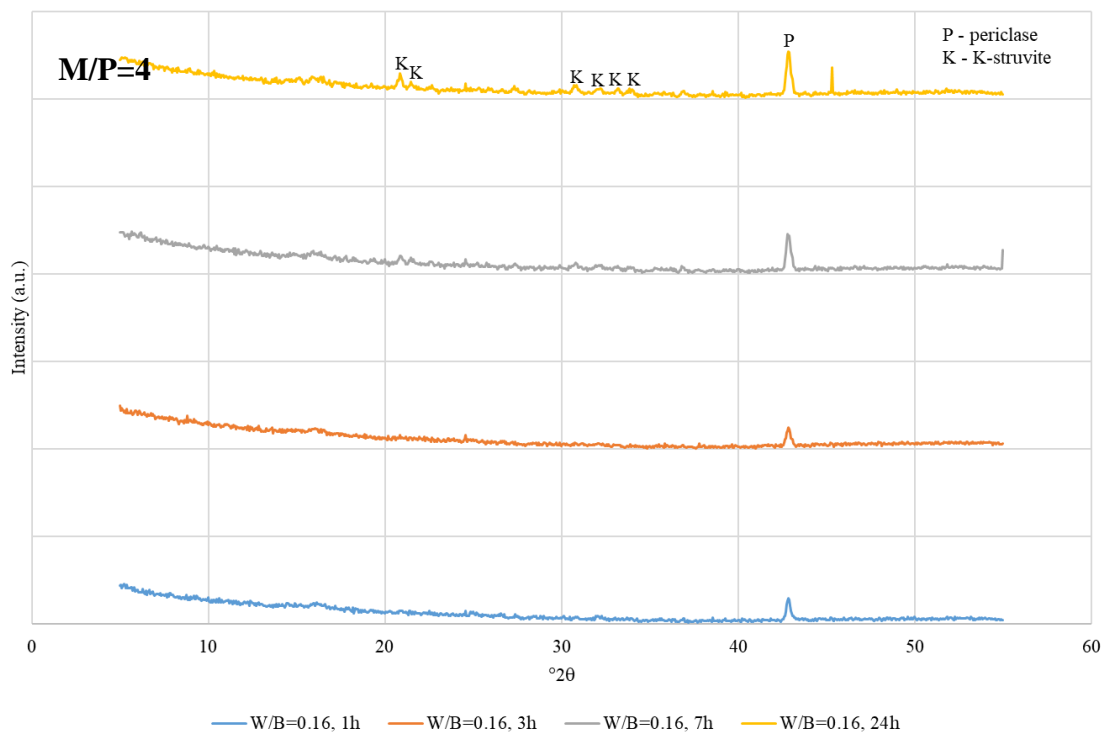


(d)

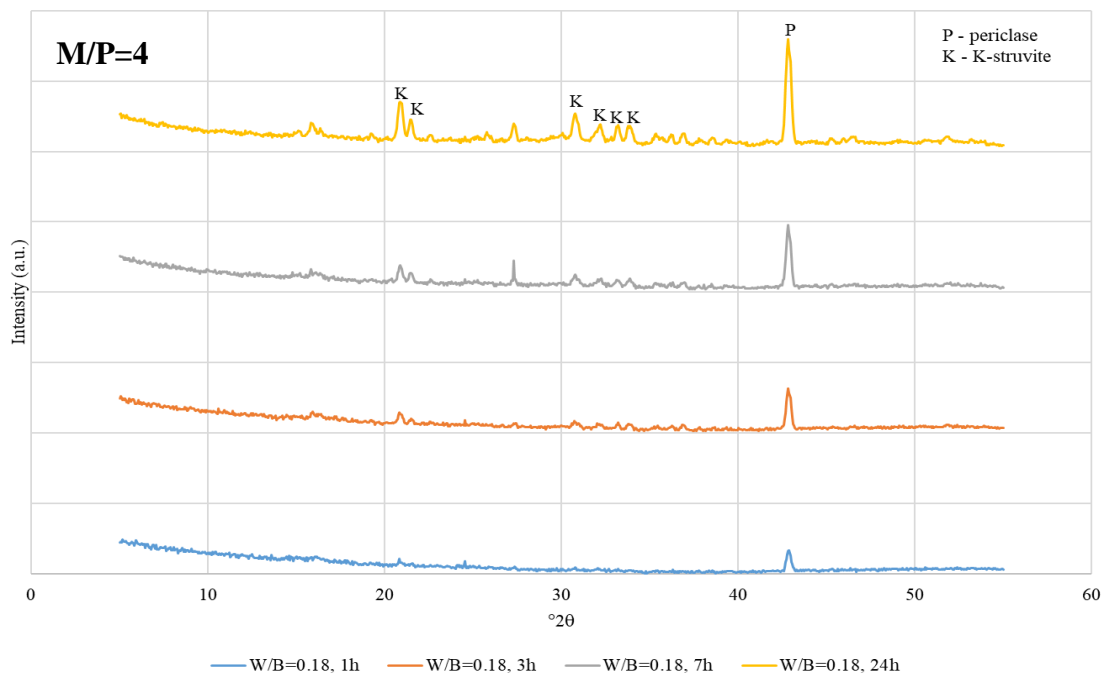
Figure D.2 (a) 1 h (b) 3 h (c) 7 h (d) 24 h XRD results for M/P = 3 mixtures with W/B = 0.14, 0.16, 0.18, and 0.20



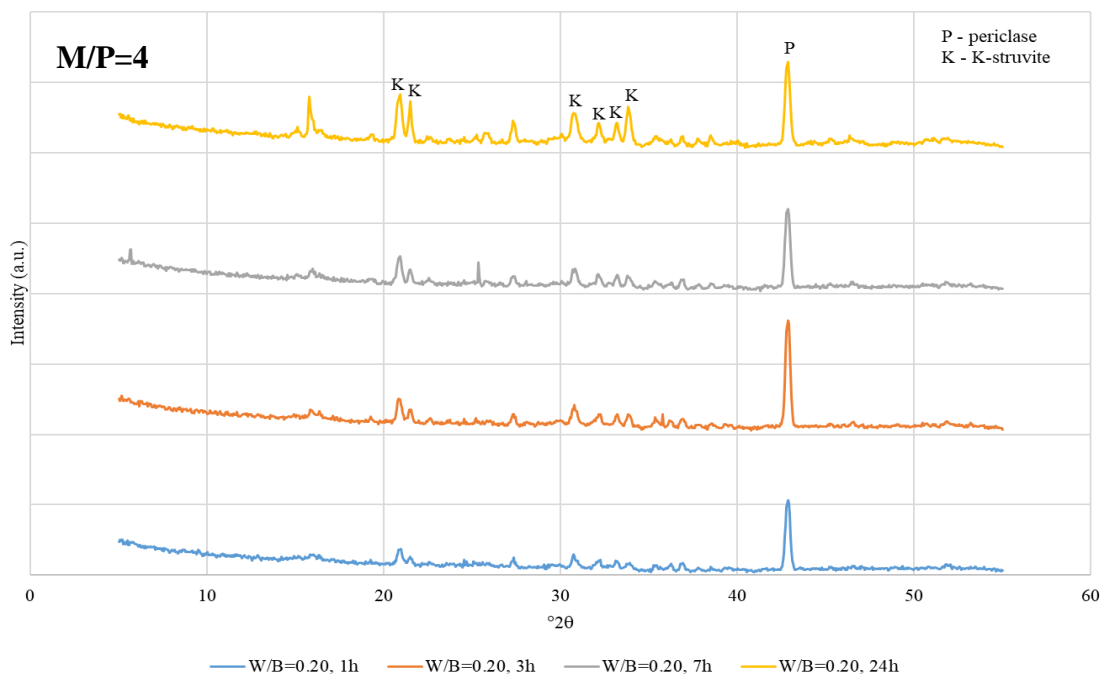
(a)



(b)

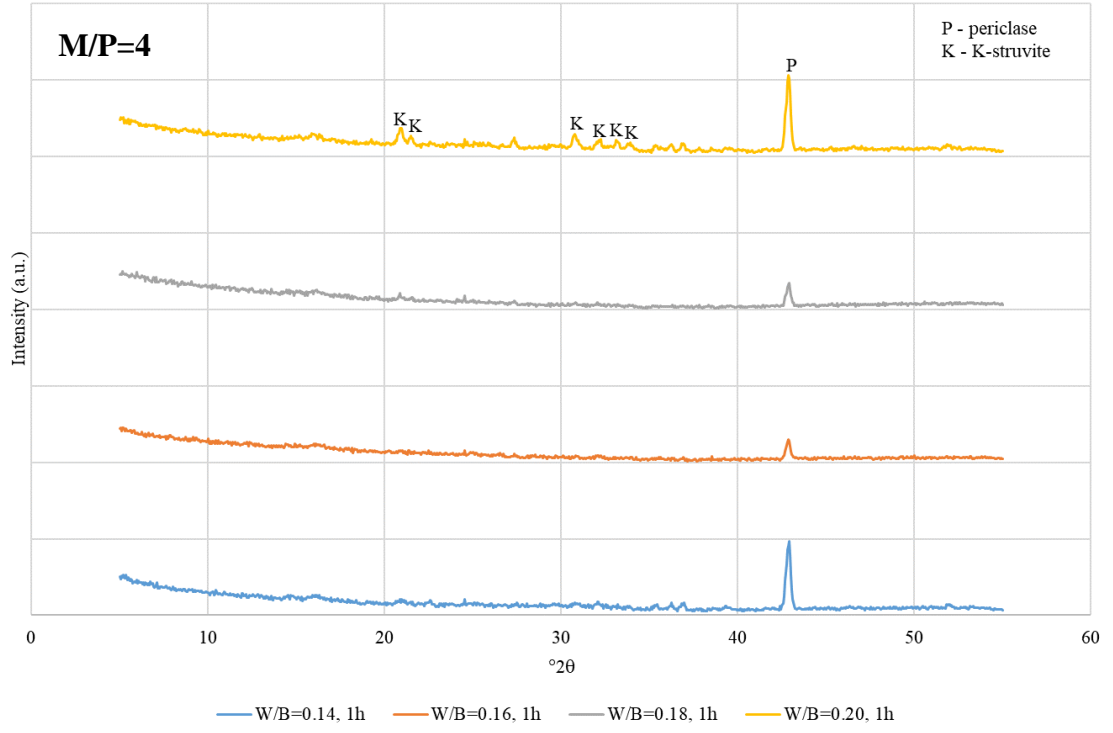


(c)

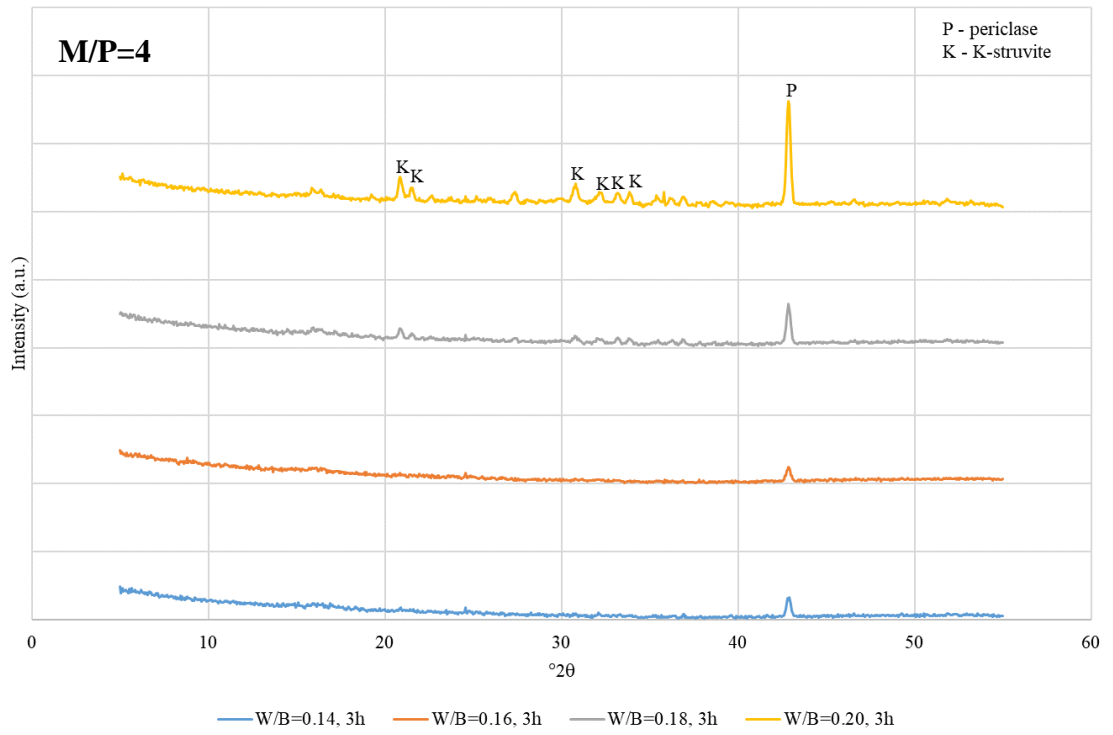


(d)

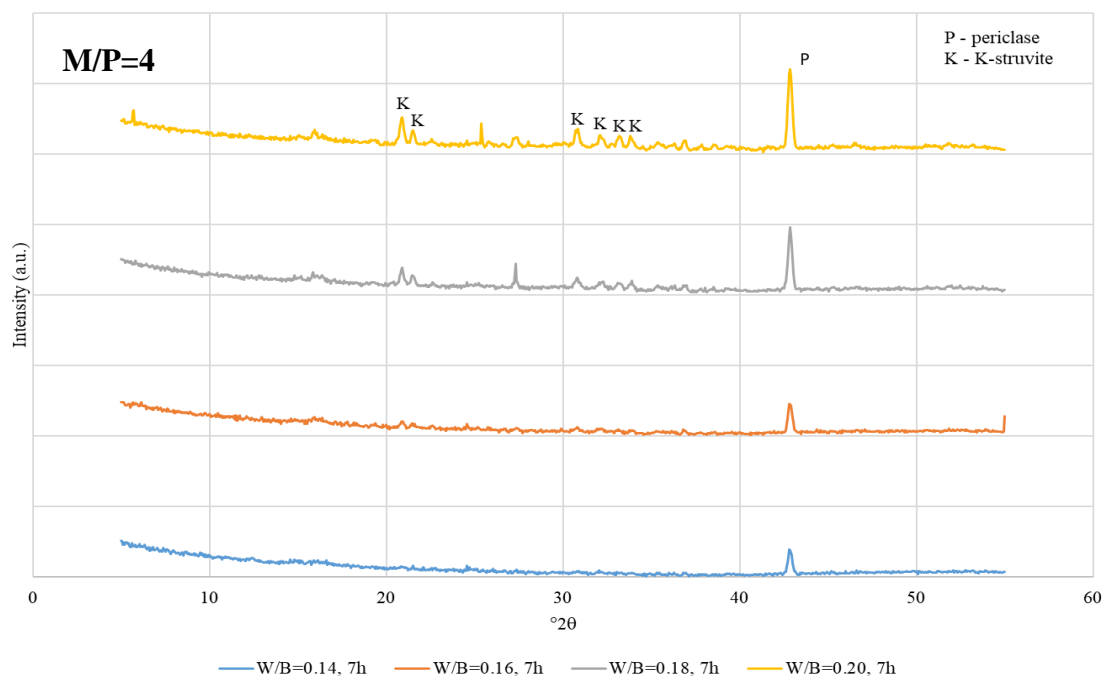
Figure D.3 (a) W/B = 0.14, (b) W/B = 0.16, (c) W/B = 0.18, (d) W/B = 0.20 XRD results for M/P = 4 mixtures



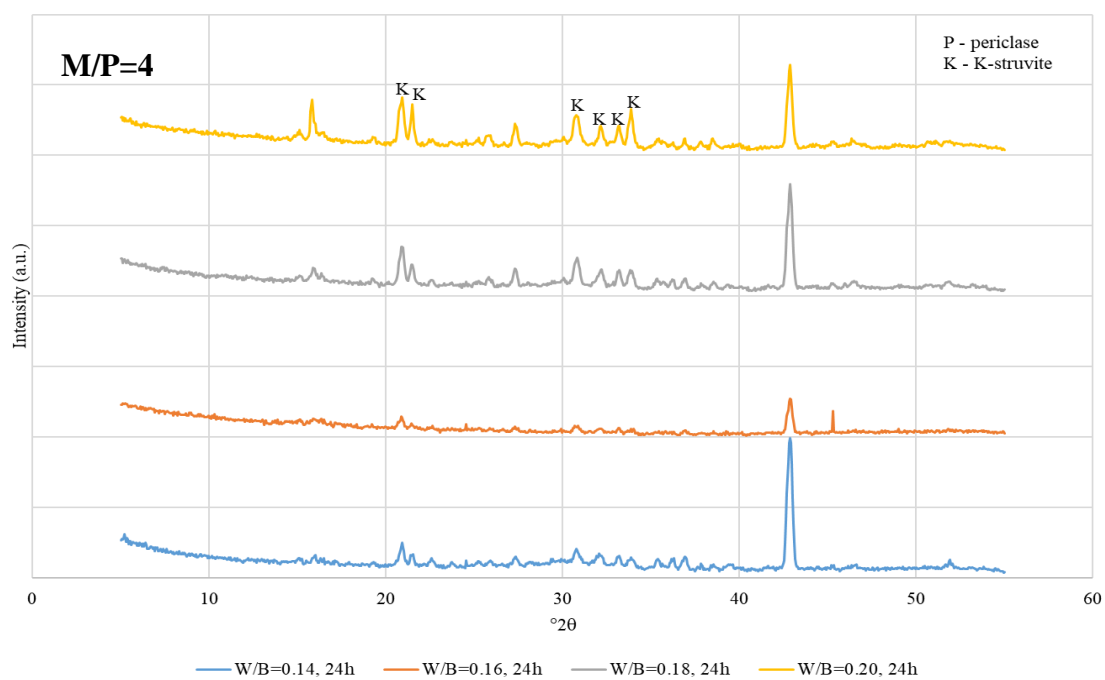
(a)



(b)

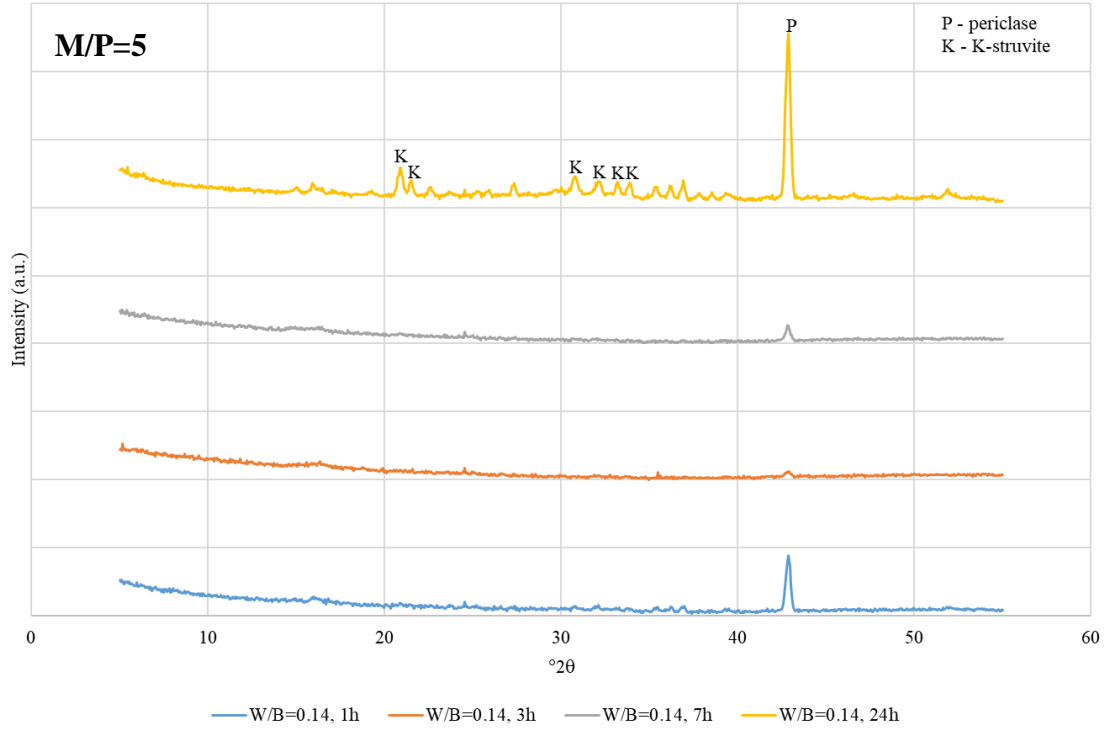


(c)

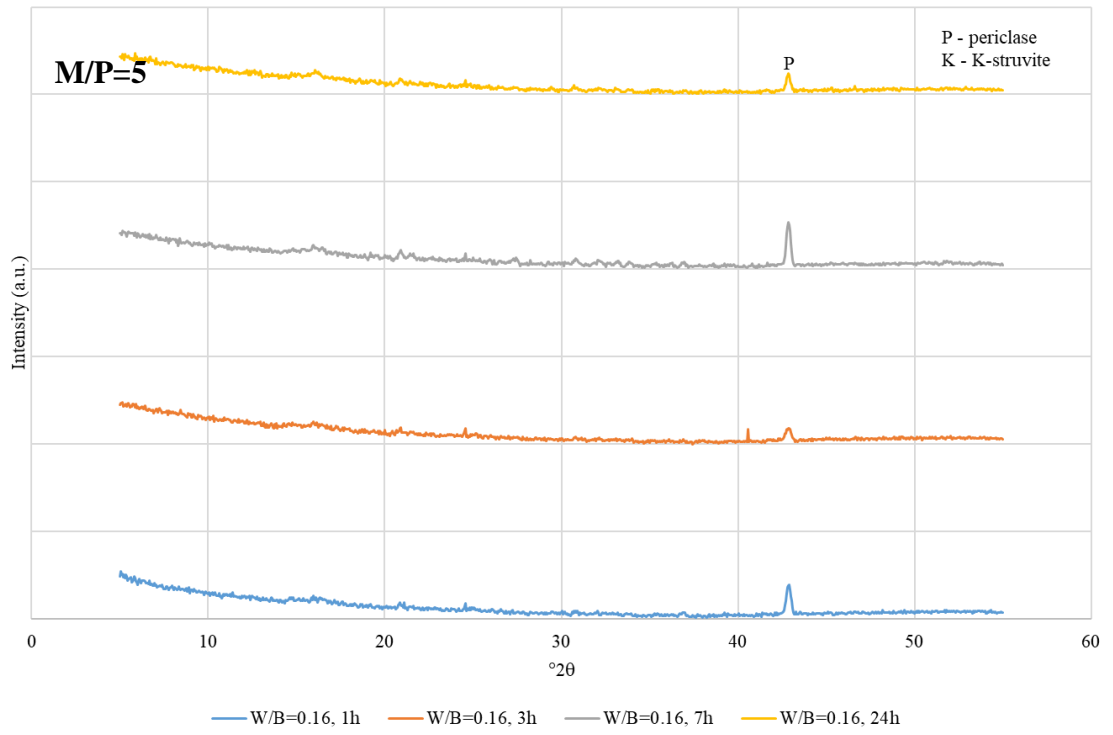


(d)

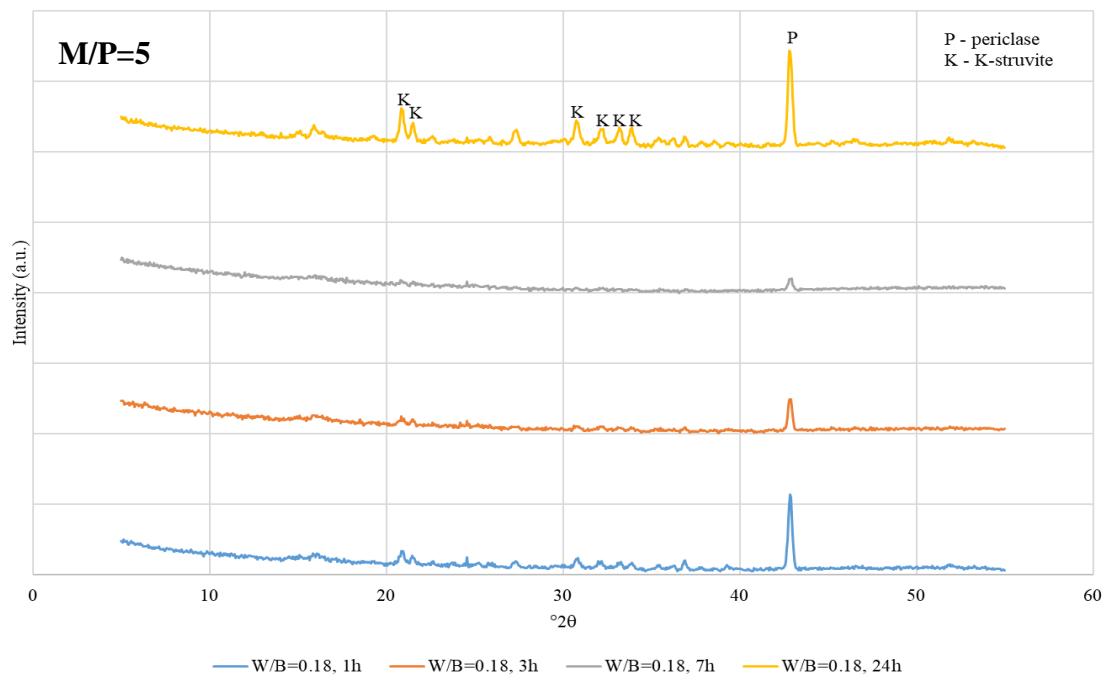
Figure D.4 (a) 1 h (b) 3 h (c) 7 h (d) 24 h XRD results for M/P = 4 mixtures with W/B = 0.14, 0.16, 0.18, and 0.20



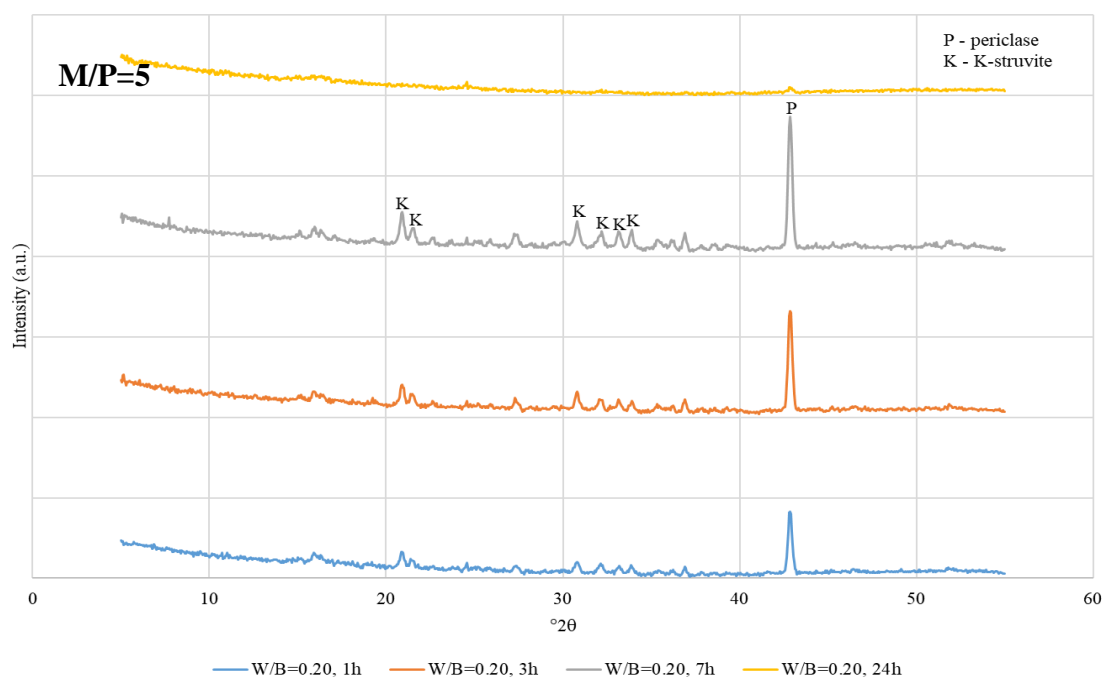
(a)



(b)

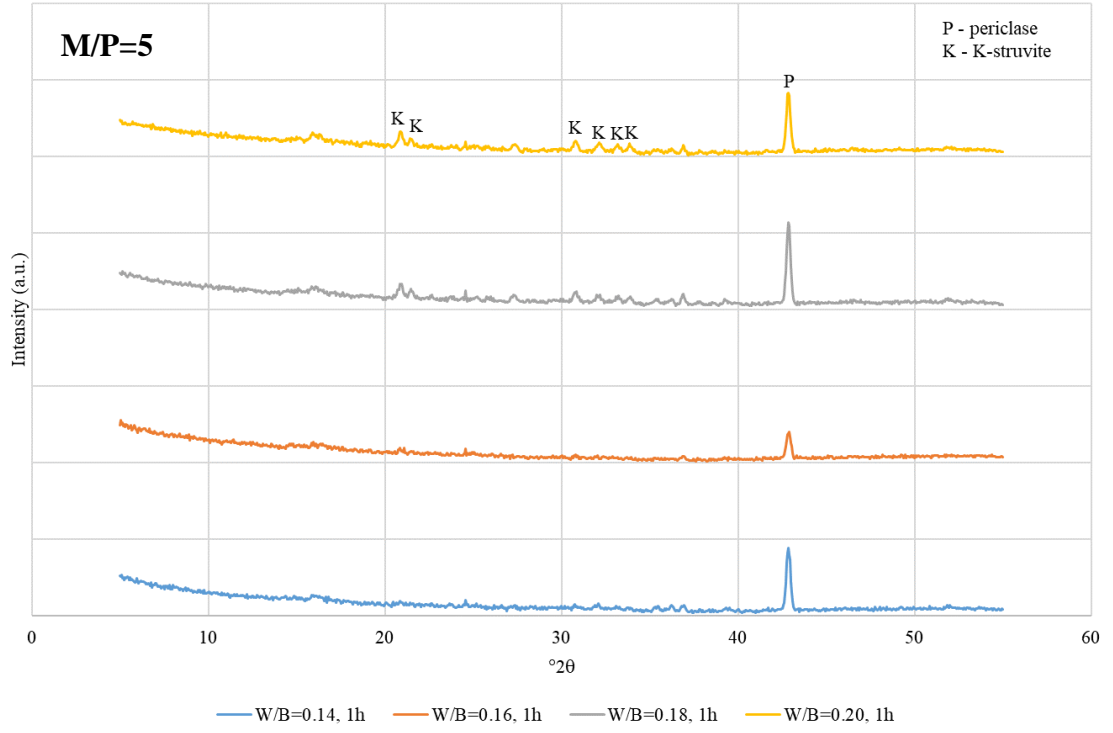


(c)

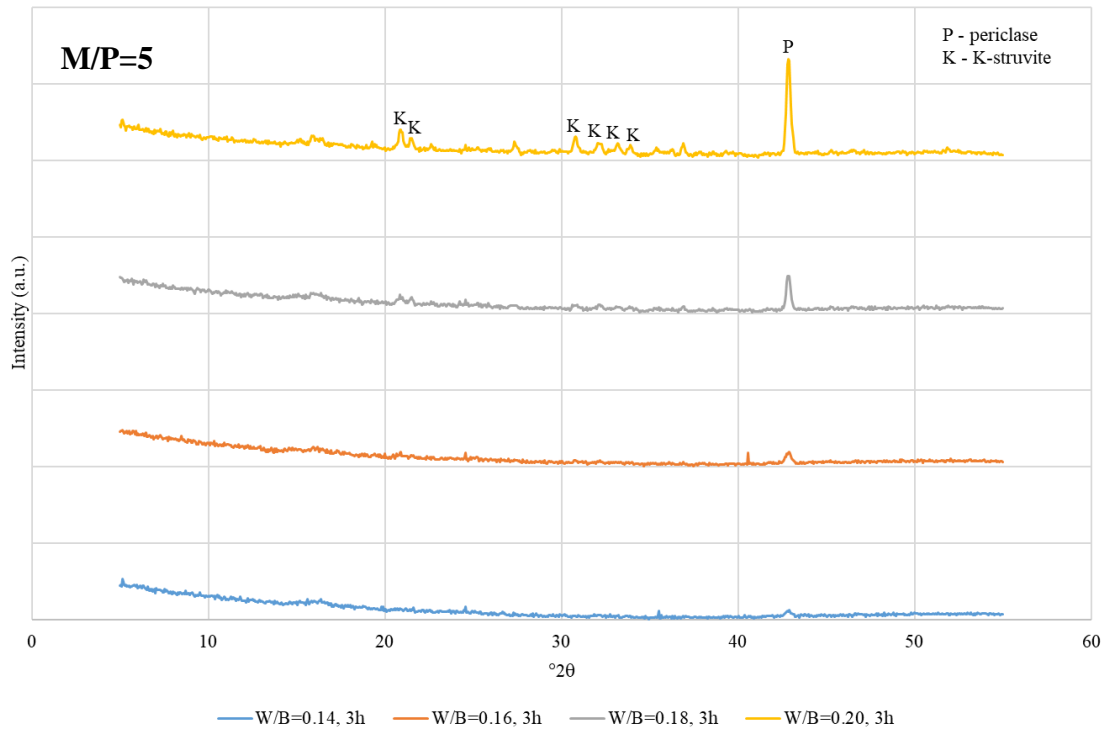


(d)

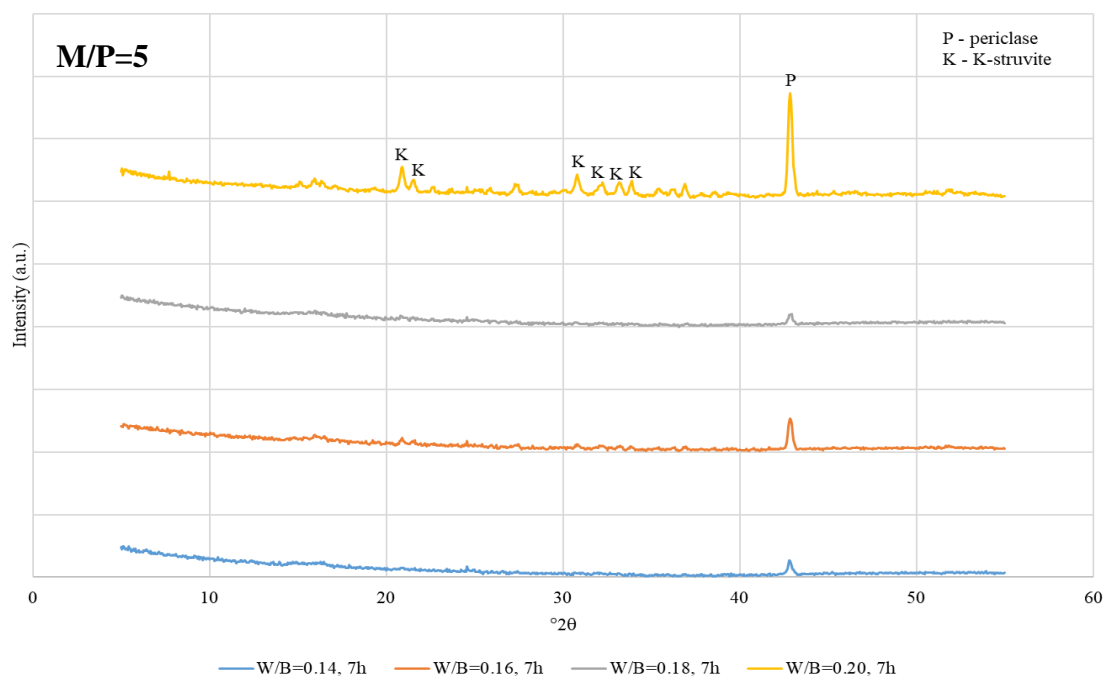
Figure D.5 (a) W/B = 0.14, (b) W/B = 0.16, (c) W/B = 0.18, (d) W/B = 0.20 XRD results for M/P = 5 mixtures



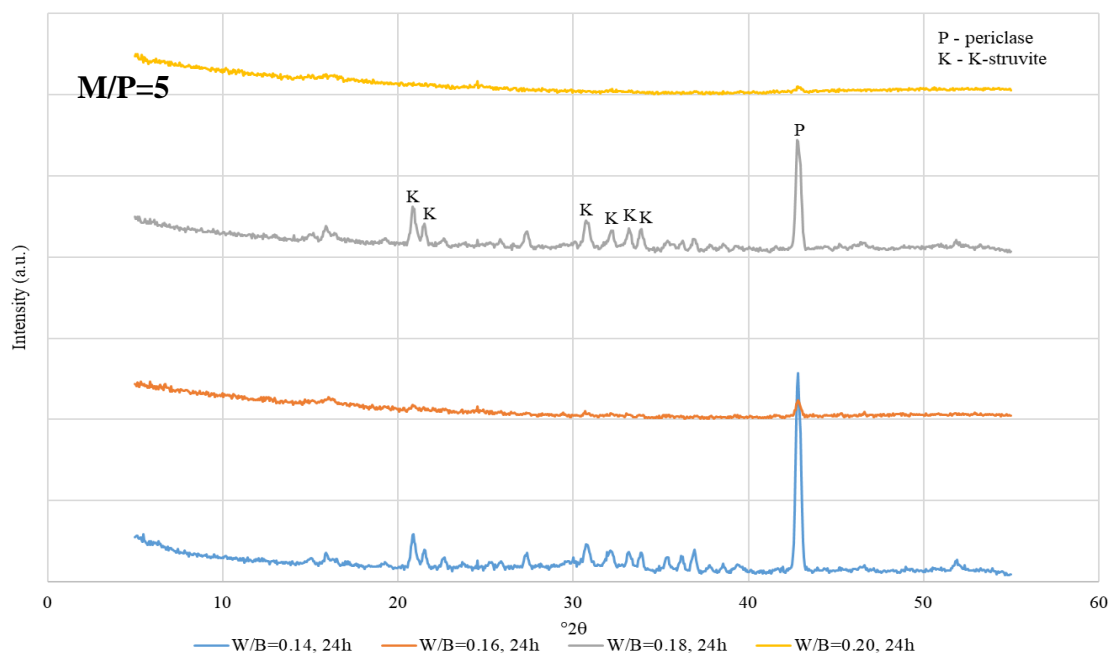
(a)



(b)

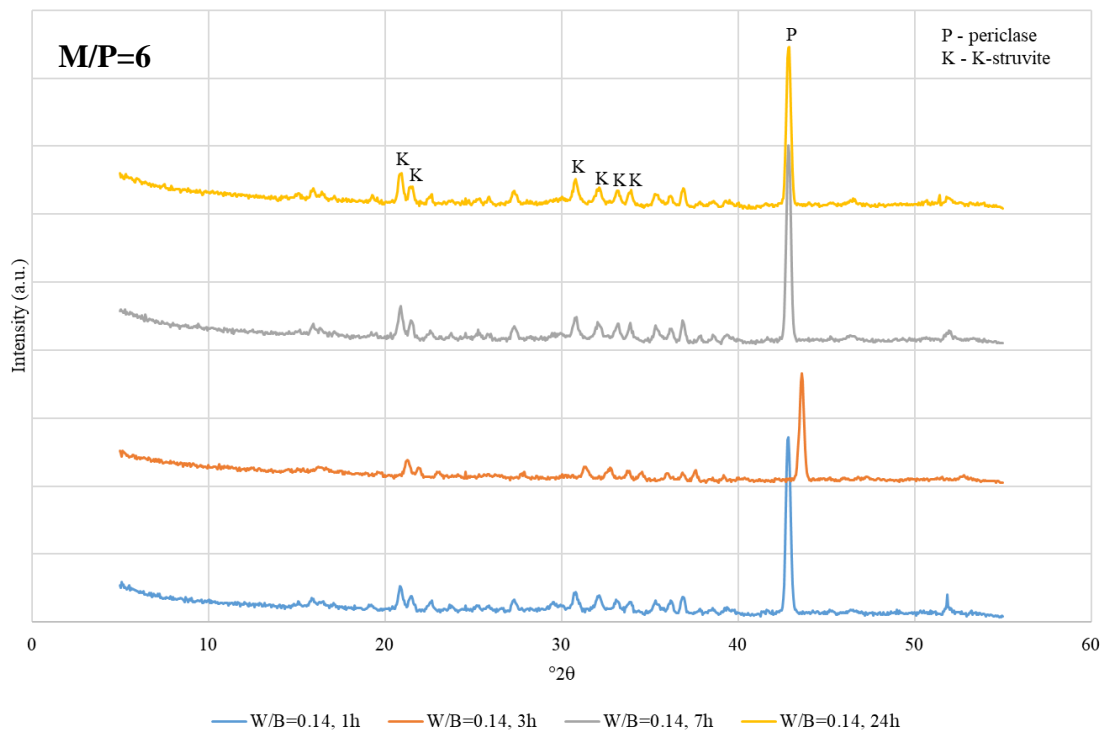


(c)

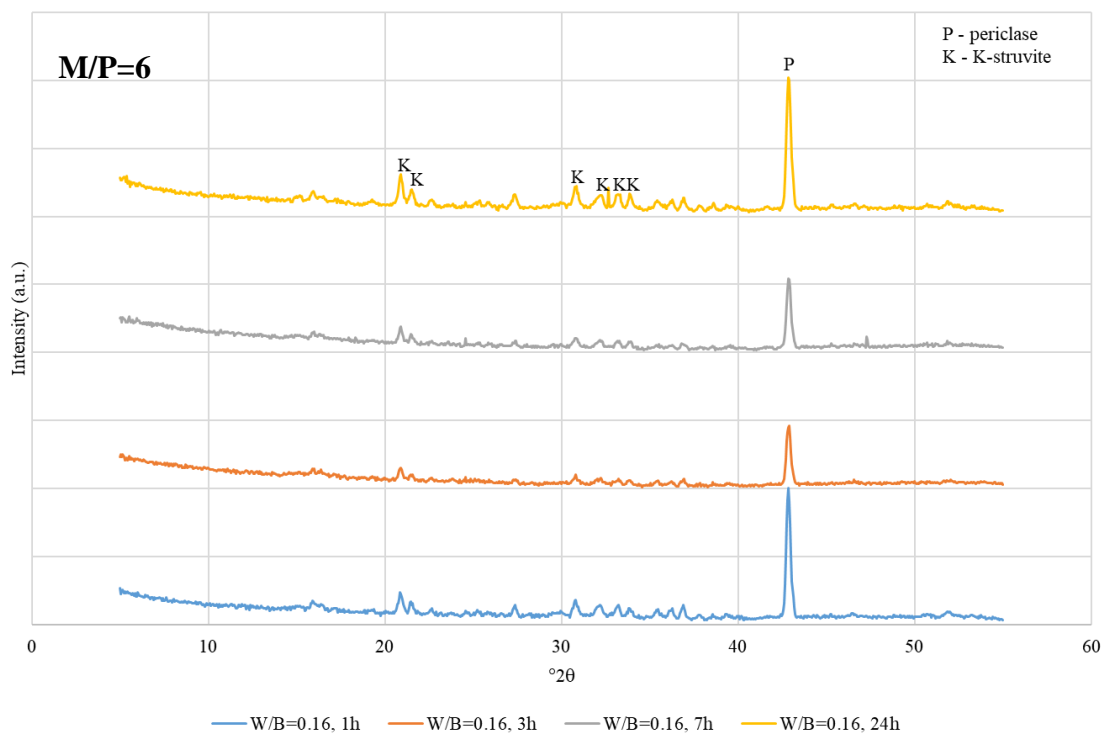


(d)

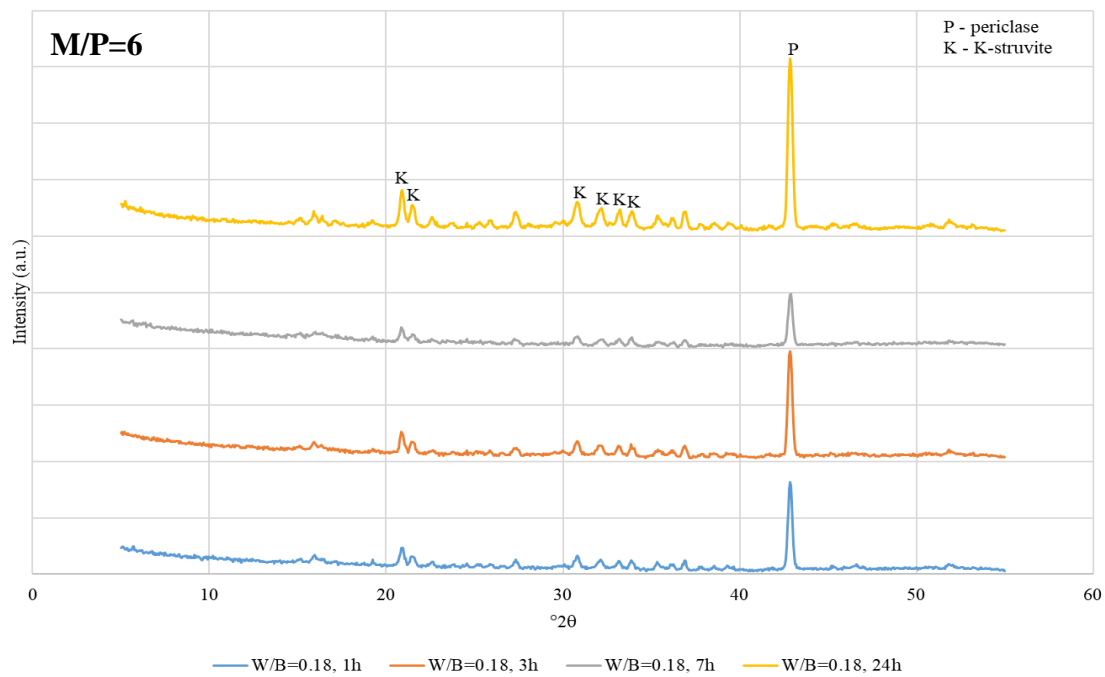
Figure D.6 (a) 1 h (b) 3 h (c) 7 h (d) 24 h XRD results for M/P = 5 mixtures with W/B = 0.14, 0.16, 0.18, and 0.20



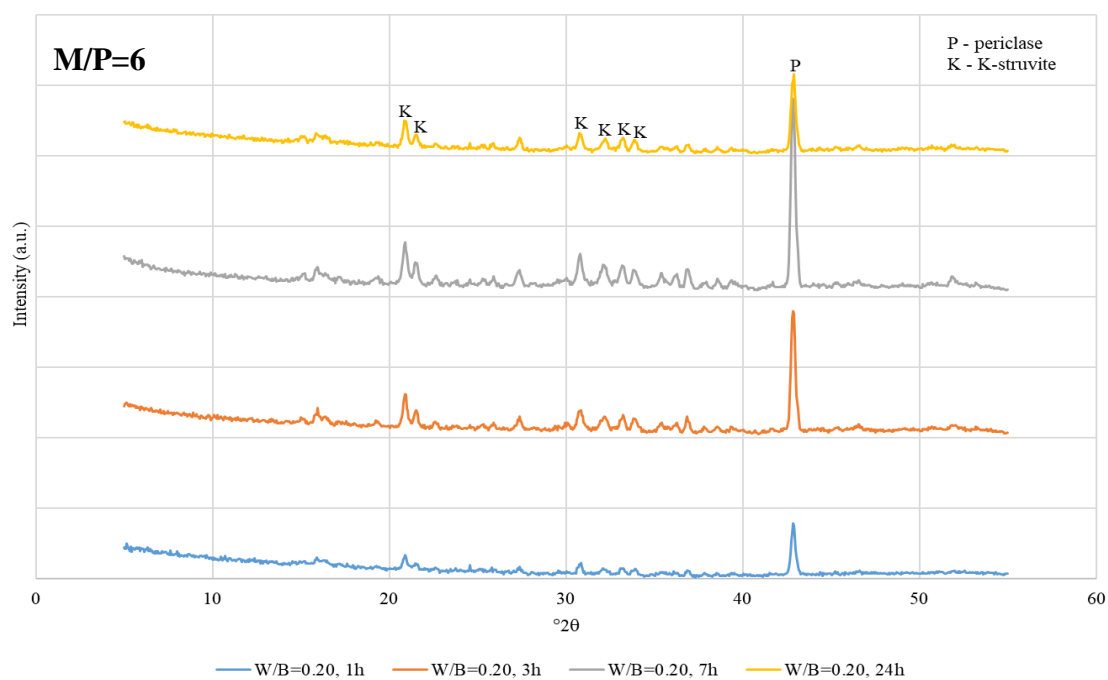
(a)



(b)

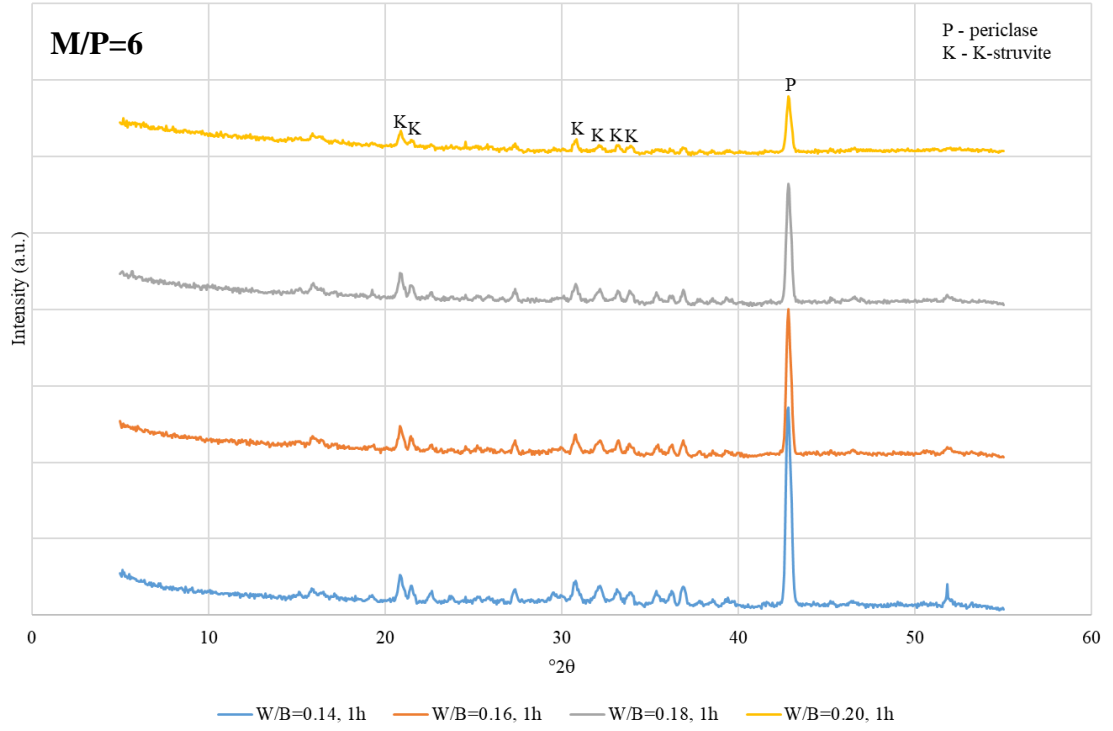


(c)

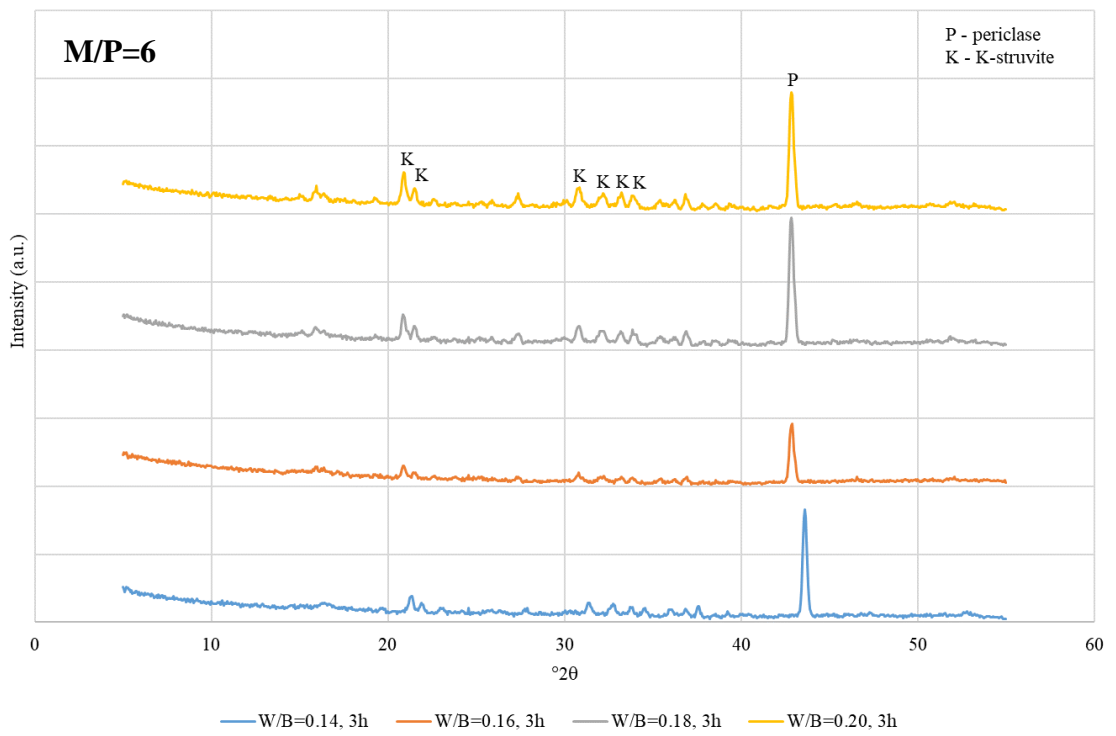


(d)

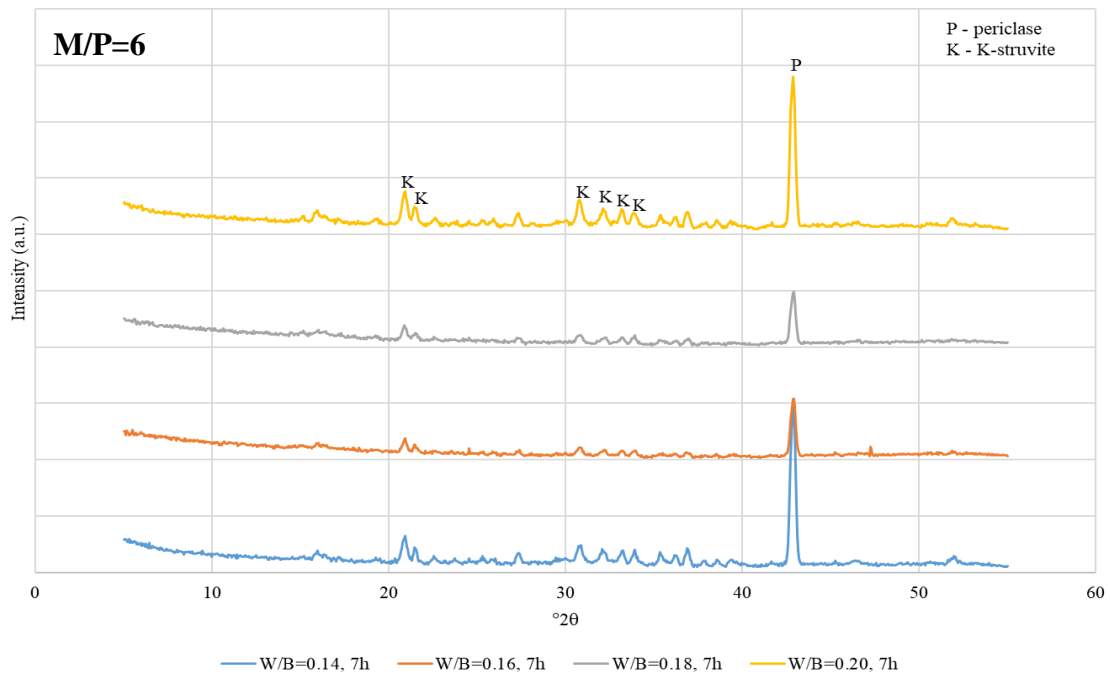
Figure D.7 (a) W/B = 0.14, (b) W/B = 0.16, (c) W/B = 0.18, (d) W/B = 0.20 XRD results for M/P = 6 mixtures



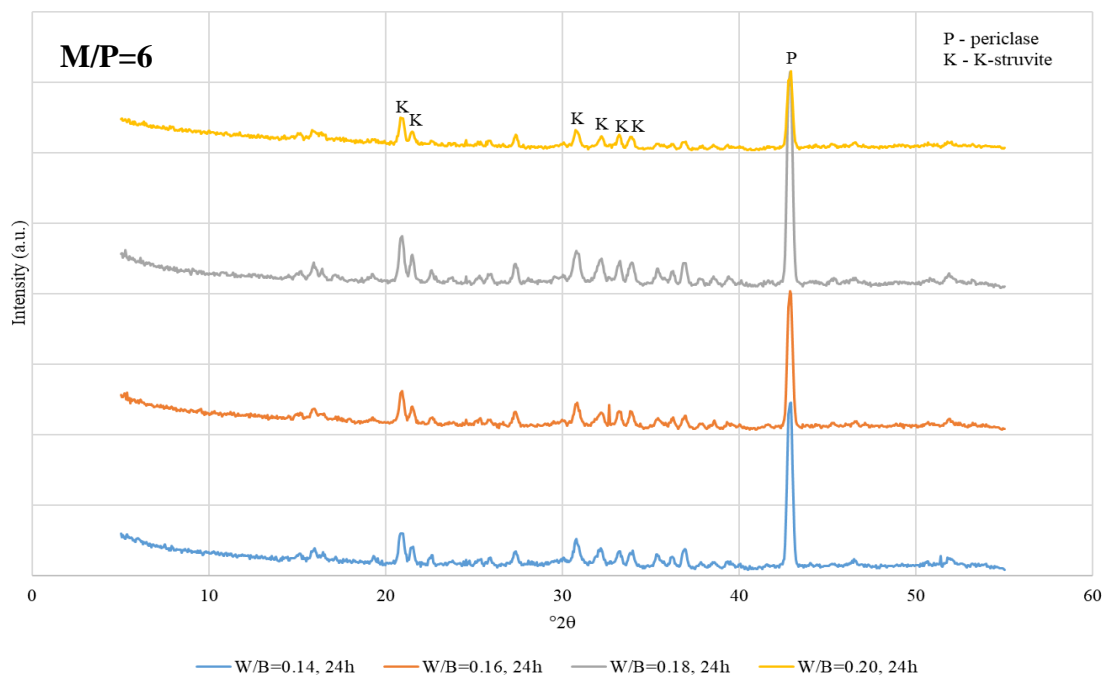
(a)



(b)



(c)



(d)

Figure D.8 (a) 1 h (b) 3 h (c) 7 h (d) 24 h XRD results for M/P = 6 mixtures with W/B = 0.14, 0.16, 0.18, and 0.20